Università degli Studi del Molise

FACOLTA' DI SCIENZE MM. FF. NN. (ISERNIA)

Dottorato di Ricerca in Ambiente e Territorio
XXIV ciclo

Epitope mapping of a mAb against the factor H binding protein (fHbp) of *N. meningitidis* by phage display

(BIO/18)

Coordinatore:
Ch.mo Prof. Claudio Caprari

Candidato:
Lorenza Zippilli

Tutor:
Ch.mo Prof. Franco Felici

a.a. 2011/2012

Contents

List of Figures

List of Tables

Chapter 1

Introduction

1.1 *Neisseria meningitidis*

N. meningitidis is a gram-negative microorganism member of the bacterial family Neisseriaceae. *Neisseria meningitidis* is a human-specific organism, often diplococcal in form, and is recognized as the main cause of bacterial meningitis (Fig. 1.1).

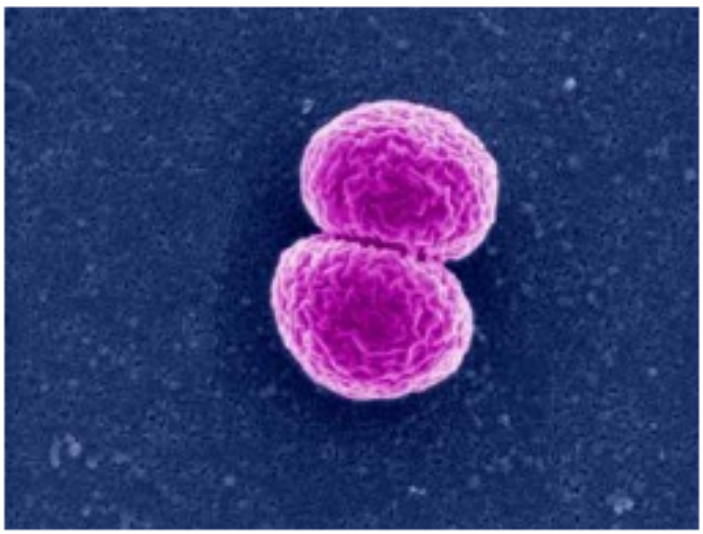

Figure 1.1: *Neisseria meningitidis* picture at scanning electron microscope.

The genus Neisseria also includes another pathogenic species *N. gonorrhoeae*, the cause of gonorrhoea, which shares numerous common features with *N. meningitidis*. However, *N. meningitidis* is present mainly in the nasopharyngeal whereas *N. gonorrhoeae* prefers the urogenital tracts but also the nature of diseases caused suggests significant

differences exist between these pathogens, borne out of the identification of variations at the genetic level (Stabler *et al.*, 2005).

One of principal difference between the two organisms is the expression of surface polysaccharide capsule which is absent in *N. gonorrhoeae*, whereas *N. meningitidis* strains commonly express one of several capsule types, which form the basis of their primary classification in 13 serogroups (Cartwright, 1995).

Although 13 meningococcal serogroups have been described (A, B, C, D, 29E, H, I, K, L, Y, W-135, X and Z), the majority of disease is caused by organisms expressing one of five capsule types, namely A, B, C, Y and W-135.

Meningococcal disease in Europe and America is predominantly caused by serogroups B and C, whereas in Africa the principal causes are serogroups A and C. Serogroup W-135 causes outbreaks around the world, while serogroup Y is generally associated with disease in the U.S.A. and Canada. The factors that determine such geographic variation are not completely understood (Stephens *et al.*, 2007).

Generally, mortality occurs in up to 10% of patients with invasive meningococcal disease. Mortality rates are dependent on the type and severity of invasive disease, and are greatest for fulminant septicaemia (up to 55%) followed by meningitis with associated septicaemia (up to 25%), and lowest for meningitis without sepsis (generally $<5\%$). However, patients who survive invasive meningococcal disease often live with physical and mental sequelae, including amputation of limbs and digits, scarring of skin, deafness, speech impairment and seizures (Brandtzaeg, 2006)

1.1.1 Capsule of meningococci

N. meningitidis can be either encapsulated or not. However, the strains that cause invasive disease and isolated from sterile sites like blood and cerebrospinal fluid are invariably encapsulated. The capsule is essential for the survival of the organism in the blood as it provides resistance to antibody complement-mediated killing and inhibits the phagocytosis. The main meningococcal capsular polysaccharides associated with invasive disease are composed of sialic acid derivatives, except for the serogroup A capsule, which consists of repeating units of N-acetyl-mannosamine-1-phosphate (Fig. 1.2).

In meningococci, capsular genes are clustered within a single chromosomal locus, *cps*, divided into three regions.

Region A encodes enzymes for the biosynthesis and polymerization of the polysaccharide, and regions B and C carry the genes responsible for its translocation from the cytoplasm to the cell surface (Frosch *et al.*, 1989).

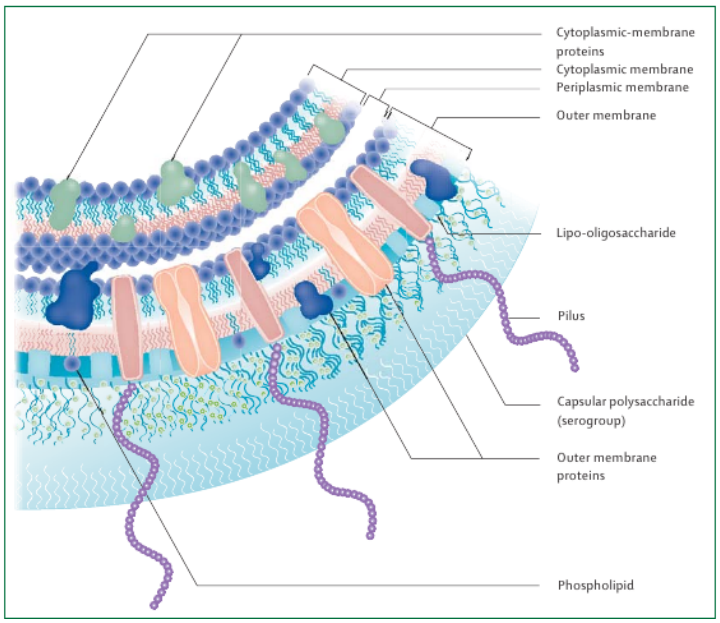

Figure 1.2: cross-sectional view of the meningococcus.

The capsular polysaccharides of the serogroups B, C, W-135 and Y contain sialic acid (5-N-acetyl-neuramic acid), and cps region A of these serogroups harbours a set of conserved genes siaA, siaB and siaC. These are responsible for the synthesis of sialic acid in the form of CMP-NANA, required for incorporation into the capsular polysaccharide. The fourth gene in this region, siaD, encodes a serogroup-specific polysialyltransferase involved in capsule polymerization (Claus *et al.*, 1997).

Genetic similarities in the structures of the capsule loci of all serogropus except for the serogroup A apparently favour horizontal exchange of portions of the capsule biosynthetic operon between different serogroups. This phenomenon, described as capsule switching, can render ineffective antibodies in controlling the spread of the pathogen (Swartley *et al.*, 1997).

1.2 Meningitis

Meningitis is an inflammetion of the protective membranes covering the brain and the spinal cord, known colletively as meninges. The inflammation may be caused by several microorganism, including viruses, bacteria, parasites and fungi.

Meningitis usually follows invasion of the bloodstream by organisms that have colonised mucosal surfaces. In the neonatal period, pathogens are acquired mainly, al-

though not exclusively, during birth by contact and aspiration of intestinal and genital tract secretions from the mother. In infants and children, meningitis usually develops after encapsulated bacteria, that have colonised the nasopharynx, are disseminated in the blood. Viral infections of the upper respiratory tract commonly precede invasion of the bloodstream. Subsequently, organisms penetrate vulnerable sites of the blood-brain barrier (eg, choroid plexus and cerebral capillaries) and reach the subarachnoid space (Leib, 1999).

The intense inflammation within the subarachnoid space noted in lumbar cerebrospinal fluid (CSF), and the resulting neurological damage, are not the direct result of the pathogenic bacteria but rather of activation of the host's inflammatory pathways by the microorganisms or their products (Sáez-Llorens *et al.*, 1990). When the pathogens have entered the central nervous system, they replicate rapidly and liberate active cell wall or membrane associated components—ie, lipoteichoic acid and peptidoglycan fragments of gram-positive organisms, and lipopolysaccharide of gram-negative bacteria. Antibiotics that act on cell walls cause rapid lysis of bacteria, which can initially cause enhanced release of these active bacterial products into the CSF (Mertsola *et al.*, 1989; Arditi *et al.*, 1989). These potent inflammatory substances can stimulate astrocytes and microglia, cerebral capillary endothelia, or both, to produce cytokines such as tumour necrosis factor, interleukin-1, and other inflammatory mediators and macrophage-derived proteins.

The cytokines activate adhesion promoting receptors on cerebral vascular endothelial cells and leucocytes, attracting neutrophils to these sites. Subsequently, leucocytes penetrate the intercellular junctions of the capillary endothelium and release proteolytic products and toxic oxygen radicals. These events result in injury to the vascular endothelium and alteration of blood-brain barrier permeability. Dependent on the potency and duration of the inflammatory stimuli, the alterations in permeability allow penetration of serum proteins of low molecular weight into the CSF, and lead to vasogenic oedema. Additionally, large numbers of leucocytes enter the subarachnoid space and release toxic substances that contribute to the production of cytotoxic oedema. As a result of the high protein and cell content, the increased viscosity of the CSF contributes to generation of interstitial oedema.

The clinical picture of acute bacterial meningitis mainly depends on the patient's age. The classic manifestations noted in children and adults are rarely present in infants. Classic meningitis of children and adults usually begins with fever, chills, vomiting, photophobia, and severe headache. Occasionally, the first sign of illness is a convulsion that

can recur during progression of the disease. Irritability, delirium, drowsiness, lethargy, and coma can also develop. As the CSF inflammatory response intensifies in bacterial meningitis, the most consistent physical finding, in children and adults, is the presence of nuchal rigidity associated with Brudzinski's and Kernig's signs.

These signs and symptoms are common to all types of meningitis (Kaplan, 1999). Other manifestations, however, are associated with specific infections.

Meningitis caused by the bacterium *N. meningitidis*, known as "meningococcal meningitis", can be differentiated from meningitis with other causes by a rapidly spreading petechial rash which may precede other symptoms (Theilen *et al.*, 2008). The rash consists of numerous small, irregular purple or red spots ("petechiae") on the trunk, lower extremities, mucous membranes, conjuctiva, and (occasionally) the palms of the hands or soles of the feet. The rash is typically non-blanching: the redness does not disappear when pressed with a finger or a glass tumbler. Although this rash is not necessarily present in meningococcal meningitis, it is relatively specific for the disease; it does, however, occasionally occur in meningitis due to other bacteria.

Although the overall clinical pattern of meningococcal disease is similar in all epidemiological situations, the number of patients presenting specific clinical features can vary from outbreak to outbreak for reasons that are not well understood. Fulminant septicaemia is recorded less frequently during African epidemics than it is for patients in industrialised countries.

In endemic and epidemic disease outbreaks in industrialised countries, haemorrhagical skin lesions are present in 28–77% of patients with invasive meningococcal disease on admission. In adults, a severe headache is the most common symptom of meningitis occurring in almost 90% of cases of bacterial meningitis, followed by nuchal rigidity.

A definitive diagnosis of meningitis is dependent on examination and culture of CSF. Whenever the physician suspects meningitis, a lumbar puncture should be undertaken. Early diagnosis followed by appropriate medical management can have a favourable effect on outcome. In neonates, the procedure should be considered when sepsis is suspected, because meningitis accompanies sepsis in 20–25% of cases. In infants, fever and convulsions may be the only initial signs of meningitis.

Examination of the CSF of a patient with acute bacterial meningitis characteristically reveals a cloudy fluid, consisting of an increased white blood cell count and predominance of polymorphonuclear leucocytes, a low glucose concentration in relation to serum value, a raised concentration of protein, and a positive stained smear and culture for the causative microorganism (Portnoy, 1985).

A promising diagnostic device has been developed, in which a broad range of bacterial primers for DNA amplification is used, to rapidly detect conserved regions of the microbial 16S RNA gene in the CSF. Preliminary results have been associated with high sensitivity, specificity, and predictive values to diagnose bacterial meningitis. If these findings are confirmed and techniques are commercially implemented, many of the pretreated, culture-negative cases could be identified (Pollard *et al.*, 2002).

1.2.1 Epidemiology

Meningococcal disease occurs worldwide with incidence rate from very rare to over 1000 cases per 100 000 population every year (Rosenstein *et al.*, 2001) (Fig. 1.3). Serogroup A of *N. meningitidis* causes the highest incidence of disease. Repeated pandemics of serogroup A disease have taken place in Sahelian and sub-Sahelian countries of Africa, known as the African meningitis belt, every 5–10 years since 1905, and to a lesser extent in China and Russia over the past 25 years (Maiden *et al.*, 1998; Wang *et al.*, 1992). Outbreaks of serogroup A disease took place in other industrialised countries until World War II, but for reasons not understood these outbreaks have vanished.

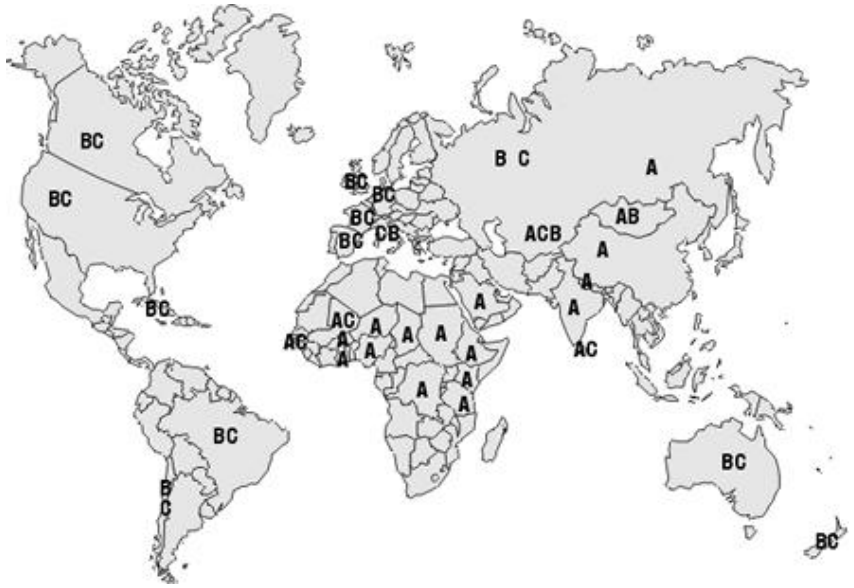

Figure 1.3: worldwide distribution of major meningococcal serogroups.

The rates of meningococcal disease in many parts of Africa are several times higher between epidemics than are the endemic rates in industrialised countries, emphasising the need for routine meningococcal vaccine prevention strategies.

Serogroup B is usually associated with a lower incidence of disease than serogroup A, and is generally absent in sub-Saharan whereas is the primary concern in industrialized countries, where it has been responsible for hyperendemic waves of disease.

Serogroup C has caused major epidemic outbreaks, case clusters, and local outbreaks. Serogroup C (ST-11) has accounted for a higher proportion of cases of invasive meningococcal disease in adolescents and young adults (Stephens *et al.*, 2007; Caugant, 2008). Since the mid 1990s, serogroup Y has caused increased rates of disease in the USA and Israel, while serogroup W135 and X meningococci have been responsible for epidemics in sub-Saharan Africa since 2002 (Gagneux *et al.*, 2002).

Rates of meningococcal disease are highest for young children (related to waning of protective maternal antibody) and increase again for adolescents and young adults (Goldschneider *et al.*, 1969). In endemic situations, serogroup B is most common in infants, serogroup C in adolescents, and serogroups B or Y in older adults.

In countries of the African meningitis belt, the epidemiology of meningococcal disease is unique. Major epidemics happen every few years a pattern seen nowhere else in the world. The reasons for this trend are still not understood, although studies have confirmed that environmental factors such as absolute humidity and dust concentration are important (Connor *et al.*, 2003) Researchers are exploring the possibility of using climatic data to provide early warning of an impending epidemic, but this technique is not yet validated (Thomson *et al.*, 2006). African outbreaks are generally very large; over 150.000 cases were reported during the serogroup A outbreaks in the mid to late 1990s in the African meningitis belt. African epidemics usually start at the beginning of the dry season and end with the coming of the rains, but the reason for this striking seasonality is not known.

1.3 Vaccines

Prevention of disease can effectively be accomplished by vaccination. Immunization was made possible in 1969 when it was discovered that protection from disease correlates with the presence in the serum of antibodies able to induce complement-mediated killing of bacteria, and that purified capsular polysaccharide was able to induce them.

Tetravalent vaccines against serogroups A, C, W-135, and Y have been available since 1984 (Gotschlich *et al.*, 1969; Lepow *et al.*, 1986). Although effective in adults, polysaccharide vaccines are less efficacious in infants and young children and do not induce immunological memory, so that they have not been used for universal vaccination.

Conjugate vaccines against serogroup C have been introduced in the UK, Ireland, and Canada (Ramsay *et al.*, 2001). These are immunogenic in infants and children, induce immunological memory and show overall efficacy of more than 90%.

A quadrivalent group A, C, W-135, and Y polysaccharide-protein conjugate vaccine was introduced in the United States and is recommended for routine use beginning at 11 years of age (Pace *et al.*, 2009). A more immunogenic quadrivalent conjugate vaccine (Perrett *et al.*, 2009) and a *Haemophilus influenzae* type b–meningococcal group C and Y conjugate vaccine, both suitable for infants, are in late-stage clinical development.

Unfortunately, the conjugate approach cannot be easily applied to serogroup B. Therefore, serogroup B of *N. meningitidis*, which causes 50% of meningococcal-disease cases worldwide, is the only serogroup whose infection is not preventable by vaccination.

The B polysaccharide is a polymer of a(2-8)-linked N-acetyl-neuraminic acid (or polisyalic acid), which is also present in glyco-proteins of developing and adult neural tissues of mammals, which are tolerant to it. The poor immune response, together with a high risk of autoimmunity, has been a main obstacle to the development of a capsular-polysaccharide-based vaccine (Finne *et al.*, 1983; Finne *et al.*, 1987). For this reason, research has been focused on the identification of noncapsular antigens. At present the vaccines of this type are composed of outer membrane vesicles (OMVs) prepared by detergent extraction from the bacteria. OMVs derived from clinical isolates have been developed in Cuba (serosubtype P1.19, 15), Norway (serosubtype P1.7, 16), and the United States (serosubtype P1.7-2, 3). Although it has been shown to be efficacious in clinical trials (Bjune *et al.*, 1991; Boslego *et al.*, 1995), the main limitation of OMV is that PorA, the immunodominant antigen, shows sequence and antigenic variability, and consequently, the protection induced is mainly strain specific. As a consequence, the conventional approach to vaccine development has failed to deliver a universal vaccine.

For this reason has been used a new strategy, named reverse vaccinoloy, that starts in silico using the genetic information rather than the patoghen itself. Using reverse vaccinology, regions of genomic DNA were screened by computer analysis while the MenB nucleotide genome sequence was being determined (Tettelin *et al.*, 2000). Six hundred novel genes were predicted to code for surface–exposed or exported proteins. These were cloned and expressed in Escherichia coli as fusions to the glutatione transferase or to a histidine tag. Of these fusion proteins, 350 were successfully expressed, purified and used to immunize mice. The sera obtained were used to confirm the surface exposure of the proteins by ELISA and FACS analysis, and to test for the ability to induce complement-mediated in vitro killing of bacteria, a test that correlates with vaccine efficacy in hu-

mans. Within 18 months, while the nucleotide sequence was still being finalized, 85 novel surface-exposed proteins were discovered and 25 of these were shown to induce bactericidal antibodies. These novel proteins have provided an optimal basis for the development of a novel and effective vaccine against MenB (Pizza *et al.*, 2000).

1.3.1 Factor H binding protein

One of the most promising of the new protein antigens is fHbp, which is a surface-exposed lipoprotein present in all *N. meningitidis* strains. The protein is characterized by a signal peptide with a lipo-box motif of the type -LxxC-, where the cysteine residue is followed by a serine, an amino acid generally associated with outer membrane localization of lipoproteins. The mature protein has a molecular weight of 26,964 Da in MC58. No homologous proteins were found in prokaryotic and eukaryotic sequence databases suggesting that it is specific for Neisseria. The low homology of a small domain with the C-terminal portion of the transferrin-binding protein TfbA of *Actinobacillus pleuropneumoniae*, is likely to be only structural, since the recombinant protein does not bind human transferrin in vitro. The protein is lipidated in Neisseria meningitidis, it is surface-exposed and expressed by all strains and the level of expression varies considerably from strain to strain.

Sequencing of the gene in a number of meningococcal isolates revealed the presence of three variants, which have been named variants 1, 2 and 3. Amino acid identity is 74.1% between variants 1 and 2, 62.8% between variants 1 and 3, and 84.7% between variants 2 and 3. Sequences within each variant group are generally highly conserved (Masignani *et al.*, 2003).

Fletcher and co-workers assigned fHbp variants into two subfamilies, designated A and B (Fletcher *et al.*, 2004). Subfamily B corresponded to variant group 1 of Masignani and co- workers, and subfamily A included strains with fHbp in the variant 2 or 3 groups.

Recently, based on phylogenetic analysis of 70 unique fHbp amino acid sequences, the molecular architecture of fHbp was shown to be modular, consisting of five variable segments that flanked blocks of two to five invariant residues. Based on the positions of the blocks of invariant amino acids, the overall architecture could be divided into an amino-terminal repetitive element and five modular variable segments, which have been designated V_A–V_E (Fig. 1.4. Segments V_B and V_D contained 15 and 19 amino acids, respectively, while segments V_A, V_C and V_E contained 69, 62 and 71 amino acids, respectively. Within each of the modular variable segments, there were both invariant and variable amino acids (Beernink, 2009).

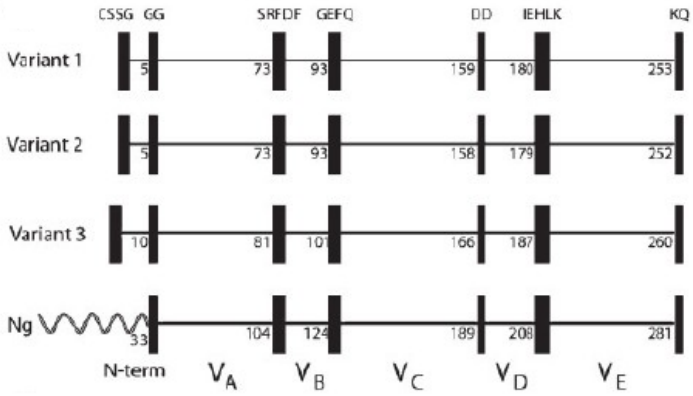

Figure 1.4: schematic representation of fHbp, showing positions of blocks of invariant residues (shown as black vertical rectangles). The top three panels show representative architectures of three *N. meningitidis* fHbp variants in groups 1, 2 and 3 (peptide ID nos 1, 16 and 28, respectively). The amino acid positions of the last residue in each variable segment are shown. With the exception of a longer, unrelated, amino-terminal element, two *N. gonorrhoeae* orthologues (Ng, GenBank accession nos AE004969 and CP001050) had the identical six invariant blocks of residues that flanked segments V_A to V_E (from Beernink, 2009).

An important function of fHbp is to bind the human complement protein fH. Binding of fH to the bacterial surface accelerates decay of C3/C5 convertase, which decreases alternative pathway activation and contributes to the ability of the organism to avoid complement-mediated killing by nonimmune human serum or blood (Madico *et al.*, 2006; Schneider *et al.*, 2006).

In the presence of anti-meningococcal antibodies, binding of fH to the bacteria also decreases complement-mediated serum bactericidal antibody titers by enhancing factor I–mediated degradation of C3b, which decreases classical complement pathway activation, and by decreasing alternative complement pathway amplification. Binding of fH to *N. meningitidis* was reported to be specific for human fH (Granoff *et al.*, 2009). This human specificity explain why *N. meningitidis* is strictly a human pathogen.

In a study of Madico *et al.* (2006), the authors observed that the amount of factor H-binding to bacterial cells correlates with the amount of fHbp expressed on the cell surface. Factor H binds whole bacteria and recombinant fHbp representing each of the three variants, despite their sequence diversity. Antibodies to fHbp can induce bacterial killing through a dual mechanism: directly, by activation of the classical complement pathway, and indirectly by inhibition of binding of factor H to the bacterial surface.

The crystal structures of fHbp in the variant group 1 and a crystal structure of a portion of fH in complex with fHbp have been reported (Fig. 1.5; Fig. 1.6).

Figure 1.5: solution structure of menigococcal factor H binding protein. The image was derived from coordinates of RCSB PDB database accession numbers 2KC0 (Cantini *et al.*, 2006).

Currently fHbps are part of 2 promising meningococcal vaccines being investigated in humans. One vaccine, referred to as LP2086, contains 2 recombinant lipidated proteins from the fHbp subfamilies A and B. The second vaccine contains fHbp in the variant 1 group (subfamily B) as part of a multicomponent vaccine. Two of the components are fusion proteins (GNA 2091 fused with fHbp and GNA 2132 fused with GNA 1030), and the third component is recombinant NadA (Fig. 1.7). Of these 5 antigens, fHbp, GNA 2132, and NadA were reported to be responsible for most of the serum bactericidal antibodies responses in mice (Giuliani *et al.*, 2006).

1.3.2 Epitope mapping of fHbp

Studies have confirmed the importance of fHbp in inducing bactericidal antibodies against *N. meningitidis* and have shown that protection in the infant rat model using

Figure 1.6: structure of a complex between *N. meningitidis* factor H binding protein and CCPS 6-7 of human complement. The image was derived from coordinates of RCSB PDB database accession numbers 2W80 (Schneider *et al.*, 2009).

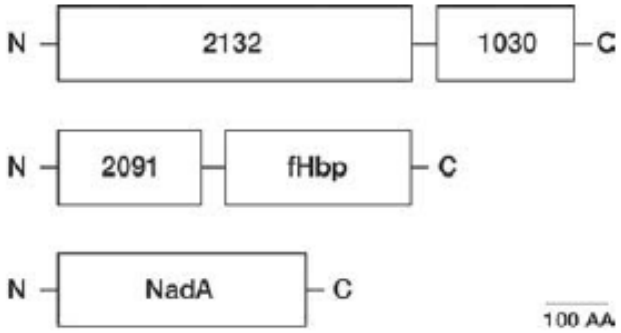

Figure 1.7: schematic showing 3 recombinant proteins (5 antigens) contained in a multicomponent meningococcal vaccine. The scale bar represents 100 amino acids (AAs), (from Granoff, 2010).

monoclonal antibodies (mAbs) against fHbp can also be achieved in the absence of measurable bactericidal activity (Fletcher *et al.*, 2004; Welsch *et al.*, 2004).

The gene encoding fHbp is present in all meningococcal strains, however fHbp exists in at least three variant groups, based on amino acid sequence identity and antibody cross-reactivity. In general, antiserum prepared against fHbp in the variant 1 (v.1) group is bactericidal against other *N. meningitidis* strains expressing fHbp in the v.1 group but not against strains expressing fHbp in the v.2 or v.3 group and vice versa, although a degree of cross-reactivity has been observed (Masignani *et al.*, 2003; Beernink *et al.*, 2006; Beernink *et al.*, 2008).

A multicomponent vaccine containing fHbp should be made with a single rfHbp capable of eliciting serum bactericidal antibodies against strains expressing fHbps from the different major antigenic variant groups. For this reason the knowledge of the locations of region containing bactericidal epitopes would allow to design a vaccine consisting of a single recombinant chimeric protein eliciting serum bactericidal antibody responses against genetically diverse strains expressing fHbp from different variant groups. Antisera raised against each variant were used to map the immunogenic regions, through epitope mapping on overlapping dodecapeptides. On the basis of the different peptide recognition pattern for each variant, it was possible to define three regions, named A (8-101), B (101-164), and C (164-255) which were then expressed in *Escherichia coli* separately or in combination, purified and used to immunize mice. The BC fragment, corresponding to residues 101–255 of the MC58 protein (variant 1) retained all the bactericidal activity of the full-length protein, suggesting that most of the bactericidal epitopes were included in this region (Giuliani *et al.*, 2006).

By immunization of mice with the variant 1 have identified a number of monoclonal antibodies, one of which, named mAb 502, has high bactericidal activity. By FACS and Western blot analysis the arginine in position 204 was identified as an essential residue for antibody recognition. The analysis of immunological data, NMR mapping, and molecular docking carried out on fHbp protein in the presence of mAb502, unequivocally have demonstrated that the fHbp contact area with the antibody is formed by three independent loops plus the N-terminal α-helix of the C-terminal domain fHbp, evidencing the conformational nature of the mAb502 epitope and confirming the key role of Arg204, as well the minor role of residues Glu146–Arg149 (Scarselli *et al.*, 2009).

Other monoclonal antibodies have been pruduced by Welsch *et al.*, 2004, immunizing mice with the variant 1 of fHbp (strain MC58) and tested their immunogenicity against nine strains of *N. meningitidis*. These mAbs, named JAR 1 (IgG2), JAR 3 (IgG3), JAR 4 (IgG2a) and JAR 5 (IgG2b), recognized epitopes which included the residues 121 and 122 of B domain.

Instead, no information was available on the epitopes expressed by fHbp in the variant 2 (v.2) or variant 3 (v.3) group that are recognized by bactericidal antibodies.

In a study of Beernink *et al.* (2008), has been prepared and characterized a panel of anti-fHbp monoclonal antibodies (mAbs) from mice immunized with v.2 or v.3 recombinant fHbp (rfHbp) proteins. The mAbs prepared against the v.2 protein were designated JAR 10, 11, and 13 and were IgG1, IgG2a, and IgG2a, respectively. Four newly prepared mAbs against the v.3 protein were designated JAR 32, 33, 35, and 36. Two of these, JAR 32 and 33, were IgG2a, and the other two, JAR 35 and 36, were IgG2b. As determined by ELISA, all seven mAbs showed concentration-dependent binding to the respective recombinant proteins that were used for the immunization of the mice. In addition, JAR 13 cross-reacted with the v.3 protein, and JAR 36 cross-reacted with the v.2 protein. None of the mAbs individually was bactericidal with human complement. However, each of the mAbs was bactericidal when combined with a second anti-fHbp mAb. Likely because binding by an individual mAb did not result in sufficient immune complex to engage C1q and activate classical complement pathway bactericidal activity. As previously reported by Madico *et al.*, 2006 the anti-fHbp MAbs JAR 3 and 5, but not JAR 4, inhibited the binding of human fH to the surface of live bacterial cells of *N. meningitidis*. Three of the mAbs isolated from mice immunized with fHbp v.2 or v.3 (JAR 13, 32, and 35), gave ∼75% inhibition of the binding of fH to rfHbp v.2 or v.3, while four other mAbs gave partial (JAR 11 and 36) or no inhibition (JAR 10 and 33).

The authors used the alignments of fHbp sequences from *N. meningitidis* strains differing in their reactivity with the respective mAbs to predict the potential amino acid residues involved in the mAb epitopes. The epitope for mAb JAR 10, which was raised against a v.2 fHbp, was predicted from sequence alignments to involve both a Lysine (K) at position 180 and a Glutamate (E) at 192. Indeed, the respective residues in the JAR 10-negative strains were R180 or D192. The reactivity of mAb JAR 33, which was raised against a v.3 fHbp, also was associated with residues at positions 180 and 192, which corresponded to those of JAR 10 reactivity with the v.2 protein. The reactivity of JAR 32 and JAR 35 was associated with the presence of a Lysine residue at position 174 (K174). The immunoblotting of wild-type and KO mutant clones indicated that both JAR 32 and JAR 35 reactivity was abolished in a mutant of M1239 fHbp containing the K174A substitution.

The mAb JAR 11 recognized an epitope with an Alanin in the same position (A174). The JAR 13 epitope was associated with the presence of a Serine residue at position 216 (S216). As previously reported, the epitope recognized by the mAbs JAR 3 and JAR 5

involved the residues G121 and K122, moreover the epitopes are overlapping, since each of these antibodies inhibited the bindig of the other to fHbp. All of the epitopes of MAbs from mice immunized with the v.2 or v.3 proteins were affected by residues spanning amino acids 174 to 216, which were located within an eight-stranded beta-barrel of the C domain (Cantini *et al.*, 2006). In contrast, the expression of the epitopes for JAR 3 and JAR 5, which bound specifically with fHbp v.1, were affected by amino acid substitutions of residues G121 or K122, which were located in the B domain. In figure 1.8 are shown all the residues affecting the epitopes mapped.

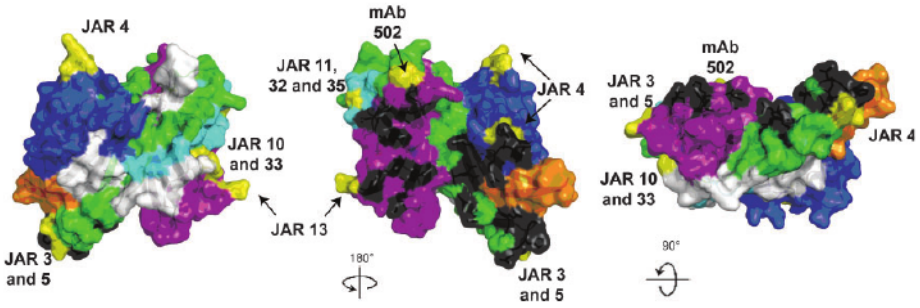

Figure 1.8: space-filling structural models of fHbp based on the coordinates of the protein in a complex with a fragment of human fH (Schneider *et al.*, 2009). The five variable segments VA to VE are depicted in different colours (VA, blue; VB, orange; VC, green; VD, light blue; VE, violet) and the invariant blocks of residues separating each of the variable segments are shown in white. The fH contact residues are depicted in black, and the residues affecting the epitopes of anti-fHbp mAbs are shown in yellow (from Beernink, 2009).

1.3.3 JAR 4

Using multiple allignment and site-specific muatgenesis, it was not possible to map the epitope recognized by the anti-fHbp monoclonal antibodies JAR 4 and JAR 36. JAR 4 is an IgG2a mAb that was isolated from a mouse immunized with recombinant fHbp in the variant 1 group (Welsch *et al.*, 2004). The mAb was not bactericidal with human complement when tested alone, even against strains with relatively high fHbp expression. However, the mAb activated C3b deposition on strains expressing fHbp in the variant 1 or 2 groups and elicited cooperative, complement-mediated bactericidal activity with other non-bactericidal mAbs specific for fHbp in the variant 1 or 2 groups (Beernink, 2008; Welsch *et al.*, 2008).

In a study of Beernink *et al.* (2009), by using filamentous bacteriophage libraries displaying random peptides (see 2) that were recognized by JAR 4, the authors identified a consensus tripeptide, DHK, that matched residues 25-27 in the N-terminal domain of fHbp. Since DHK was present in both JAR 4-reactive and non-reactive fHbps, the tripeptide alone was necessary but not sufficient for reactivity. The results indicated that the JAR 4 epitope was discontinuous and involved DHK residues beginning at position 25; YGN residues beginning at position 57; and a KDN tripeptide that was present in variant 3 proteins beginning at position 67 that negatively affected expression of the epitope (Fig. 1.9). Thus, the region of fHbp encompassing residues 25 to 59 in the N-terminal domain is important for eliciting antibodies that can cooperate with other anti-fHbp antibodies for cross-reactive bactericidal activity against strains expressing fHbp from different antigenic variant groups.

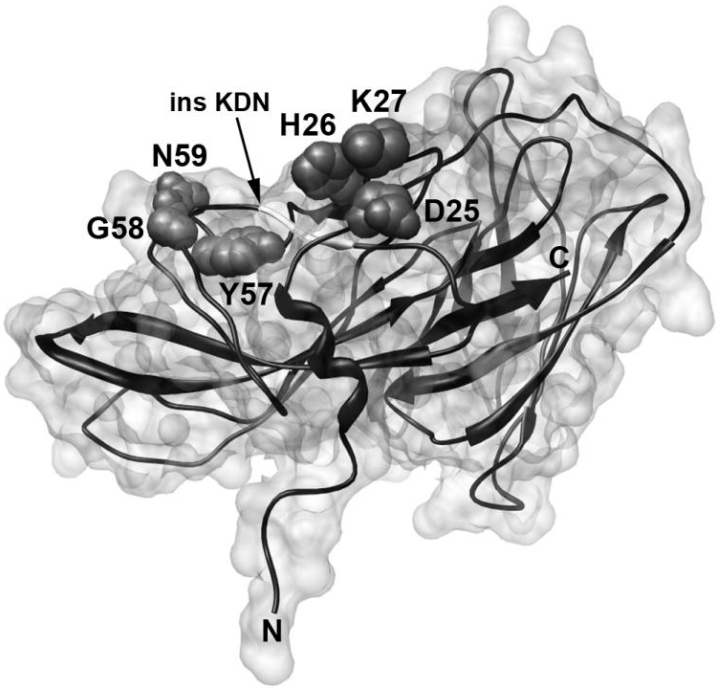

Figure 1.9: structure of fHbp variant 1, where the relative positions of the DHK and YGN tripeptides that affect binding of JAR 4 are shown. The location of amino acids 67-69, which in the variant 3 protein contains the KDN tripeptide that negatively affects JAR 4 binding and is not present in variant 1 or 2 proteins, is shown as a white insert in the ribbon next to the arrow (from Beernink *et al.*, 2009).

Chapter 2

Phage Display technology

2.1 Introduction

Phage display is a method for the study of protein–protein, protein–peptide, and protein–DNA interactions that uses bacteriophage to connect proteins with the genetic information that encodes them. The display of peptides and proteins on the surface of bacteriophage represents a powerful methodology for carrying out molecular evolution in the laboratory. The ability to construct libraries of enormous molecular diversity and to select for molecules with predetermined properties has made this technology applicable to a wide range of problems.

The origins of phage display date to the mid–1980s when George Smith first expressed a foreign segment of a protein on the surface of bacteriophage M13 virus particles. As a test case he fused a portion of the gene encoding the EcoRI endo–nuclease to the minor capsid protein pIII (Smith, 1985). Using a polyclonal antibody specific for the endonuclease, Smith demonstrated that phage containing the EcoRI–gIII fusion could be enriched more than 1000–fold from a mixture containing wild-type (nonbinding) phage by using affinity purification through an immobilized polyclonal antibody. From these first experiment emerged that, using recombinant DNA technology, it should be possible to build large libraries wherein each phage displays a unique random peptide. Moreover, the methodology provides a direct physical link between phenotype and genotype.

The phage display technology is based on the insertion of foreign nuclotide sequences into genes encoding coat proteins of bacteriophage, resulting in a heterogeneous mixture of phages, each carryng a distinct peptide sequence on the fusion coat proteins.

The bacteriophage M13, f1, fd are made up of a proteic envelope, constituited by several copies of five different proteins (pIII, pVI, pVII, pVIII and pIX) and a single–

strand DNA molucule carrying the phage genetic information (Fig.2.1). When exogenous DNA is cloned in frame at the 5'–end of the gene encoding for one of the two capsid proteins pIII or pVIII, the corresponding fusion product is displayed on the surface of the virion. These bacteriophage infect *E. coli* and grow without the lysis of the host cell, giving very high titers of ligand displaying phage (up to 10^{12} particles/ml of culture supernatant).

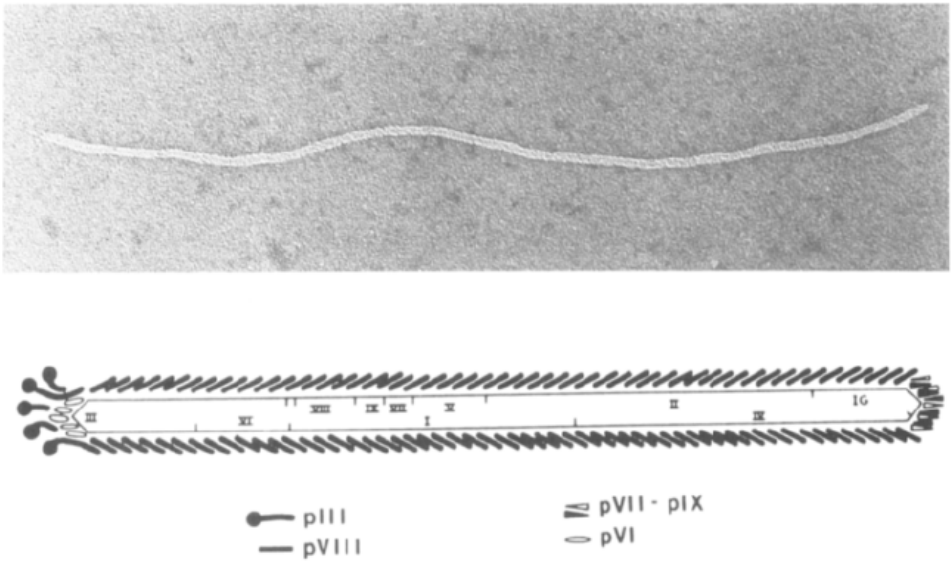

Figure 2.1: the Ff bacteriophage particle. Top is an electron micrograph of a negatively stained particle with the pVII-plX end at the right. Bottom is a schematic representation of the phage particle showing the location of the capsid proteins and the orientation of the DNA (from Webster, 1985).

One of the most impressive aspects of phage display is the variety of uses for the technology. The approach has been applied, for example, to isolate new ligands, as antigenic epitopes, inhibitors, antagonist, agonist, or substrate that bind to particular amino acid sequences. Moreover, large collection of antibody fragments have been displayed on phage particles, and successfully screened with different antigens. Libraries of short peptides of random sequence have been displayed on phage and screened with antibodies or other molucules, leading to the identification of new ligands (Rodi, 1999; Zwick *et al.*, 1998; Deroo, 2001).

2.2 Biology of filamentous bacteriophage

A number of filamentous phage have been identified which are able to infect a variety of gram negative bacteria. They have a single–stranded, covalently closed DNA genome which is encased in a long cylinder approximately 7 nm wide by 900 to 2000 nm in length. The best characterized, because extensively studied and utilized in molecular biology, are M 13, fl, and fd phage. They infect *Escherichia coli* containing the F conjugative plasmid (either F^+ or Hfr). The genomes of these three bacteriophage have been completely sequenced and are 98% homologous (Van Wezenbeek *et al.*, 1980; Beck, 1981; Hill, 1982). As a result of their similarity and dependence on the F plasmid for infection, M13, fl, and fd are collectively referred to as the Ff phage.

2.2.1 Genome and coat proteins

The genome of the Ff phage is a single–stranded covalently closed DNA molecule, which encodes 11 genes. Two of these genes, X and XI, overlap and are in–frame with the larger genes II and I (Model, 1988; Rapoza, 1995). The genes are grouped on the DNA according to their functions in the life cycle of the bacteriophage (Fig.2.2). One group encodes proteins required for DNA replication, the second group encodes the proteins which make up the capsid and the third group encodes three proteins involved in the membrane associated assembly of the phage. There also is the "Intergenic Region", a short stretch of DNA which encodes no proteins. It contains the sites of origin for the synthesis of the (+) strand (phage DNA) or (-) strand as well as a hairpin region which is the site of initiation for the assembly of the phage particles (packaging signal).

Genes II, V, and X encode cytoplasmic proteins (pII, pV and pX) which are involved in the replication of the phage DNA. The infecting single–stranded genome is converted to a supercoiled double–strand or RF DNA by bacterial enzymes, pII binds and introduces a specific cleavage on the (+) strand of the RF DNA allowing the host enzymes to use the resulting 3' end as a primer for synthesis of a new (+) strand. This rolling circle replication continues for one round and the resulting (+) strand is circularized by pII. The new (+) strand either is converted to another replicative form DNA by host enzymes or is bound by the phage pV subsequent to packaging into phage particles. Dimers of pV bind single–strand DNA in a highly cooperative manner. It is this binding that prevents the conversion of the newly synthesized single–stranded DNA to RF and thus sequesters the (+) strand DNA for assembly into the phage particle. The result of this interaction is a pV–DNA structure approximately 880 nm long and 8 nm in diameter

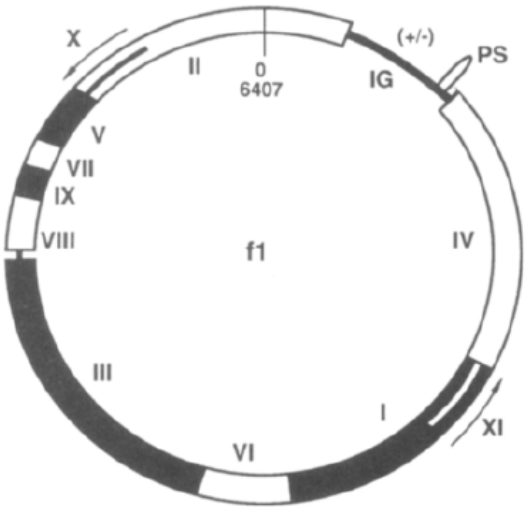

Figure 2.2: the genome of the fl bacteriophage. The single–stranded DNA contains 11 genes. It has 6407 nucleotides which are numbered from the unique *HindII* site located in gene II (represented by 0). IG, Intergenic Region; PS, the packaging signal; (+/-), the position of the origin of replication of the viral and complementary DNA strands; arrows indicate the location of the overlapping genes X and XI. (Model, 1988).

containing one (+) strand and approximately 800 pV dimers (Gray, 1989; Skinner *et al.*, 1994). The structure appears to be wound in a left–handed helix with the pV dimers binding two strands of single–stranded DNA running in opposite directions along the helix. The packaging signal (PS) is at one end of this rod–like structure, allowing it to be available for the initiation of phage assembly (Bauer, 1988). pX is essential for the proper replication of the phage DNA and appears to function, in part, as an inhibitor of pII function (Fulford, 1984).

The products of the genes, III, VI, VII, VIII, and IX, constitute the capsid proteins of the phage particle. All these proteins reside in the cytoplasmic membrane until they are assembled into a phage particle.

pVIII is the most abundant capsid protein, as approximately 2700 molecules are needed to form the protein cylinder around the DNA, for these reason is called the *major coat protein*. The mature protein consist of 50 amino acid residues and adopts an alpha helical conformation with the C–terminal 30 residues traversing the membrane and extending into the cytoplasm in an orientation perpendicular to the surface of the membrane (McDonnell *et al.*, 1983). Its structure has been determinated by Marvin *et al.* (2006) (Fig. 2.3).

Figure 2.3: molecular structure of fd filamentous bacteriophage refined with respect to X–ray fibre diffraction. The image was derived from coordinates of RCSB PDB database accession numbers 2C0W (Marvin *et al.*, 2006) using PyMol (DeLano, 2006)

The remaining four *minor capsid proteins*, which make up the ends of the phage particle, are also located in the membrane prior to assembly into mature bacteriophage (Endemann, 1995).

The proteins pVII and pIX are small hydrophobic proteins of only 32 (pVII) and 33 (pIX) amino acids. The structure of these two proteins has not been solved and their arrangement in the virion has not been determined. Genetic analysis showed that the residues near the C–terminus are involved in interactions with the packaging signal, a DNA hairpin that targets phage genome for packaging (Russel, 1989). For both proteins, once an addition to the N-terminus has been made, a signal sequence is required for successful incorporation of these chimeric proteins into the virion and display on the surface of the virion (Gao *et al.*, 1997; Gao *et al.*, 2002).

Proteins pIII and pVI are added to the virion at the end of assembly. They form a distal "cap" of the filament and at the same time release the virion from the cell (Rakonjac *et al.*, 1999; Rakonjac, 1998). These two proteins are required for the structural stability of the virion and also for termination of assembly. Moreover, pIII mediates entry of the phage into the host cell and either pIII and pVI are integral membrane proteins (Boeke, 1982).

pVI is a 112-residue and is the mostly hydrophobic protein. It is integral membrane protein prior to assembly into the virion (Endemann, 1995), predicted to contain three

transmembrane α helices, with the N terminus in the periplasm and the C terminus in the cytoplasm (Krogh *et al.*, 2001). Instead, the protein pIII at 406 amino acids in length, is distinctly larger than the other four virion proteins. pIII is composed of three domains (N1, N2 and C) separated by long glycine–rich linkers. The N1 and N2 domains of pIII interact with the host receptors and their structure has been determined using X–ray crystallography and NMR (Holliger *et al.*, 1999; Lubkowski *et al.*, 1998) (Fig. 2.4).

Figure 2.4: cristal structure of N–terminal domain of bacteriophage minor coat protein g3p. The image was derived from coordinates of RCSB PDB database accession numbers 1g3p (Lubkowski *et al.*, 1998) using PyMol (DeLano, 2006)

The three-dimensional structure of the C domain, which is required for termination of phage assembly, formation of a detergent-resistant virion cap and for late steps in phage infection, is yet to be determined.

2.2.2 Life cicle

The primary receptors for filamentous phage are pili, long filamentous structures on the surface of bacterial cells. Infection of *E. coli* by the Ff bacteriophage is at least a two-step process (Model, 1988). The first involves the interaction of the pIII end of the phage particle with the tip of the F conjugative pilus. Retraction of the pilus, presumably by depolymerization of the pilin subunits into the inner membrane, brings the tip of the phage to the membrane surface. The second step involves the integration of the pVIII *major capsid protein* and perhaps the other capsid proteins into the inner membrane

together with the translocation of the DNA into the cytoplasm.

After entry into the cytoplasm, the Ff ssDNA genome positive (+) strand serves as a template to synthesize the negative (-) strand. This step is independent of phage proteins, and is initiated by host RNA polymerase. The prokaryotic promoters are recognized by bacterial RNA polymerase and viral genes are transcribed in one polycistronic RNA strand and simultaneously translated. The newly synthesized structural proteins reach the membrane of the host, where waiting to be incorporated into the capsid of phage particles forming. The non-structural proteins, indead, take part in the replication of genetic material and the process of packing. Through the intervention of the phage protein pII, the viral genome is duplicated many times to form a pool of double–stranded molecules, called replicative forms (RF). From the replicative forms, through the mechanism of replication by rolling circle, are made structures of single–stranded phage DNA molecule. This process involves the formation of single–stranded break, which allows the DNA polymerase of *E. coli* uses the filament (-) as a template and, as a trigger, the end helix (+). In this way multimers are synthesized, susequently they are cut from phage protein to form monomers. Each monomer then closes to form a circular shape. The circular molecules of single–stranded newly–synthesized genetic material will be included within the virions. To avoid that the sigle–stranded DNA is converted in a doudle–strended, the pV phage protein, which is a single–stranded DNA binding protein, covers the molecule completely, thus blocking *E. coli*'s repair enzymes from accessing to nucleic acid.

The ssDNA–pV complex, called prophages, migrate to the inner membrane host, where they are released through a mechanism regulated by the intergenic region. The structural proteins, that lie in the membrane, are assembled around the DNA, covering it, simultaneously with its release from the bacterial cell, leading the formation of new phage particles: the strand of nucleic acid is covered first by pVII and pIX, successively by pVIII, and at the end by pIII and pVI.

When a newly formed phage crosses the membrane, the protein V, which covers the DNA, is replaced by the *major coat protein* (pVIII). pV thus detaches and returns to cytoplasm, where it is available to bind new molecules of the phage genome.

All the above biological processes act without the lysis or death of the host cell. The major phenotypic affect of phage infection and production is a slowing down of bacterial growth rate, which causes the formation of plaques (consisting of slowly doubling phage–infected cells) on a bacterial lawn of noninfected cells.

2.3 Vectors for Phage display

A range of vectors are available for exogenous expression on the surface of bacteriophage M13 virus particles. The display sites most commonly used are within genes III or VIII, although there have been reports of successful cloning in all the other genes VI, VII and IX (Hufton *et al.*, 1999, Gao *et al.*, 2002, Løset *et al.*, 2011). In pVIII display, the number of copies of the foreign insert per virion depends on the size of the displayed peptide. Ilìchev *et al.* (1989) first showed that pVIII proteins carryng short amino terminal extensions can assemble into functional viral capside. Later, Felici *et al.* (1991) and Greenwood *et al.* (1991), found that a substantial number of hybrid pVIII carryng peptides longer than six residues can be incorporated into phage only when interspersed in an otherwise wild–type capside. Although this size limit is not absolute (Iannolo *et al.*, 1995), pVIII libraries are more conveniently assembled in pahgemid vectors. Felici *et al.* (1991) and Luzzago (1998) have used plasmid pC89 to costruct a large library of nonapeptides and dodecapeptides inserted near the aminoterminus of pVIII.

Only the C domain of pIII is required for assembly of the virion, hence also this domain alone can be used in display as long as it is preceded by a signal sequence (Barbas III *et al.*, 1991; Griffiths *et al.*, 1993). Given that N1 and N2 domains of pIII are required for infectivity of the particles, if truncated pIII is used for display, a wild-type (full length) pIII must be provided in order to allow easy amplification of phage. As with pVIII, the inserted sequence must be in frame with the upstream signal sequence and downstream mature (or truncated) pIII. The pIII display system has been developed by Smith and collaborators who have built a versatile collection of vectors derived from fd Tet, each containing a different restriction endonuclease recognition site in the sequence encoding the amino terminus of pIII (Parmley, 1988; Scott, 1990). An important property of these vectors is that they confer resistence to tetracycline on the infected host and can thus be propagated like a plasmid, indipendently of phage function. Since peptides of 6-20 amino acids do not normally abolish pIII function and phage infectivity, pIII phagemide display vectors have been exploited mostly for the purpose of presenting relatively large peptide (Bass *et al.*, 1990).

2.4 Fusion strategy

As mentioned, pIII and pVIII are the most suitable phage proteins for expression of foreign peptide sequences and the insertion takes place at or near the amino-terminus of the protein molecule. The main types of phage-derived vectors can be grouped into

two classes. The first type of vectors is used to obtain recombinant phage particles where all copies of the capside protein are modified. This mechanism, named *one–gene system* (Felici *et al.*, 1995), has been described mainly for pIII, whose biological function does not seem to be significantly affected by N-terminal fusion. In contrast, the insertion of peptides in all the copies of pVIII interferes with the assembly of phage particles. The presence of a BamHI restriction endonuclease site near the middle of the protein sequence, led Smith to show that pIII could be used to display peptides on the surface of filamentous bacteriophage. Parmley and Smith 1988 described phage vectors where foreign DNA fragments can be inserted into the region just downstream the signal peptide of gene pIII in phage derivative of fd-tet, which carry the gene for resistence to tetracycline and can thus be propagated like a plasmid (Zcher III AN, 1980).

The second type of vectors can be utilized to produce chimerical virions bearing either wild–type and recombinant versions of the capside protein, this strategy is called *two–gene system* (Felici *et al.*, 1995). The concomitant expression of recombinant and wild–type structural proteins pIII and pVIII is possible by costructing a tandem repeat of the corresponding gene in the phage genome, where one of the two copies is modified, or using a phagemid system. In this last method recombinat genes III or VIII are present in expression plasmids containing the origin of replication of the phage named phagemids or phsmids (Dente *et al.*, 1983). Superinfection of bacteria containing such plasmids results in the release of hybrid phage in the supernatant, with both recombinat and wild–type coat proteins present on the phage coat. Using this *two–gene system* the density of exogenous peptides on phage surface is reduced, allowing the cloning of molecules of different sizes.

2.5 Phage and Phagemid vectors

The vectors developed to display peptide can be divided into two groups. To the first one belong M13 (fd) derivatives that have been engineered to introduce suitable unique restriction endonuclease recognition sites in the genetic loci that code for the protein regions that dispaly foreign peptides (N-terminus of pIII or pVIII).

The second class of vectors includes phagemids that contain the engineered version (with unique restriction endonuclease recognition sites) of the phage genes encoding either pIII or pVIII.

2.5.1 Phage vectors

Vectors belonging to this group allow the construction of hybrid phage where each copy of the relevant capsid protein display the inserted peptide. Therefore, pIII phage vectors will display approximately three to five copies of the foreign peptide, while, in the pVIII phage vectors, all the surface of the filament will be saturated by 2700 copies (Cesareni *et al.*, 1995).

2.5.2 Phagemid vectors

The main disadvantage of phage vectors is the limitation of insert size. For this reason phagemids have been developed, plasmide vectors that carry the replication origin of filamentous bacteriophage (Dente *et al.*, 1983; Cesareni, 1987; Felici *et al.*, 1991). They normally replicate under control of the plasmid replication. However, when the plasmid containing bacteria are superinfected by a wild–type bacteriophage, the phage replication origin is activated by the product of gene II. Single stranded phagemid chromosome are then produced and incapsidated into phage particles.

2.6 Peptide Libraries

One important application of phage display has been to construct combinatorial peptide libraries. A peptide library is made up of a collection of phages, each displaying a different peptide fused to one of the phage coat proteins. Synthetic oligonucleotides, fixed in length but with unspecified codons, can be cloned into genes III or VIII of M13 by cassette mutagenesis, where they are expressed as a plurality of peptides: capsid fusion proteins. The libraries, often referred to as random phage-displayed peptide libraries, can then be tested for binding to target molecules of interest. This is most often done using a form of affinity selection known as "biopanning" (Parmley, 1988). For storage purpose libraries originally conatining 10^7–10^8 indipendent clones are normally amplified by growing them for a limited number of generations. Thus, peptide libraries consist of a phage suspension (10^{11}–10^{14} phage/ml) containing several copies of each original clone. The first large peptide libraries of random peptides fused to pIII was reported in 1990 (Scott, 1990; Devlin *et al.*, 1990; Cwirla *et al.*, 1990), while the first library of random peptides displayed on pVIII was described the year after by Felici *et al.*, 1991.

The displayed peptides have a free amino terminus thus allowing the peptide considerable flexibility much like peptides free in solution. Because these peptides are relatively

short in length it is unlikely that they fold into stable secondary structures. In order to lower the entropy of such peptides for the sake of enhancing their affinity for binding to a target molecule, several constrained peptide libraries have been built. These include cyclization of the random peptide sequences by flanking cysteines residues which form disulfide bonds (Luzzago *et al.*, 1993).

2.6.1 Aplications

Since phage dispaly technology was introduced by George Smith (1985), it has been widely used for generating and screening peptide libraries, in many different ligand/ligate systems. A few of the many applications are listed and discussed below.

Epitope mapping –One of the main application of phage peptide libraries is the determination of epitopes. A B or T epitope, also known as *antigenic determinant*, is the part of an antigen that is recognized by the immune system, while in the humoral resonse the part of an antibody that recognizes the epitope is called paratope. Antibodies recognize their cognate antigen by establishing energetically favourable interactions with its amino acids. In some cases, the recognition site is essentially represented by a continuous segment of the antigen sequence, but much more often the epitope is "conformational", i.e. the antibody recognizes the location and type of exposed antigen side chains that are not necessarily contiguous in the antigen's sequence, but brought together by its threedimensional structure. Identifying the location of the epitope on the protein, i.e. mapping it, is of paramount importance because it is instrumental for understanding of the molecular and functional details of the immune response, for identifying structural-functional relationships of antibody activity, for the development of diagnostic or biotechnological tools and of recombinant vaccines.

Since peptide libraries became available they were used by many authors with the purpose to map epitopes. The first demostration of the validity of random peptide libraries in mapping an epitope has been demostrated by Felici *et al.*, 1991. They screened a pVIII based nanopeptide library with a mAb raised against the peptide VQGEESNDK (residues 163–171 of human Interleukin 1–beta protein). This mAb is able to recognize both the synthetic peptide and the entire protein. After two round of selection, several indipendent phage were isolated for their ability to bind the mAb. All these clones displayed peptides with a consensus sequence SND/E, which is also contained in the nonapeptide used to elicit the antibody, suggesting which peptide sequence was critical for the mAb binding. Stephen, 1992 identified a previously unmapped epitope that was

unmasked by a conformational change induced by a point mutation in the protein p53.

As mentioned above, the majority of antibodies recognize residues that are distant in the primary sequence and become spatially close only after the folding process (conformational epitope).

The first evidence that a linear peptide library could be used to isolate phage mimicking assembled epitopes was provided by Felici *et al.*, 1993. By scrrening of a nonapeptide library displayed on pVIII with a mAb raised against a confomational epitope of *Bordetella pertussis* toxin, they found mimotopes whose binding to the mAb could be competend by the natural antigen, indicating that the selected clones were binding to the antigen binding-site.

Luzzago *et al.* (1993), were the first reporting mapping of a discontinuous epitope by screening a cistein–constrained nonapeptide library in pVIII with the mAb H107 recognizes recombinat human H ferritin whose three–dimensional structure is known. Comparing the peptide sequences of positive phages with that of the H ferritin it has been possible identify two different ferritin regions that are distinct in the primary sequence, but close together in the folded molecule. In this case the epitope maping has been possible by combining the phage sequence informations with the antigen 3D structure.

Phage as immunogens –With the work of De la Cruz *et al.*, 1988, the use of phage as carriers for immunogenic peptides, became an alternative approch to that chemical synthesis. They expressed repeat regions derived from the circumsporozoite protein of the human malaria parasite *Plasmodium falciparum* on phage as pIII N–terminal fusions. Compared to the conventional technique based on chemical synthesis of peptide, the phage as immunogens has the advantage of producing large quantities of antigen at minimal cost and without need for extensive purification of the recombinant protein (Felici *et al.*, 1995). However, as showed by Greenwood *et al.*, 1991, the antigenic determinants of the circumsporozoite protein of the human malaria parasite *Plasmodium falciparum*, were much more immunogenic when expressed in multiple copies as pVIII fusion, than when expressed in pIII, indicating that pVIII is better suited for this application.

Nonantibody molecules –A further application of phage display technology is the screening of phage peptide libraries with nonantibody ligates, aimed at identifying peptide mimics of unknown natural target. Devlin *et al.*, 1990, first isolated peptide ligands for a target protein that is not an antiboby. By screening of a pentadecameric library fused to pIII using the biotin-binding protein streptavidin, they found that all the isolates shared the tripeptide sequence HPQ. From the solution of the crystal structure of a

streptavidin/peptide complex was possible to observe that this tripeptide is important in stabilizing the complex. Phage bearing the consensus sequnces YPY were selected from two different group by screening a hexapeptide and an octapeptide library using the plant lectin concanavalin A (con A) as a ligate (Scott *et al.*, 1992; Oldenburg *et al.*, 1992). The authors found that this tripeptide was strictly selective for con A and that the phage presenting these peptides do not bind closely related pea or lentil lectins.

Chapter 3

Aim of work

Despite approximately half of the cases of meningococcal disease in the United States are caused by capsular group B strains of *N. meningitidis* (MenB) and a even higher frequency is registered in Europe (90%), no broadly effective vaccine is yet available to prevent the disease caused by this pathogen. The conventional approaches to vaccine development against MenB have been used for four decades without significant progress. The main limitation is because the capsular polysaccharide, which was used to develop conventional and conjugate vaccines against all other pathogenic meningococci, in this case could not be used as the MenB capsule is chemically identical to an α2–8 linked polysialic acid present in many human tissues. Therefore, a capsular-polysaccharide-based vaccine against MenB would be poor immunogenic and could give risk of autoimmunity. For this reason, research has been focused toword the discovery of non capsular antigens.

Effective non capsular vaccines are composed of outer membrane vesicles (OMVs) but their main limitation is that PorA, the immunodominant antigen, shows sequence and antigenic variability, and consequently, the protection induced is mainly strain specific.

The genome sequence of a serogroup B strain (MC58) allowed the *in silico* analysis of the entire gene repertoire, through a strategy named "reverse vaccinology", and the discovery of novel surface-exposed antigens able to induce antibodies with bactericidal activity. One of the antigens identified by the genomic approach is the factor H binding protein (fHbp, also known as GNA 1870 or lipoprotein 2086), which is a surface-exposed lipoprotein, present in all *N. meningitidis* strains, that binds human factor H (fH). The presence of fH on the bacterial surface is critical to circumvent host defenses while, in the absence of bound fH, the organism becomes susceptible to bacteriolysis. Based on the sequence variability of the entire protein, fHbp has been divided into 3 variant groups or

2 sub-families and its architecture is modular, consisting of 5 variable segments.

The fHbp is a component of two serogroup B meningococcal vaccines currently in clinical development (Granoff, 2010).

The work of the present thesis is plugged in to a wider project aim identifying the immunogenic regions of fHbp able to elicit antibodies with bactericidal activity.

Previously, a panel of anti-fHbp mAbs has been produced from mice immunized with the 3 variants of fHbp and their epitopes have been mapped using multiple allignment and site-specific muatgenesis. However this method has been not successful to map the epitope recognized by one of the mAbs named JAR 36. This antibody was isolated from a mouse immunized with fHbp of the antigenic variant 3 group, but it cross-reacts with all fHbp sequences in the variant 2 group and elicits complement-mediated cooperative bactericidal activity with JAR 11 and JAR 13 (Beernink *et al.*, 2008).

The present work is aimed at widening, by using the phage-display technology, the knowledge about the residues that are important for the epitopes recognized by anti-fHbp mAbs, particularly mapping the epitope of JAR 36, which remains still unknown.

Peptide display on the bacteriophage surface represents a very effective technology, which is an important tool for the selection and identification of specific ligands. Such approach provides significant advantages when compared to conventional methods for the screening and the discovery of new molecular interactions: very large combinatorial libraries (over 10 million clones) of phage particles, each expressing a different peptide sequence, can be easily constructed, and their composition can rapidly be deduced by sequencing the corresponding region in the viral DNA. Moreover it allow fast identification of specific clones among the heterogeneous mixture of library phage particles. These features have made phage display a largely exploited tool for many different applications, as described in the section 2.6.1.

One of the main applications of phage display techonology is the epitope mapping. Several examples of identification of antigenic determinants utilizing phage peptide libraries have been described. The identification and characterization of epitopes by combinatorial phage display peptide analyses is based on the principle that unique peptides can be affinity purified (with antibodies) from an enormous collection of random peptides. Moreover, once affinity selected, the peptide sequence can be elucidated, as it is physically linked to its DNA sequence. In most cases the peptide sequence exposed by the affinity selected clones reveal a sequence similarity with the original epitope. However often they do not share a common sequence and/or a similarity with the linear sequence of an antigen, but combining the phage sequence informations with antigen structural

data, is sometimes possible circumvent this obstacle.

In the present research a total of five previously built libraries of random peptides fused to the N-terminal region of the major coat protein (pVIII) of filamentous phage will be used. Three of these libraries contain linear peptides composed of random 9-mers, 12-mers and 15-mers, respectively. The remaining two libraries are composed of 9-mers and 12-mers in which the presence of two cysteine residues create a collection of disulfide constrained loops of different sizes.

Affinity selection of already available libraries, by using JAR 36 as target, will allow to selecte peptides with high affinity with the mAb. Selection procedures will be optimized in order to enrich the pool of specific sequences, by using two different solid supports: magnetic beads and Petri plates. The first, coated with protein G, can bind the antibody; by using a magnetic device, antibody-binding phage particles are then separated from the library mixture. Petri plates, which are coated with protein G, tether antibody-specific phage particles complexes, while unbound phage particles are discarded by washing solution.

After a number of selection rounds, enrichment of phage pool reacting with the antibody JAR 36 will be tested by ELISA. Single positive phage clones will be isolated from the reactive enriched pools through immunoscreening and tested by ELISA. Sequence analysis of the inserts of positive clones will allow to identify peptide sequences capable to mimic the epitope of JAR 36 and to determine whether they correspond to regions of the primary sequence of fHbp.

The results of the above analysis will be used to produce mapping hypotheses which will be confirmed by constructing of point mutants in the fHbp gene.

The protein antigen fHbp, component of a new vaccine for prevention of group B meningococcal disease, shows antigenic variability and/or variable expression in different *N. meningitidis* strains. Therefore, it would be desirable to use a single rfHbp capable of eliciting serum bactericidal antibodies against strains expressing fHbps from every different major antigenic variant group.

The identification of residues involved in the binding of the mAb JAR 36, represents an important step for the achievement of this goal. The mAb JAR 36 is particularly important because it cross reacts with the variant groups 2 and 3 and partially inhibits the binding of fH. The results should provide further information for engineering chimeric fHbp molecules containing epitopes from all the three antigenic variant groups.

Chapter 4

Materials and methods

4.1 Phage displayed libraries

In the present work we have used five different libraries that display random peptide sequences of different sizes, fused to the N-terminal region of the major coat protein (pVIII) of filamentous phage. The pVIII-9aa, pVIII-12aa and pVIII-15aa libraries are composed of random 9-mers, 12-mers and 15-mers, respectively. The pVIII-9aa.Cys library has random sequences of 9 residues flanked by two Cyssteine residues (CX_9C), and the pVIII-Cys.Cys library has random sequences of 12 residues with two Cysteine residues present 2 to 10 residues apart ($CX_{10}C$, CX_9CX, XCX_8CX, XCX_7CX_2, $X_2CX_6CX_2$, $X_2CX_5CX_3$, $X_3CX_4CX_3$, $X_3CX_3CX_4$, $X_4CX_2CX_4$), which creates a collection of disulfide constrained loops of different sizes (Felici *et al.*, 1991; Luzzago, 1998). The vector pC89 (Fig. 4.1) was used to insert oligonucleotides of random sequence in the 5' of the gene VIII as previously described by Felici *et al.*, 1991. Briefly, a fragment of f1 phage, containing the entire gene VIII, has been treated with restriction endonucleases, purified and inserted into the SmaI site of $pEMBL19^+$. Clones containing the insert in an orientation that puts gene VIII under pLac control, have been selected thanks to their capability to form blue colonies on X-gal indicator plates. To prepare a library of peptides with random amino acid sequences, pC89 DNA has been linearized by digestion with the enzymes *EcoRI* and *BamHI* to allow the insertion of oligonuclotides and subsequently recircularized by ligation.

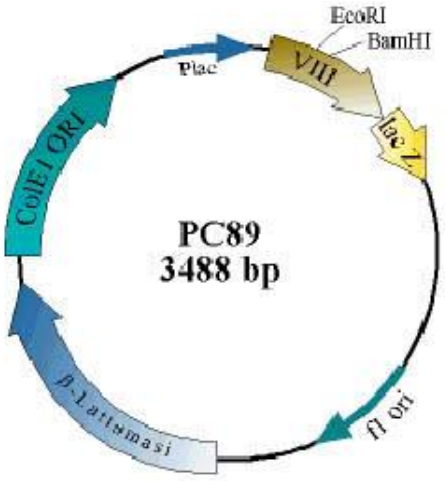

Figure 4.1: genetic map of the phagemid pC89.

4.2 Monoclonal antibody

The monoclonal antibody designated JAR 36 has been produced immunizing mice with the fHbp in the variant group 3 (a gene from strain M1239) as reported by Beernink *et al.*, 2008. This mAb is an IgG2b and, as determinated by ELISA, it showed concentration-dependent binding to the respective recombinant protein that was used for the immunization of the mice, moreover it was cross-reactive also against the variant group 2.

4.3 Screening of peptide libraries

Specific phage clones were isolated from the libraries using two different techniques: Biopanning and Dynabeads. Three round of selection have been performed by using JAR 36 as target, alternating biopanning and dynabeads rounds in order to reduce the limitations that the methods might present, which may lead to the enrichment of unspecific clones.

4.3.1 Biopanning

In the biopanning approach, 1 μg/ml of JAR 36 mAb was incubated overnight at 4°C with 10^{10} transducing units (TU) of each library, in a total volume of 20 μl of PBS (Reaction A). In the Reaction B, 0.8 μg of biotinylated goat anti-mouse IgG antibody (Fc specific, Sigma, St Louis, MO, USA), was added to $3 \bullet 10^{10}$ UV-inactivated M13KO7 phage particles and incubated overnight at 4°C. This step prevent non-specific binding. Falcon

plates (⊘ 6 cm) were coated with 4 ml of Coating Buffer 1X and 40 μl of streptavidin (stock solution 1 mg/ml) and incubated overnight at 4°C. The Reaction A was mixed with the Reation B and incubated 4 hours at room temperature. The Coating Buffer was removed and after Blocking Buffer the plates were washed with Washing Solution 3 times. The mixture A+B was added to a streptavidin-coated plates and incubated for 10 min at room temperature. After 10 washes with 1 ml of Washing Solution, bound phages were eluted with 800 μl 0.1 N HCl, adjusted to pH 2.2 with glycine and 10 mg/ml BSA. The solution was neutralized using 60 μl of 2 M Tris–HCl, pH 9.6 and the phages were amplified by infecting *E.coli* TG1 cells.

The second and third rounds of selection were done in the same way, except 10 ng/ml and 1 ng/ml of the mAb were used, respectively.

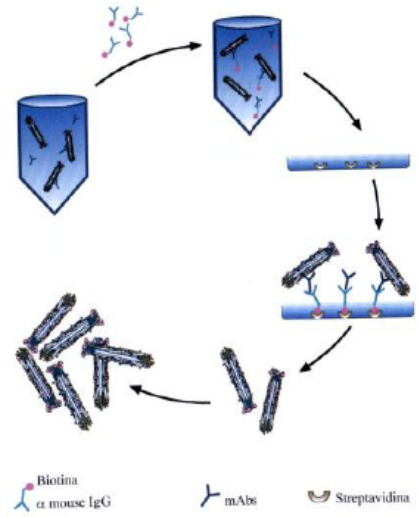

Figure 4.2: schematic rappresentation of a biopanning screening round.

4.3.2 Dynabeads

The JAR 36 mAb (1μg/ml) was incubated with magnetic beads conjugated with protein G (50 μg protein G-Dynabeads®, Dynal, Norway) for 1h at room temperature under agitation. The beads were washed 3 times with Washing Solution (PBS, 0,5% Tween-20), and approximately 10^{10} ampicillin-transducing units of library preparation (10^{11} phage particles) in a volume of 100 μl, were added to 900 μl of Blocking Solution (PBS, 5% non-fat dry milk, 0.05% Tween-20) and agitated for 3 to 4 h at room temperature. After 10 washes with 1 ml of Washing Solution, bound phages were eluted with

500 μl 0.1 N HCl, adjusted to pH 2.2 with glycine and 10 mg/ml BSA. The solution was neutralized and the phages were amplified by infecting *E.coli* TG1 cells.

The second and third rounds of panning were performed as described above, but using 10^{10} ampicillin-transducing units obtained from the first and the second round of amplified phage pools, respectively.

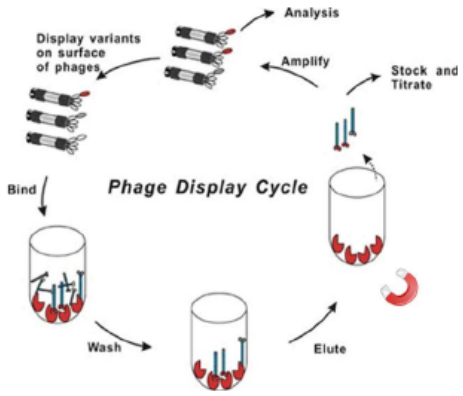

Figure 4.3: schematic rappresentation of a dynabeads screening round.

4.4 Amplification of selected phages

The phage particles selected through the two methods described above, were amplified infcting *E.coli* TG1 cells grown in Luria-Bertani broth (LB) at 37°C under agitation up to an OD_{600nm} of 0.8.

In the I *step*, 800 μl of cell culture were infected with 200 μl of phage eluted from the selections, and kept in incubation for 15 min without agitation and 30 min with shaking. *E.coli* TG1 cells were infected with selected phage and plated onto Luria-Agar (LA) added with ampicillin and glucose at finally concentration of 50 μg/ml and 10 μg/ml. After incubation at 37°C overnight, cells were scraped and resuspended in 8 ml Luria Broth (LB) containing 50 μg/ml ampicillin (stok solution 1000x) and 2 ml glycerol (final concentration 20%). The scraping was stored at -20°C.

In the II step, 50 μl of scraping was inoculated in 10 ml LB containing 10 μl ampicillin (stok solution 2000x) and incubated at 37°C under agitation up to an OD_{600nm} of 0.2. IPTG (10 μl from a stok solution 500x) was added and the cells were super-infected with 10 μl M13K07 (stock solution 10^{12} phage/ml) to have a final concentration 10^9 phages/ml. After incubation at 37°C for 15 min without agitation and 4 h with vigorous

shaking, cultures were centrifuged at 3000 rpm for 30 min at 4°C, the supernatants were collected and added with sodium azide (4 ml from a stock solution 5% for each ml of supernatant recovered) and stored at 4°C.

4.5 Titration of TUs

The titration is useful to determine the number of phage particles per unit volume. The titre can be determine by the TU (transduction units) value. Infecting the cells with the phage solution that needs to be titreted and using a selective media (containing ampicillin) only the growth of colonies containing the phagemid DNA is possible, because the gene for the antibiotic resistance is carried by the pC89 vector. *E.coli* TG1 cells were grown in LB at 37°C under agitation. When they reached an OD_{600nm} of 0.6-0.8, 100 μl they were transferred into an Eppendorf tube. Phages (eluted or amplified) were serially diluted in PBS 1x as follows:

100 μl of phages	+	900 μl of PBS 1X	1:10
100 μl of phages diluted 1:10	+	900 μl of PBS 1X	1:100
ecc.			

100 μl of *E.coli* TG1 cells were infected with 10 μl of each serial dilution and incubated for 15 min without shaking and 30 min under agitation. The mixture (5 μl) was plated onto LA with ampicillin and incubated at 37°C overnight. From the number of grown colonies is possible estimate the number of phages as Ampicillin transducing units (Amp TU)/ml:

$$TU/ml = n \circ colonies \bullet 10^x \bullet 100 \bullet 10$$

4.6 Immunoscreening

Positive phage clones were identified through immunoscreening, as described by Felici *et al.*, 1993. After three rounds of affinity selection, using the libraries either individually or in combination, phage particles from scraping, were mixed with 2 ml of a culture of *E.coli* TG1 (OD_{600nm} 0.4). Five hundred μl of this culture were infected with M13KO7 helper phage ($\sim 10^9$ pfu) and incubated 15 min at 37°C plus 30 min with shaking. Serial dilutions of infected bacteria were plated on Luria–Bertani (LB) agar plates containing ampicillin, kanamycin and IPTG, and incubated overnight at 37°C. Nitrocellulose filters (Protran BA85, 0.45 mm, Schleicher and Schuell, Keene, NH) were

layered on the plates containing 50–200 colonies, and left at room temperature for 1 h. Filters were blocked for 1 h with Blocking Solution, and incubated with mAb JAR 36 (1μg/ml in blocking solution) for 2 h at room temperature with gentle shaking. After 3 washes an AP-conjugated anti-mouse IgG secondary Ab (Sigma, St. Louis, MO, 1:5000), was added for 1 h at room temperature. Filters were washed and developed with nitro-blue-tetrazolium and 5-bromo-4-chloro-3-indolyl-phosphate (Sigma).

4.7 Positive phage recovery

After the detection of positive colonies from immunoscreening, they were isolated and amplified. To identify recombinant phage particles blue/white screening was used by α-complementation. The basis of its approach lies on the β-galactosidase enzyme that can be split in two peptides, LacZα and LacZω, neither of which is active by itself but when both are present together, spontaneously reassemble into a functional enzyme. This property is exploited in many cloning vectors where the presence of the lacZα gene in a plasmid can complement in *trans* another mutant gene encoding the LacZω in specific laboratory strains of *E.coli*. However, when DNA fragments are inserted in the vector, the coding sequence of LacZα is interrupted, the cells therefore show no β-galactosidase activity. The presence or absence of an active β-galactosidase may be detected by X-gal, which produces a characteristic blue dye when cleaved by the enzyme, thereby providing an easy means of distinguishing the presence or absence of cloned product in a plasmid.

Positive colonies from immunoscreening were resuspended in 50 μl of 1x PBS and heated at 70°C for 15 min to kill the bacterial cells. After centrifugation for 5 min at 14000 rpm (16000 g), the supernatant containing positive phage particles was collected. Five μl of recovered supernatant was amplified by infecting *E.coli* TG1, incubated 15 min at 37°C and additional 30 min with shaking, and finally plated on LA containing ampicillin. After incubation at 37°C overnight, single colonies were plated as drop spots both onto a plate with LA/Amp and onto LA/X-Gal/IPTG/Amp. The colonies in LA/Amp proved to be blue on X-Gal plates, were inoculated into LB containing 50 μg/ml ampicillin and incubated at 37°C with vigorous shaking; when OD_{600nm} was 0.2, M13KO7 helper phage (10^9 pfu) and IPTG (0.1 mM) were added, and the cultures were then incubated for 15 min at 37°C and additional 4 h with shaking. After centrifugation at 12,000 g for 30 min, the supernatant containing positive phage was recovered.

4.8 ELISA assay

The JAR 36 reactivity with the phage pools selected by biopanning and/or dynabeads, or with the single clones positive in immunoscreening, was verified by PHAGE-ELISA using an HRP–anti M13 mAb conjugate.

Ninety-six well plates were coated with mAb JAR36 (100 μl/well, 0.2 μg/ml in 50mM $NaHCO_3$, 0,02% (w/v) NaN_3, pH 9.6) and incubated overnight at 4°C. The plates were washed 8 times with Washing Solution (50mM Tris–HCl,150mM NaCl, pH 7.5, 0.05% (v/v) Tween-20). One hundred μl per well of phage supernatant were added and the plates were incubated for 2 h at 37°C. After washing, 100 μl of an HRP–anti M13 mAb conjugate (Amersham Biosciences, Buckinghamshire, UK, 1:5000) was added and incubated for 1 h at 37°C. Antibody binding was detected by 3,3',5,5'-tetramethylbenzidine (TMB) (Sigma) through reading at 450 nm after 45 min by an automated ELISA reader (Labsystem multiskan).

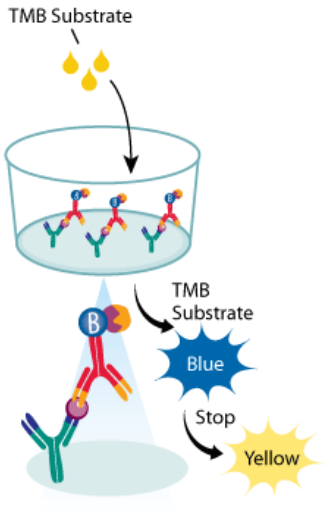

Figure 4.4: schematic rappresentation of ELISA assay

4.9 Single strand DNA extraction and sequencing

A solution of 2.5 M NaCl, 20% PEG (1/4 of the volume) was added to phage supernatants and the mixture was left for 15–30 min at room temperature; after centrifugation at 12,000 g for 15 min the pellets were resuspended in TE pH 8.0. Deproteinization was obtained through phenol and phenol/chloroform extraction, DNA was precipitated by

MIX	$[]_f$	**μl/sample**
Buffer 10X	1X 1.5 mM	0.25
MgCl2 [25 mM]	2.5 mM	2.5
dNTP [2.5 mM]	0.2 mM	0.5
PF [20 μM] E24 forw	1 μM	1.25
PR [20 μM] 40 rev	1 μM	1.25
AmpliTaq DNA Polymerase [5 U/μl]	1.25 U/μl	0.25
H_2O	final volume 25 μl	

Table 4.1: PCR mixture

using cold ethanol and centrifuged. Purified DNA was resuspended in TE and checked by agarose gel electrophoresis.

After extraction, the DNA of phage particles positive for the reactivity with JAR 36, was amplified by PCR using specific *primers*: M13-40 reverse (5'-GTTTTCCC AGTCACGAC-3') and E24 forward (5'-GCTACCCTCGTTC CGATGCTGTC-3'). One μl of each DNA sample was added to 24 μl of mixture PCR reaction (Table 4.1).

All amplification reactions were carried out using a PCR System (Applied Biosystems, Foster City, CA, USA). The thermal cycling conditions consisted of 5 min at 94°C, followed by 25 cycles at 94°C for 30 s, 52°C for 30 s and 72°C for 30 s. At the end an extension for 7 min at 72°C.

The amplified products (5 μl) were checked by agarose (1%) gel electrophoresis in TBE (0,04 M Tris-acetate, 0,001 M EDTA), the remainder was purified by QIAquick PCR purification Kit (QIAGEN) and sequenced using the *primer* M13-40 reverse.

For the pVIII-15 library two additional *primers* were specifically sinthesized for being used in this work: 15J36 forward (5'-TCTGGTCCGACAAGGACAG-3') e 15J36 reverse (5'-TCGGCCTTGCTGGTAATATC-3'), with the aim to eliminate phage particles carrying peptides already selected. Indeed, the *primer* 15J36 forward is complementary to the sequence that includes both the vector and the insert coding for the 15-mer peptide. Therefore, this primer can only amplify clones carrying this insert. The thermal cycling conditions consisted of 5 min at 94°C, followed by 25 cycles at 94°C for 30 s, 58°C for 30 s and 72°C for 30 s. At the end an extension for 7 min at 72°C.

The samples not amplified in this reaction were amplified with the *primers* M13-40 reverse ed E24 forward as reported above, and than sequenced.

4.10 M13KO7 preparation

To prepare the helper phage M13KO7 we have infected *E.coli* TG1 cells with the phage and incubated for 15 min without shaking and 30 min under agitation. Ten μl of infected cells were added to 200 μl of uninfected cells and mixed with Top Agar, then plated onto LA plates and incubated overnight at 37°C. The day after a plaque was inoculated in 3-4 ml of LB and incubated for 2 h. This culture was transferred in 100 ml of LB and incubated for 2-4 h at 37°C, then was added 400 ml of LB plus 70 μg of kanamycin and incubated overnigt in the same conditions. After centrifugation, the supernatant was added at PEG 20% + NaCl 2,5 M, left in ice for 30 min and centrifuged at 10.000 rpm for 15 min. The pellet was resuspended in 100 ml of TBS 1X, centrifuged again, mixed with PEG 20% + NaCl 2,5 M and centrifuged at 8000 rpm for 15 min. At the end the pellet was resuspended in 2 ml of TBS 1X, titrated and diluted to obtain a final concentration of $1 \bullet 10^{12}$ pfu/ml.

4.11 Titration of M13KO7

The titration is necessary to determine the number of infecting phage particles per unit of volume. The titre can be determinated through the PFU (plaque-forming unit) value; it is a functional measurement rather then a measurement of the absolute quantity of particles: viral particles that are defective or which fail to infect their target cell will not produce a plaque and thus will not be counted. A plaque is a visible structure formed within a cell culture, such as bacterial cultures within some nutrient medium (e.g. agar). The bacteriophage viruses replicate and spread without lysis or death of the host cells but the slow growth of infected cells compared to uninfected, produce zones having a lower bacterial density and hence named plaques (Fig. 4.5).

An *E.coli* TG1 colony was inoculated in LB and incubated at 37°C under agitation up to an OD_{600nm} of 0.6-0.8. At the same time the phages were diluted in serial dilutions with PBS 1X:

10 μl of phages	+	990 μl of PBS 1X	1:10 (10^{-2})
10 μl of phages	+	990 μl of PBS 1X	1:100 (10^{-4})
100 μl of phages	+	900 μl of PBS 1X	1:10 (10^{-5})
100 μl of phages	+	900 μl of PBS 1X	1:10 (10^{-6})
100 μl of phages	+	900 μl of PBS 1X	1:10 (10^{-8})

One hundred μl of *E.coli* TG1 were dispensed in Eppendorf tubes and infected with

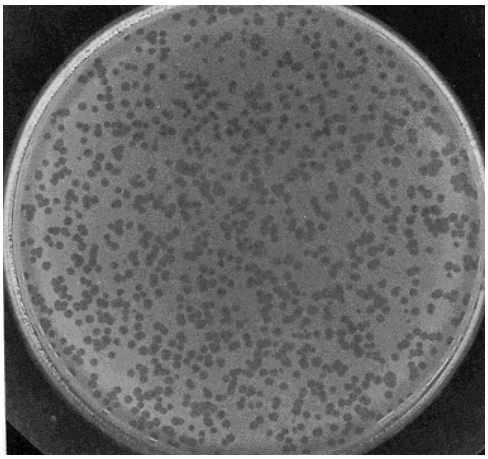

Figure 4.5: exemple of filamentous phage plaques on LA plate.

10 μl of each phage dilution. The mixture was incubated at 37°C without shaking and 30 min under agitation. Ten μl of infected cells were mixed to 200 μl of non-infected cells, added to 5 ml of Top Agar and plated onto LA plate, than incubated at 37°C overnight.

The day after, is possible estimate the number of phage particles per ml on the basis of the number of plaques formed (PFU), according to:

$$PFU/ml = n \circ plaques \bullet 10^x \bullet 100 \bullet 10$$

4.12 Solutions and Buffers

Blocking Buffer for Biopanning :
BSA 0,5 g
$NaHCO_3$ 10 ml (Stock 1M)
Streptavidin 10 μl (Stock 1 mg/ml)
Add. H_2O up to final volume of 100 ml.
Store at -20°C.

Blocking Buffer 2X :
PBS 2X 20 ml (Stock 10X) Tween20 100 μl Not Fat Dry Milk 10 g NaN3 (0.1%) 2 ml (Stock 5%) Add. H_2O up to final volume of 100 ml.
Store at -20°C.

Developing Solution for ELISA :
Dissolve a tablet of SIGMA 104 in 5 ml of Substrate Solution.

Protect from light.

Developing Solution for Immunoscreening :
NBT 66 μl (Stock 50 mg/ml*)
BCIP 33 μl (Stock 50 mg/ml*)
Into 10 ml of Substrate Buffer. Store at 4°C.
* NBT: 0,5 g in 10 ml of Dimethylformamide 70%
* BCIP: 0,5 g in 10 ml of Dimethylformamide 100%

Coating Buffer 10X pH 9,6 for ELISA :
$NaHCO_3$ 2,93 g
Na_2CO_3 1,59 g
Add. H_2O up to final volume of 100 ml.

Elution Buffer :
HCl 0,1 N
Glycine up to pH 2,2
Add. H_2O up to final volume of 1L.
Just before use add BSA [10 mg/ml].

H_2SO_4 **2 M** :
H_2SO_4 19,6 ml
Add. H_2O up to final volume of 100 ml.

PEG/NaCl 5X :
Polyethilene glycol 200 g
NaCl 150 g
Dissolve in 1L of H_2O.

PBS 10X :
Na_2HPO_4 27,7 g
NaH_2PO_4 6,6 g
NaCl 29 g
Add. H_2O up to final volume of 1L.

PBS-Tween20 0,05% (Washing Buffer for Immunoscreening and ELISA) :
PBS 100 ml (Stock 10X)
Tween20 0,5 ml
Add. H_2O up to final volume of 100 ml.

PBS-Tween20 0,5% (Washing Buffer for Biopanning e Dynabeads) :
PBS 100 ml (Stock 10X)
Tween20 5 ml
Add. H_2O up to final volume of 100 ml.

Streptavidia – solution 1 mg/ml :
Resuspend 1 mg of streptavidin (stored at -20°C) in 1 ml of buffer prepared as described below:
Phosfate buffer [0,01 M] 100 μl (Stock 0,1 M)
NaCl [0,15 M] 30 μl (Stock 5M)
Sodium azide [0,05%] 100 μl (Stock 0,5%)
Add. H_2O 770 μl.

Substrate Buffer for Immunoscreening :
Tri-HCl pH 9,6 5 ml (Stock 2 M)
$MgCl_2$ 0,5 ml (Stock 1 M)
NaCl 2 ml (Stock 5 M)
Add. H_2O up to final volume of 100 ml.

Substrate Solution pH 9.8 :
Diethanolamine 5 ml
$MgCl_2$ 25 μl (Stock 1M)
NaN_3 0,5 ml (Stock 5%)
Add. H_2O up to final volume of 50 ml. Protect from light.

TBE 5X :
EDTA 4,7 g
Boric acid 30 g
TRIS base 60,5 g
Add. H_2O up to final volume of 1l.

TBS 10X :
TRIS 500 ml (Stock 1 M pH 7,5)
NaCl 87 g (Stock 1,5 M)
Add. H_2O up to final volume of 1l.

TE pH 7,5 :
EDTA pH 8,0 1 nM
Tris-HCl pH 7,5 10 nM

4.13 Bacterial growth medium

BBL TOP AGAR :
Tryptone 1g
NaCl 0,5 g
Bactoagar 0,7 g
Add. H_2O up to final volume of 100 ml.

LA :
Tryptone 5g
Yeast Extract 2,5 g
NaCl 5g
Bactoagar 7,5 g
Add. H_2O up to final volume of 500 ml.

LA+Glucose+Ampicillin :
Tryptone 5g
Yeast Extract 2,5 g
NaCl 5g
Bactoagar 7,5 g
Glucose 5g
Add. H_2O up to final volume of 500 ml.
After sterilization, when the growth medium temperature is 47°C, add. 250 μl of Ampicillin 2000X (Stock 100 mg/ml).

LB :
Tryptone 1g

Yeast Extract 0,5 g
NaCl 0,5 g
Adjusted to pH 7,2 with NaOH 1 or 10 M.
Add. H_2O up to final volume of 100 ml.

Ampicillin 2000X (Stock 100 mg/ml) :
Ampicillin 1g
H_2O u.p. 5 ml
Ethanol 5 ml
Store at -20°C.

Kanamycin 1000X (Stock 10 mg/ml) :
Kanamycin 100 mg
H_2O u.p. 10 ml
Store at -20°C.

Tetracyclin 1000X (Stock 20 mg/ml) :
Tetracyclin 200 mg
H_2O u.p. 5 ml
Ethanol 5 ml
Store at -20°C.
Protect from light.

IPTG 1000X (Stock 20 mg/ml) :
IPTG 0,2 g
H_2O 10 ml
Store at -20°C.

X-gal 1000X (Stock 35 mg/ml) :
X-gal 0,35 g
Dimethylformamide 100% 10 ml
Protect from light.

Chapter 5

Results

5.1 Binding of JAR 36 mAb to natural fHbp sequence variants

JAR 36 is an IgG2b mAb that was generated from a mouse immunized with recombinant fHbp ID 28[1] from variant group 3. The mAb reacts with recombinant fHbp ID 28, which is the immunogen that was used to produce the mAb, moreover it cross-reacts with fHbp ID 77 (in variant group 2) but not with fHbp ID 1 (in variant group 1). JAR 36 mAb also cross-reacts with a natural chimeric fHbp, ID 207 (Fig. 5.1 A). As a control, mAb JAR 5, which is specific for fHbp sequence variants in variant group 1 (Welsch *et al.*, 2004), reacts with fHbp ID 1 (variant group 1) and with the chimeric fHbp ID 207, but not with fHbp ID 28 (variant group 3) or ID 77 (variant group 2) (Fig. 5.1 B).

Amino acid residues 1 to 185 (variable segments V_A through V_D)[2] of the natural chimeric fHbp ID 207 have 96% identity with the corresponding segments of fHbp ID 1, while residues 186 to 255 of segment V_E of fHbp ID 207 have 96% identity with segment V_E of fHbp ID 28. The fHbp variants that are bound by JAR 36 are denoted with asterisks (Fig. 5.2). Collectively, the data are consistent with the hypothesis that the epitope recognized by JAR 36 mAb is residing in variable segment E (V_E) derived from lineage 2 (white octagonal symbols).

[1] fHbp ID numbers are assigned in the fHbp database at http://pubmlst.org/neisseria/fHbp/

[2] As described in section 1.3.1

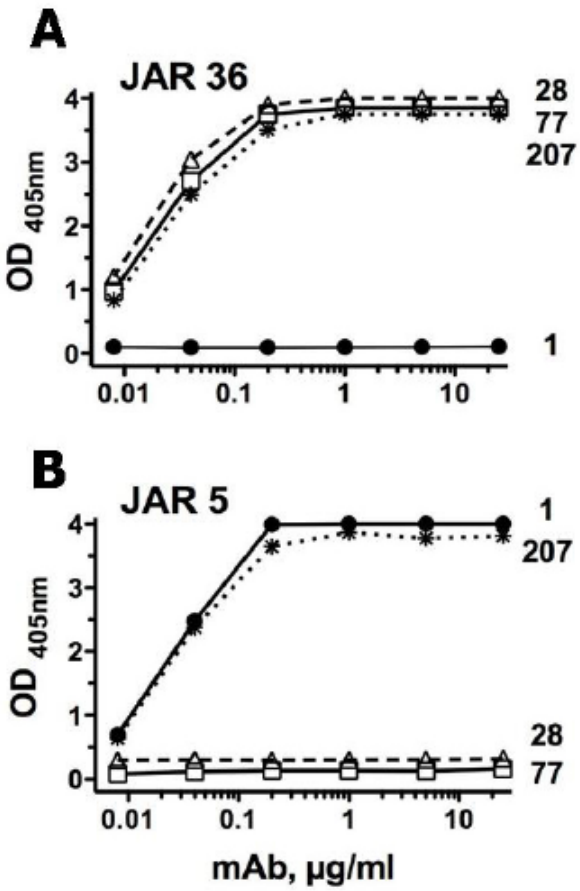

Figure 5.1: binding of anti-fHbp mAbs to purified recombinant fHbp variants by ELISA. **A**, Binding of mAb JAR 36 to fHbp ID 1 (filled circles), ID 28 (open triangles), ID 77 (open squares) and ID 207 (asterisks). **B**, Binding of mAb JAR 5 to the same fHbp variants as in Panel A.

5.2 Phage libraries screening

To identify fHbp amino acid residues affecting the JAR36 epitope, we screened five phage libraries displaying random peptides of different length fused to the N-terminus of the coat protein VIII. The screening was performed by immunoaffnity selection, using two different techniques: Biopanning and Dynabeads. Neither method is free from the risk of selecting non-specifc clones, their combined use should therefore help in minimizing this risk. For each library were carried out three rounds of selection using JAR 36 as a bait, using the libraries either individually or in combination. In the Biopanning method, after the first round, the phage pools need to be concentrated by PEG precipitation for

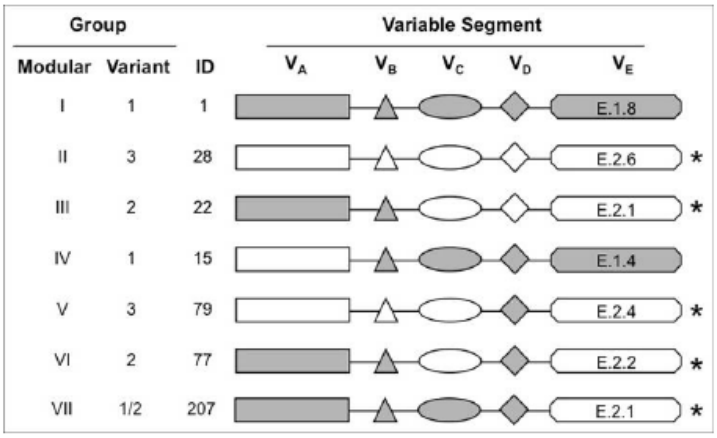

Figure 5.2: schematic of the modular architecture of fHbp. Seven different fHbp sequence variants, designated by ID numbers, are shown along with their classifications into modular groups and variant groups. fHbp ID 1 and ID 28 are designated as comprising variable segments from lineage 1 (shaded) and 2 (white), respectively. In this panel, each distinctive V_E segment is designated by two numbers, separated by a decimal point with the first number, 1 or 2, referring to the genetic lineage, and the second number referring to the ID number of the segment as annotated on the website http://pubmlst.org/neisseria/fHbp/. The variants that bind the JAR 36 mAb are designated with an asterisk.

this reason we have used this approach in the first rounds, followed by the Dynabeads method in the subsequent rounds (Table 5.1).

In order to detect the presence of non-specific clones in the selected mixtures, the reactivity of phage pools from each selection cycle was tested by ELISA, using the pC89 phage vector (i.e. displaying no recombinant insert) as a negative control (Fig. 5.4). The assay was performed using 0.8 μg/ml of JAR 36 mAb according to the calibration curve (Fig. 5.3).

As shown in figure 5.4, the phage pools have different reactivity with JAR 36. Most of them show a reactivity corresponding to an OD between 0.4 and 1.5. The phage particles derived from the Dynabeads second round with pVIII-9aa (f), pVIII-9aa.Cys (i), pVIII-12aa (m) libraries and from third round with pVIII-15aa library, show the highest reactivity (values between 2 and 3.5 OD). These results show that, although the alternate selection was expected to be more effective, the phage pools derived by Biopanning are less reactive than Dynabeads. Indeed, this last method allowed us to identify ligands with higher affinity with mAb JAR 36. The selections carried out by using Dynabeads

Library	mAb	I round	II round	III round
pVIII-9aa+pVIII-9aa.Cys	JAR 36 1 μg/ml	BIOPANNING 1μM	DYNABEADS 1 μg	DYNABEADS 1 μg
		DYNABEADS 1 μg	DYNABEADS 1 μg	DYNABEADS 1 μg
pVIII-12aa+pVIII-Cys.Cys	JAR 36 1 μg/ml	BIOPANNING 1μM	DYNABEADS 1 μg	DYNABEADS 1 μg
		DYNABEADS 1 μg	DYNABEADS 1 μg	DYNABEADS 1 μg
pVIII-9aa	JAR 36 1 μg/ml	BIOPANNING 1μM	DYNABEADS 1 μg	DYNABEADS 1 μg
		DYNABEADS 1 μg	DYNABEADS 1 μg	DYNABEADS 1 μg
				BIOPANNING 1μM
pVIII-9aa.Cys	JAR 36 1 μg/ml	BIOPANNING 1μM	DYNABEADS 1 μg	DYNABEADS 1 μg
		DYNABEADS 1 μg	DYNABEADS 1 μg	DYNABEADS 1 μg
				BIOPANNING 1μM
pVIII-12aa	JAR 36 1 μg/ml	DYNABEADS 1 μg	DYNABEADS 1 μg	DYNABEADS 1 μg
				BIOPANNING 1μM
pVIII-Cys.Cys	JAR 36 1 μg/ml	DYNABEADS 1 μg	DYNABEADS 1 μg	DYNABEADS 1 μg
				BIOPANNING 1μM
pVIII-15aa	JAR 36 1 μg/ml	DYNABEADS 1 μg	DYNABEADS 1 μg	DYNABEADS 1 μg

Table 5.1: phage libraries screening rounds

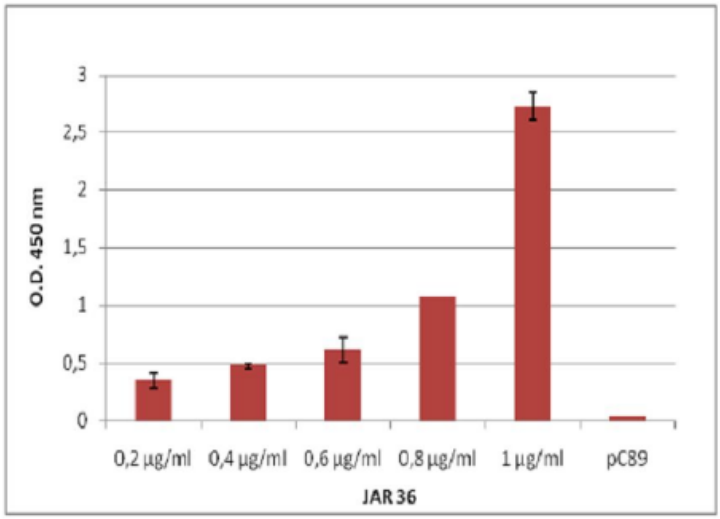

Figure 5.3: calibration curve to determine the JAR 36 concentration to be used for detect its reactivity with the phage pools.

in all three rounds display higher OD values (b, d, f, i, m, o, p) when compared to pools deriving from a first Biopanning round and a second and third Dynabeads rounds (a, c, e, h,). The phage pools that showed the highest reactivity were chosen to perform the Immunoscreening.

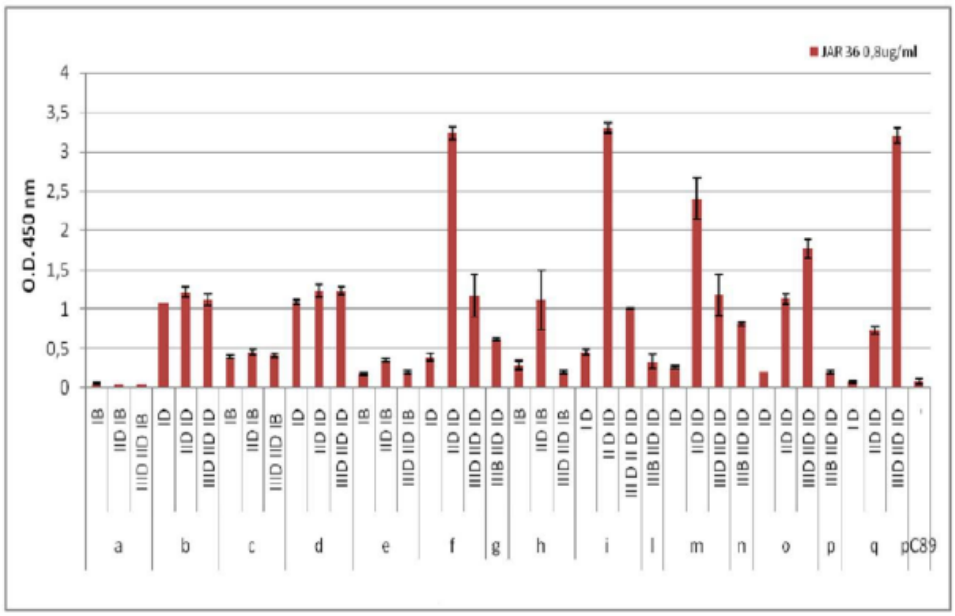

Figure 5.4: ELISA reactivity of the phage pools selected from libraries: pVIII-9aa+pVIII-9aa.Cys (a, b); pVIII-12aa+pVIII-Cys.Cys (c, d); pVIII-9aa (e, f, g); pVIII-9aa.Cys (h, i, l); pVIII-12aa (m, n); pVIII-Cys.Cys (o, p); pVIII-15aa (q).

5.3 Immunoscreening

Among the selected clones, the positive ones were identified by a suitable colony immunoscreening procedure. We have chosen the pools that had shown the highest reactivity in ELISA. Eluted phage pools were plated to form colonies, transferred onto nitrocellulose filters and tested for their ability to bind the target molecule represented by mAb JAR 36 (Fig. 5.5, 5.6 and 5.7). Moreover, the single colonies were tested on plate containing X-Gal. The phage particles containing phagemides encoding for productive random inserts should be able to produce blue colonies. Through Immunoscreening it has been possible to identify single positive clones, as shown in figures 5.8, 5.9, 5.10, and 5.11.

5.4 ELISA on single clones

The positivity of single clones, selected by Immunoscreening and Positive Phage Recovery, was verified through ELISA, using the pC89 phage vector (i.e. displaying not recombinant insert) as a negative control (Fig. 5.13, 5.14, 5.15, and 5.16). In this case 0.2 μg of mAb JAR 36 was used as suggested by the calibration curve (Fig. 5.12).

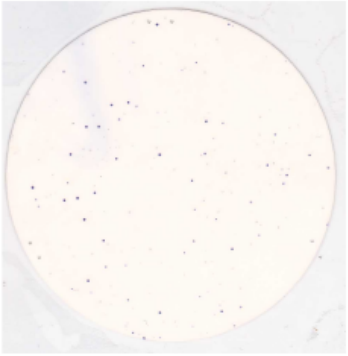

Figure 5.5: the nitrocellulose filter shows the reactivity with JAR 36 of phage pool deriving from pVIII-9aa.Cys library.

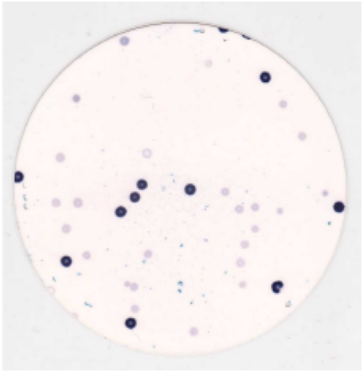

Figure 5.6: the nitrocellulose filter shows the reactivity with JAR 36 of phage pool deriving from pVIII-15aa library.

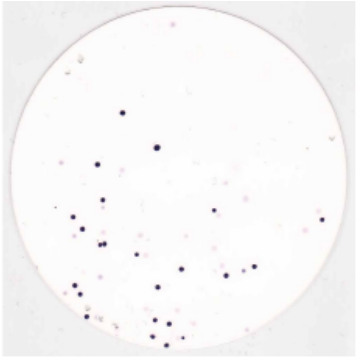

Figure 5.7: the nitrocellulose filter shows the reactivity with JAR 36 of phage pool deriving from pVIII-12aa library.

Most of selected clones show a relatively low reactivity, with an OD value between 0.1 and 0.4. The clone 18M, deriving from the libraries pVIII-12aa and pVIII-Cys.Cys

Libraries	mAb	Round	Clones
pVIII-12aa + pVIII-Cys.Cys	JAR 36 1 µg/ml	IIID IID IB	1R, 2R, 3R, 4R, 5R, 6R 7R, 8R, 9R; 1M, 2M, 3M, 4M, 5M, 6M, 7M, 8M, 9M, 10M, 11M, 12M
pVIII-12aa		IIID IID ID	13M, 14M, 15M
pVIII-Cys.Cys		IIID IID ID	16M, 17M, 18M

Figure 5.8: positive clones derived from pVIII-12aa and pVIII-Cys.Cys libraries.

Libraries	mAb	Round	Clones
pVIII-9aa	JAR 36 1 µg/ml	IIID IID ID	19M, 20M, 21M 25, 26, 27, 28, 29, 30, 31, 32; 67, 68; 88, 89, 90

Figure 5.9: positive clones derived from pVIII-9aa and library.

Libraries	mAb	Round	Clones
pVIII-9aa.Cys	JAR 36 1 µg/ml	IIID IID ID	22M, 23M, 24M; 33, 34, 35, 36, 37, 38, 39, 40; 43, 44, 45, 46, 47, 49, 53, 54, 55, 59, 61; 70, 72, 74, 75, 76; 91, 92, 93

Figure 5.10: positive clones derived from pVIII-9aa and pVIII-9aa.Cys libraries.

Libraries	mAb	Round	Clones
pVIII-15aa	JAR 36 1 µg/ml	IIID IID ID	80, 81, 82, 83, 84, 85, 86, 87; J1A-J40A

Figure 5.11: positive clones derived from pVIII-15aa library.

(Fig. 5.13) display the highest reactivity (OD 2.3), followed by 1R, 2R e 5R having an OD between 0.51 and 50 . The clones 25, 29, 31, 32, 34 and 35 (Fig. 5.14) and 43 to 61

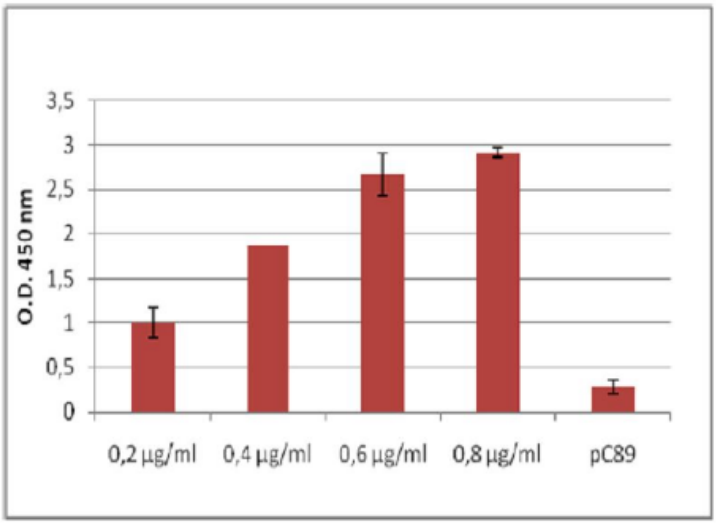

Figure 5.12: calibration curve to determine the JAR 36 concentration to detecte its reactivity with the single positive clones.

(Fig. 5.15), selected from pVIII-9aa and pVIII-9aa.Cys libraries, show a good reactivity, with an OD between 0.5 and 0.85. While the clones 33, 36, 37, 38, 39 and 40 (Fig. 5.14) and 67 to 76 (Fig. 5.15), show a lower reactivity (OD 0.3-0.4). The samples 80, 81, 83, 84 and J17A, selected from the p-VIII.15aa (Fig. 5.16), show a good reactivity with OD value between 0.5 and 0.9, vice versa the others clones have lower OD values ($\leq$0.25).

The pVIII-12aa and pVIII-Cys.Cys libraries selections allowed us to detect the clones shwing the highest reactivity with JAR 36. However, most of selected phage particles deriv from the pVIII-9aa selections. These results are not completely unexpected, indeed as reported by Iannolo *et al.* (1995), the peptides length can affect their ability to be expressed on the phage surfaces. Therefore, shorter peptide could be displayed on phage particles more efficently, and showing higher avidity with the mAb.

5.5 Identification of single clones

The positive clones, identified by immunoscreening, and showing an ELISA reactivity $\geq$0.5 OD, were sequenced after PCR amplification of nucleotide sequence and their aminoacid sequence was determined (Table 5.3).

From this analysis, we did not identify a consensus sequence common to the peptides that reacted with JAR 36, which suggest that the JAR 36 epitope is discontinuous or conformational. We hypothesized that the most abundant amino acids in the bound

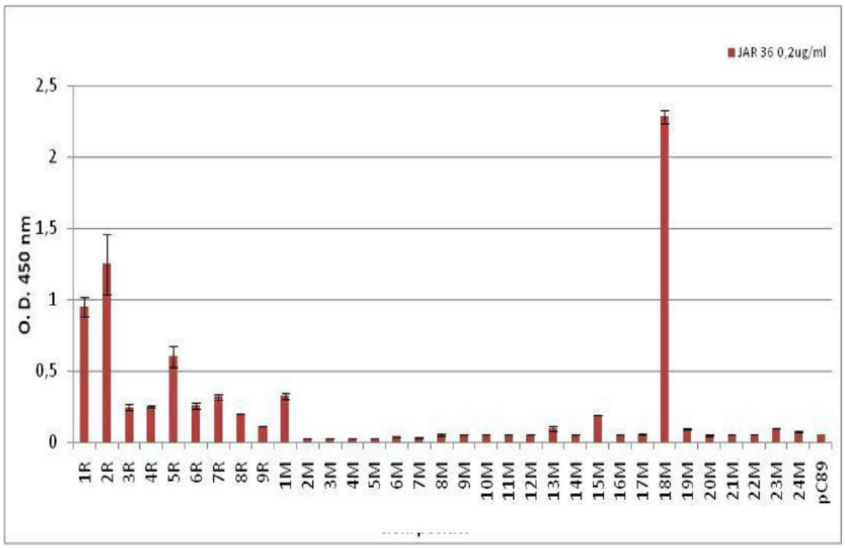

Figure 5.13: ELISA reactivity of single clones selected from libraries pVIII-12aa+pVIII-Cys.Cys (1R-9R e 1M-12M), pVIII-12aa (13M-15M), pVIII-Cys.Cys (16M-18M), pVIII-9aa (19M-21M) and pVIII-9aa.Cys (22M-24M).

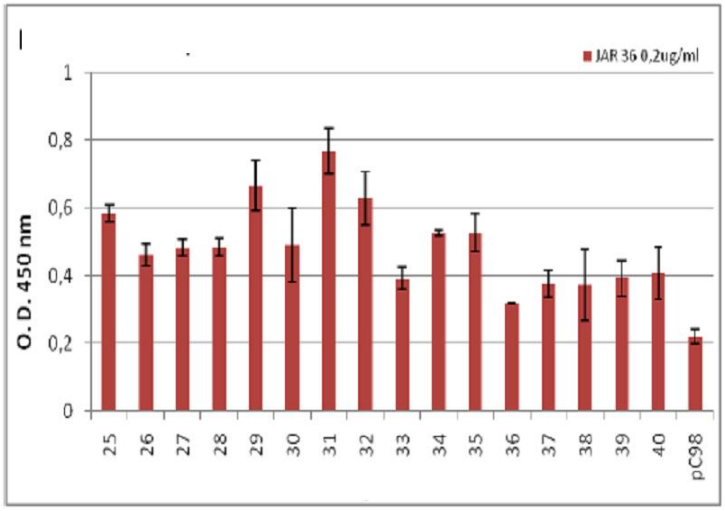

Figure 5.14: ELISA reactivity of single clones selected from libraries pVIII-9aa (25-32) and pVIII-9aa.Cys (33-40).

peptides might be important for the interaction between the immunogen and the mAb.

The observed frequency in the mimotopes was normalized by calculating for each amino acid, the ratio with the expected frequency in the library.

The observed frequency is defined as the ratio between the number of times an amino acid is observed in peptides and total length of the corresponding library clones

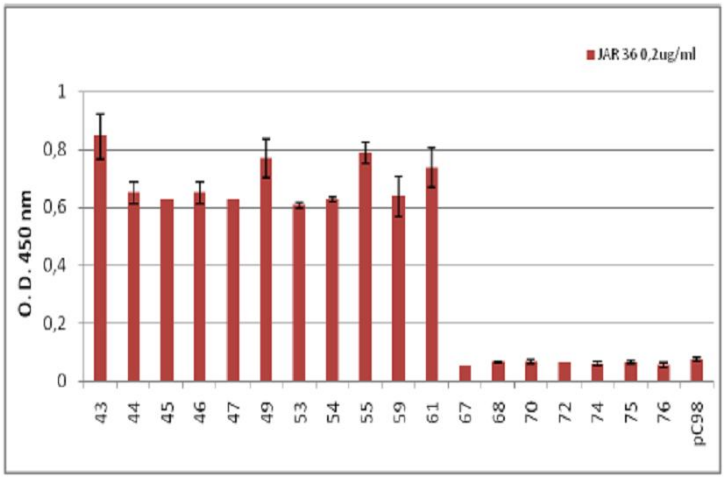

Figure 5.15: ELISA reactivity of single clones selected from libraries pVIII-9aa (67, 68) and pVIII-9aa.Cys (43-61 and 70-76).

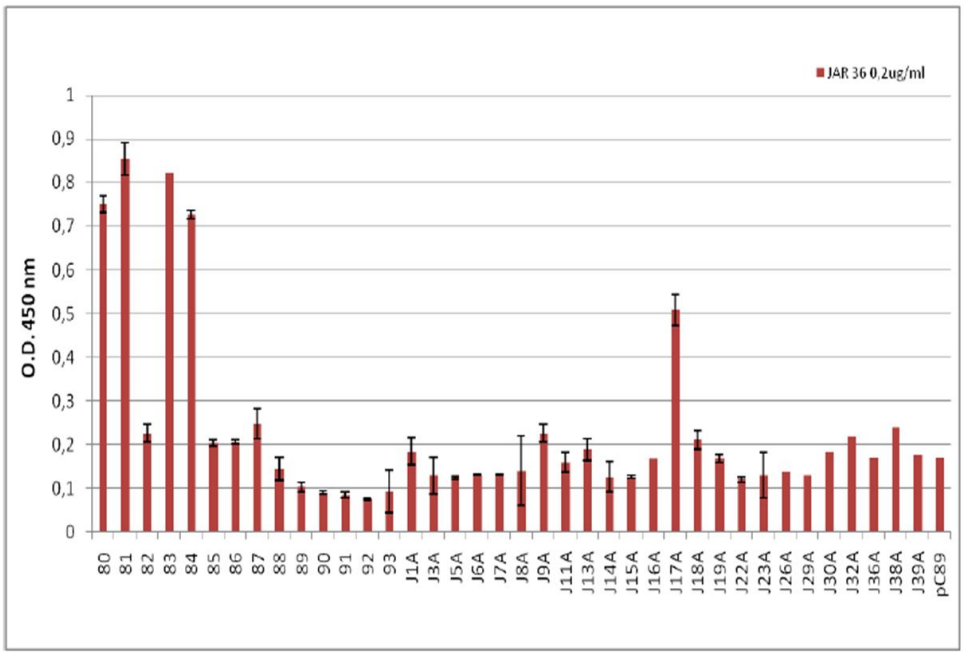

Figure 5.16: ELISA reactivity of single clones selected from libraries pVIII-9aa (88-90), pVIII-9aa.Cys (91-93) and pVIII-15aa (80-87, J1A-J39A).

inserts, the expected frequency, instead, is the ratio between the number of codons in the library for the amino acid concerned and the total number of codons that are present in the library.

Sequence[a]	Number of clones	ELISA OD[b]	SD[c]
AKWCAQFCqGYL	2	3.10	0.42
AKWCNLWCTWVG	3	2.25	0.35
GKQCAAWCEWFA	1	1.10	0.14
GKGCTRRGCDVD	2	1.00	0.39
WSDKDRNLWGLWYRE	4	0.78	0.05
qARCIVEECKWA	3	0.68	0.16
LGWCGDGLCKGV	2	0.65	0.14
NKFVSLGLA	5	0.65	0.09
QKWFALGAPWYD	3	0.60	0.10
WNINWGKPTRDE	1	0.57	0.04
GKWCLLVDCNRD	1	0.57	0.04
RPGPGDIDI	13	0.57	0.16
KVCQLWGNNCGE	2	0.55	0.07
GCGKWELDGCAA	2	0.55	0.07
VRSKWGEVGRPYDVV	1	0.45	0.08

Table 5.2: Amino acid sequences of the phage-displayed peptides mimicking the JAR 36 epitope. [a] Deduced amino acid sequences of the peptide inserts displayed through pVIII fusion on the phage library clones positive, ranked by their reactivity with JAR 36. [b] Reactivity of mAb JAR 36 clone, determined by ELISA.[c] SD value is the standard deviation of the mean (n = 2).

$$observed\,frequency = \frac{n \circ times\,an\,amino\,acid\,is\,observed\,in\,peptides}{total\,lenght\,(insert\,lenght \bullet n \circ clones)}$$

$$expected\,frequency = \frac{n \circ codons\,for\,amino\,acid\,x}{total\,n \circ codons\,in\,the\,library}$$

Whereas for the construction of pVIII-9aa and pVIII-9aa.Cys libraries all the 64 codons were used, for the pVII-Cys.Cys and pVIII-15aa libraries only 32 codons were used (NN^C_G), and for the pVIII-12aa only 20 codons were used, one for each amino acid, according to the *codon preference* of *E. coli*.

Amino acid[a]	Observed[b]	Expected OD[c]	Obs/Exp(95%Cl)[d]
Alanine (A)	0.072	0.063	1.16 (0.62, 1.94)
Arginine(R)	0.061	0.088	0.69 (0.35, 1.22)
Asparagine (N)	0.050	0.038	1.33 (0.61, 2.48)
Aspartate (D)	0.078	0.038	2.07 (1.15, 3.39)
Glutamine (Q)	0.039	0.038	1.04 (0.43, 2.11)
Glutamate (E)	0.050	0.038	1.33 (0.61, 2.48)
Glycine (G)	0.139	0.063	2.22 (1.47, 3.17)
Histidine (H)	0.006	0.038	0.15 (0.00, 0.83)
Isolaucine (I)	0.028	0.045	0.61 (0.20, 1.41)
Leucine (L)	0.078	0.088	0.89 (0.49, 1.45)
Lysine (K)	0.083	0.038	2.22 (1.25, 3.57)
Methionine (M)	0.006	0.030	0.19 (0.00, 1.04)
Phenylalanine (F)	0.028	0.038	0.74 (0.24, 1.71)
Proline(P)	0.033	0.063	0.53 (0.19, 1.15)
Serine (S)	0.017	0.088	0.19 (0.05, 0.55)
Threonine (T)	0.022	0.063	0.36 (0.10, 0.90)
Tryptophan (W)	0.111	0.030	3.74 (2.32, 5.61)
Tyrosine (Y)	0.028	0.038	0.74 (0.24, 1.71)
Valine (V)	0.067	0.063	1.07 (0.56, 1.82)

Table 5.3: Amino acid frequencies in the distinctive phage clones bound by JAR 36. [a] Cys (C) residues were eliminated from the analysis because they were fixed in a subset of the phage libraries. [b] Observed frequency of each amino acid in unique peptides bound by JAR 36. [c] Expected frequency of each amino acid in the five phage libraries used. [d] Ratio between observed frequency and expected frequency and 95% confidence interval (CI) calculated from the Gaussian distribution.

In this analysis, when the ratio is greater than 1, the amino acids in the peptides are present at an higher frequency than that expected, conversely when the ratio is less than 1, the frequency is lower. The results show greatest relative abundance of Asp(D), Gly(G), Lys(K) and Trp(W) residues in the inserts, with a value $\geq$2, and Ala (A), Asn (N) and Glu (E) having a value between 1 and 1.5.

We have downloaded from the website http://pubmlst.org/neisseria/fHbp/ and then alligned, all known fHbp sequence. Tryptophan does not occur in any of known

fHbp sequence, and Glycine has only a hydrogen atom as its side chain. Consequently, we can hypothesize that the electrostatically-charged residues Aspartate (D) or Lysine (K) might contribute to the JAR 36 epitope. Since JAR 36 reacts with fHbp sequence variants containing variable E (V_E) segments from lineage 2 (Fig. 5.2), we focused our attention on the amino acid residues, D and K, occurring frequently in the peptide sequences, and that are located between positions 186 and 255 of fHbp ID 28. This region of fHbp contains three Aspartate (D) and six Lysine (K) residues that are conserved in V_E segments from lineage 2.

5.6 Homology modeling

To decrease the number of possible residues to be tested experimentally by site-directed mutagenesis, we examined the positions of the D and K residues in a homology model of the fHbp ID 28 protein.

In the Protein Data Bank are reported three crystal structures of the full-length fHbp in the variant group 1 (Cantini *et al.*, 2009; Cendron *et al.*, 2011; Mascioni *et al.*, 2009), therefore we have performed an *Homology modeling* of the fHbp in the variant group 2 and 3 (Fig. 5.17 and 5.18).

Homology modeling, also known as *comparative modeling* of protein, refers to constructing an atomic-resolution model of the "target" protein from its amino acid sequence and an experimental three-dimensional structure of a related homologous protein (the "template"). *Homology modeling* relies on the identification of one or more known protein structures likely to resemble the structure of the query sequence, and on the production of an alignment that maps residues in the query sequence to residues in the template sequence. It has been shown that protein structures are more conserved than protein sequences amongst homologues, but sequences falling below a 20% sequence identity can have very different structure (Chothia, 1986).

The homology modeling procedure can be broken down into four sequential steps:

- template selection;
- target-template alignment;
- model construction;
- model assessment.

To perform the modeling we have used the software MOE 2010.10 (Chemical Computing Group). MOE-searchPDB searches for protein structures that are homologous to a query sequence. The software uses a two stage strategy.

First, a fast scanner is performed to create an initial list of candidates. The initial scan is performed using a version of the Fasta methodology (Pearson, 1996). Any family containing at least one high-scoring sequence is placed on the list of candidates for further inspection and an expectation value (*E-value*) is determined for each sequnce.

Second, the list is than narrowed by *Z-Score* evaluations. The list is sistematically reduced using pre-defined thresholds. For each family, the best E-value of all of its sequences is compared to two values: *E-value Cutoff* and *E-value Accept*.

- if the *E-value* is higher than *E-value Cutoff*, the family is rejected;
- if the *E-value* is lower than *E-value Accept*, the family is accepted and reported without any further evaluations. In this case, the word "Good" is shown in the *Z-Score* column of the *Results* list;
- if the *E-value* is between *E-value Accept* and *E-value Cutoff*, the *Z-Score* for the family is calculated.

After loading the "target" protein sequnce, we have performed search of the homologous families. In the *Results* list we found three hits reported. Among them we chose that with ID 2KDY.A (corresponding to the crystal structure reported by Mascioni *et al.* (2009)) and its amino acid sequence was aligned to the fHbp ID 28 sequence. Aspected, their homology ratio was high (65%). Using the command *Homology/Homology modeling*, the model was generated . The software chooses automatically as "template" the sequence without atomic coordinates and vice versa for the "target". To calculate the force-field the software Amber 99 (Wang *et al.*, 2001) was used. Following the same procedure, it was obtained the model of fHbp varinat group 2 (ID 19).

5.7 Site-specific mutagenesis of D and K residues

Six of these eight residues of D and K conserved in the segment V_E, occur in two clusters in the fHbp. Cluster 1 includes K199, D201 and K203 on one end of the C-terminal structural domain, and Cluster 2 includes D211, K241 and K245 on the other end of the same domain. In collaboration with the group of Dr. Dan Granoff at the

Figure 5.17: *Homology modeling* of the fHbp in the variant group 2 (ID 19).

Figure 5.18: *Homology modeling* of the fHbp in the variant group 3 (ID 28).

Center for Immunobiology and Vaccine Development (Children's Hospital Oakland, CA, USA), site-specific mutagenesis experiments were perfomed.

The codons for residues K199, D201 or K203 in Cluster 1 were substituted with alanine (A), and the corresponding fHbp mutants were expressed and purified. In ELISA, JAR 36 resulted to be reactive with wild-type fHbp ID 28 and the K199A and K203A mutants but not with the D201A mutant (Fig. 5.19). As a positive control, to demon-

strate that D201 mutant was normally adsorbed to the wells of the microtiter plate, in parallel it was also tested the binding of anti-fHbp mAb JAR 33, which reacted similarly with the native ID 28 and all the three mutants (Fig. 5.20).

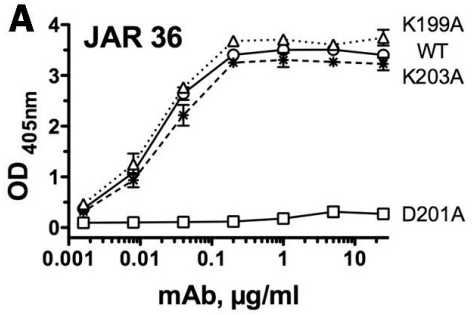

Figure 5.19: binding of mAb JAR 36 to fHbp ID 28 wild-type (WT, open circles) K199A (open triangles), D201A (open squares) and K203A (asterisks) mutants.

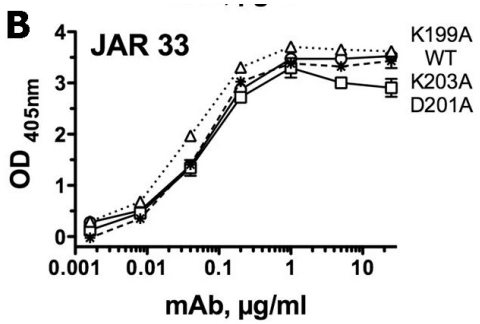

Figure 5.20: binding of control mAb JAR 33 to fHbp ID 28 wild-type (WT, open circles) K199A (open triangles), D201A (open squares) and K203A (asterisks) mutants.

Alanine substitutions of the any of three residues, in Cluster 2, had no effect on binding of JAR 31 by Western blotting or ELISA.

Since JAR 36 was previously shown to inhibit binding of human fH (Beernink *et al.*, 2008), we also analysed the crystal structure of fHbp-fH complex (PDB ID 2W80) by using the software MOE 2010.10. The results of the ligand interaction show that nineteen residues in the fHbp make contacts with the fH (Table 5.4).

The interaction types are shown in the figures 5.21, 5.22, 5.23 and 5.24.

As shown in figure 5.25, the fHbp-fH complex is held together by extensive interactions that involve both the N-terminal and C-terminal domains; however, most of fHbp contact residues are localized in the N-terminal domain including the residue D201. For this reason it was also tested the binding of fH to the fHbp mutants of Cluster 1.

fHbp	fH
Arg106	Cys357
Asp181	Lys405
Gln180	Tyr390
His184	His402
Lys191	Ser367-Ser365
Arg195	Tyr368
Gln103	His337
Gln193	Ser367
Ile199	Met340
Lys107	Glu359
Ser185	Gly403
Asp262	Tyr344
Asp266	Asn339
Glu283	Lys351
Ser274	Met340
Val272	Tyr344
Gly285	Lys351
Ser286	Lys351
Glu304	Arg341-Ser354-Tyr352

Table 5.4: name and positions of residue interactions in the fHbp-fH binding-site (according to the atomic coordinates of crystal structure PDB ID 2W80).

Binding of fH to the D201A and K203A mutants is not significantly different from the native ID 28 protein (Figure 5, Panel D) likely because the residue D201 does not establish strong interactions with the fH. In contrast and unexpectedly, binding of fH to the K199A mutant is lower than that to the native protein. This latter substitution probably influences the interaction of the neighboring residue D197 that, differently from D201, establishes strong interaction with a Tyrosine in position 344 in fH.

Thus, the amino acid residue D201, which affects binding of the JAR 36 mAb, while not decreasing fH binding, is in proximity of the fH-binding site.

As reported previously by Beernink *et al.* (2008), pairs of mAbs were bactericidal when at least one mAb inhibited binding of fH to fHbp and when the distance between residues affecting the epitopes was between 16 and 20 Å. Since JAR 36 was shown to

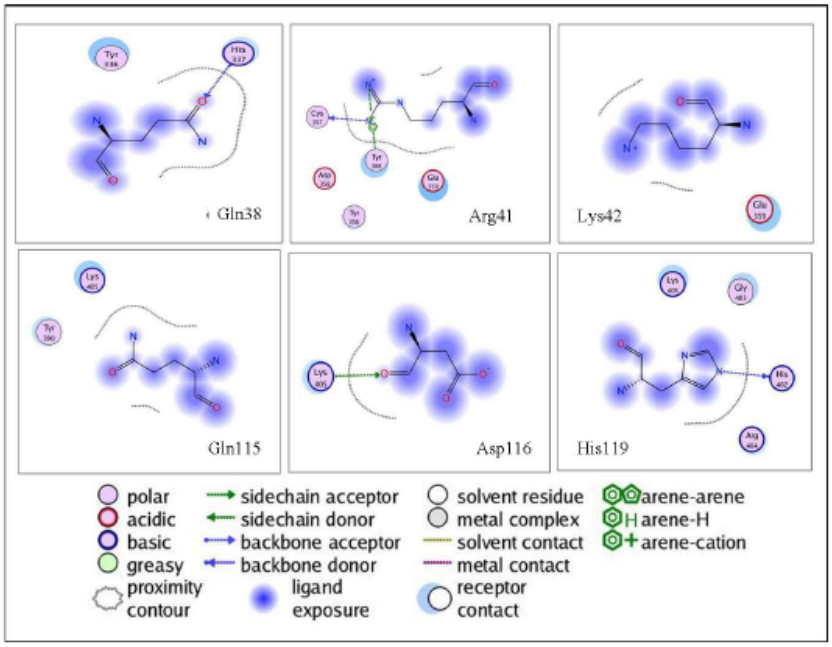

Figure 5.21: interactions of the fHbp n-terminal residues with the fH. The numbering of residues is according to the fHbp sequence ID 1.

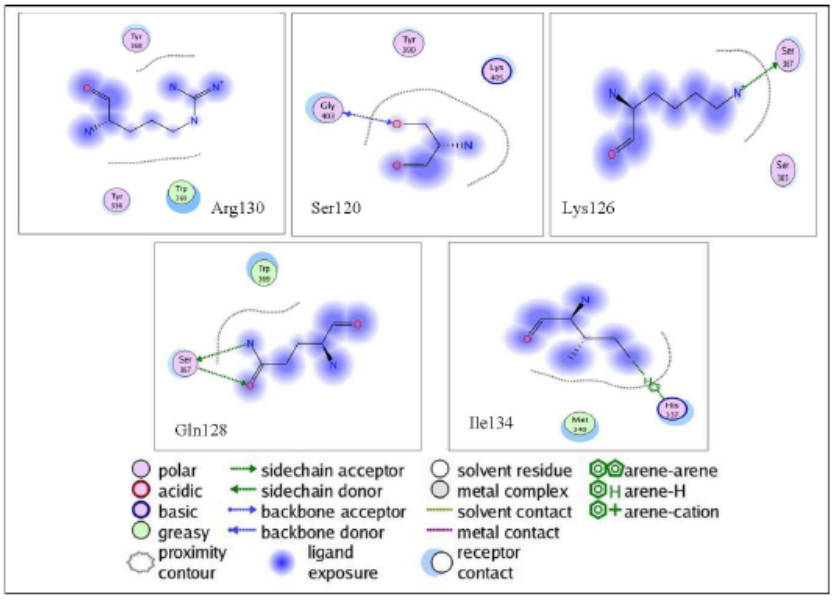

Figure 5.22: interactions of the fHbp n-terminal residues with the fH. The numbering of residues is according to the fHbp sequence ID 1.

be bactericidal when assayed with JAR 11 or JAR 13, we have measured the distances

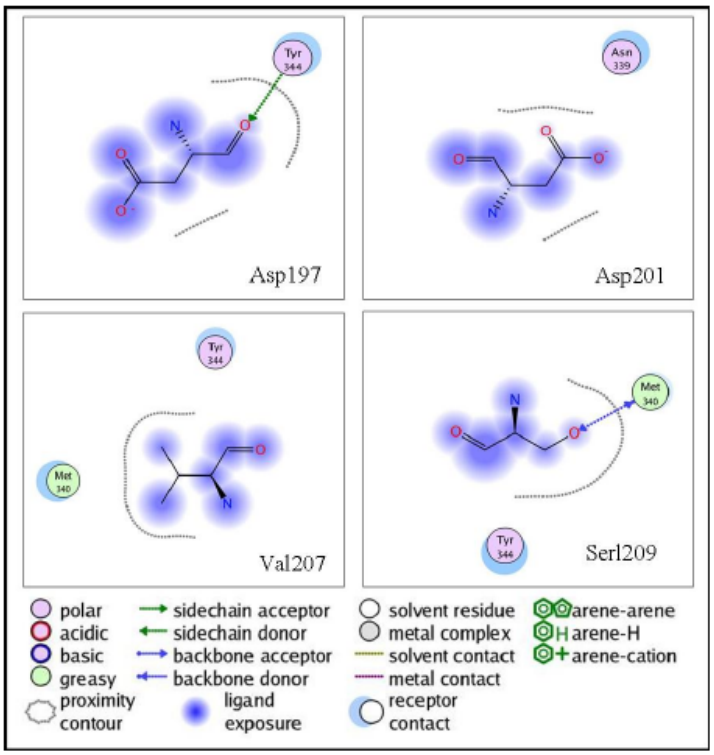

Figure 5.23: interactions of the fHbp c-terminal residues with the fH. The numbering of residues is according to the fHbp sequence ID 1.

between D201 and their epitopes. The analysis was extended to other pairs of antibodies (Table 5.5).

5.8 "In silico" epitope prediction

Despite phage display technology has become an epitope mapping experimental method widely used, it is often difficult identify with precision the actual epitope mimicked by mimotopes because, although they show a specific binding activity, comparable to that of the original antigen, they often (especially in the casa of structural and/or discontinuous epitopes) do not share obvius sequence similarities. For this reason a number of computational resources were developed for mimotope-based epitope prediction.

The first work combining computational methods and experimental results to identify epitopes from mimotope sequences was reported in 1995 (Pizzi *et al.*, 1995). Since then several computational resources, based on different approaches, have been developed. However, they often provide several alternative solutions to the putative epitope,

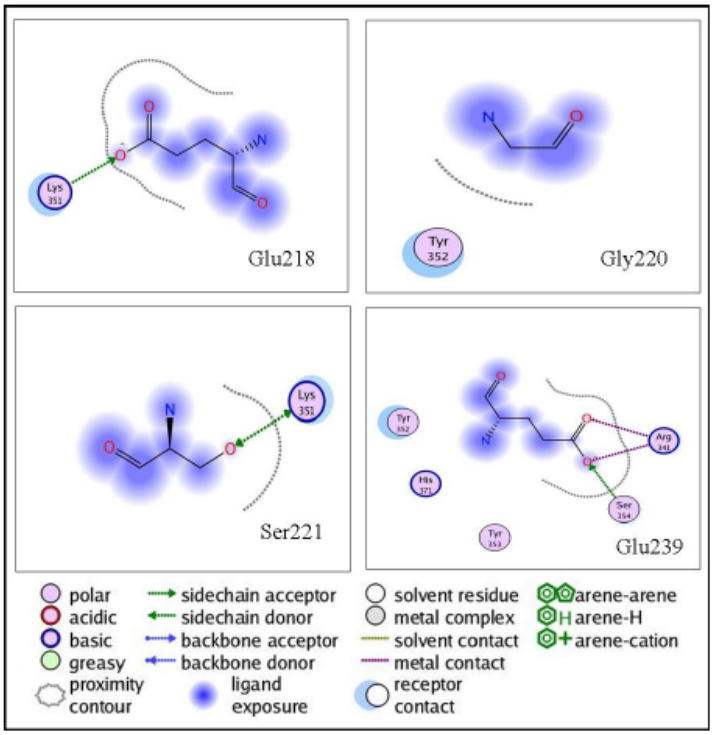

Figure 5.24: interactions of the fHbp c-terminal residues with the fH. The numbering of residues is according to the fHbp sequence ID 1.

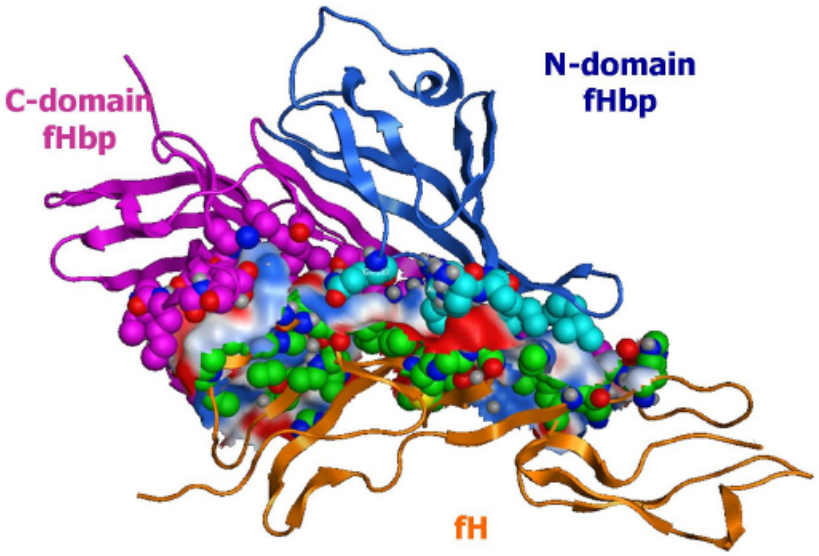

Figure 5.25: cartoon representation of fHbp-fH binding site.

	Distance (Å)[a]				
JAR MAb *pair*[b]	(*A*)[c]	(*B*)[d]	(*C*)[e]	(*D*)[f]	Cooperative *activity*[g]
JAR 10/33-JAR 11					yes
K180-A174	18.8	18.8	20.7	21.1	
E192-A174	19.6	19.2	21.1	20.6	
JAR 10/33-JAR 32/35					yes
K180-K174	18.8	18.8	20.7	21.1	
E192-K174	19.6	19.2	21.1	20.6	
JAR 3/5-JAR 10					no
G121-K180	45.4	45.5	44.5	42.4	
G121-E192	46.2	43.3	44.5	43.0	
JAR 13-JAR 11					no
S216-A174	27.4	22.3	30.5	29.3	
JAR 13-JAR 32/35					no
S216-K174	27.4	22.3	30.5	29.3	
JAR 13-JAR 10/33					no
S216-K180	12.3	12.0	11.5	11.7	
S216-E192	8.5	8.0	15.4	15.6	
JAR 3/5-502					yes
G121-R204	50.0	44.3	46.8	45.1	
JAR 36-JAR 11					yes
D201-A174	19.6	17.7	16.7	16.5	
JAR 36-JAR 13					yes
D201-S216	29.0	28.2	32.4	32.6	

Table 5.5: [a] Distances between the pairs of the MAbs calculated between alpha-carbon positions for the respective residues using MOE (Chemical Computing Group). [b] The numbering of the residues is based on the amino acid sequence of MC58 v.1 fHbp. [c] Distance calculated on the crystal structure PDB ID 2KC0. [d] Distance calculated on the crystal structure PDB ID 3KVD. [e] Distance calculated on the homology model of fHbp v.2. [f] Distance calculated on the homology model of fHbp v.3. [g] As reported by Beernink *et al.* (2008).

and some of them rely more on information regarding mimotope sequences than on relationships between protein surface characteristics and features of every peptide.

We have used a recently introduced computer program named LocaPep (Pacios *et al.*, 2011). It uses an algorithm that focuses on protein structure surface features for predicting potential epitopes from the input given by phage display selected peptides . LocaPep is written in Fortran90 and runs in commmand-line mode.

The program starts reading an input file named "locapep.inp". The first line specifies the name of the file with the 3D protein structure in PDB format. The four following lines give values for parameters that control run options: KRun, KSea, KMin, and KPrn (Fig. 5.26).

KRun controls whether the SES (solvent-excluded surface) is calculated (KRun = 0) or the surface data from a previous run are read instead (KRun $\neq$0). KSea selects the strategy to organize the searching process in the clusters algorithm. KMin sets the minimum number of residues localized in a cluster to consider it valid. KPrn is a parameter that only controls the amount of printing in output. The last line (NSeq) gives the number of peptide sequences to be read.

```
fHbp_v3.pdb
0              ! KRun
0              ! KSea
0              ! KMin
0              ! KPrn
15             ! NSeq
AKWCAQFCqGYL
AKWCNLWCTWVG
GKQCAAWCEWFA
GKGCTRRGCDVD
WSDKDRNLWGLWYRE
qARCIVEECKWA
LGWCGDGLCKGV
NKFVSLGLA
QKWFALGAPWYD
WNINWGKPTRDE
GKWCLLVDCNRD
RPGPGDIDI
KVCQLWGNNCGE
GCGKWELDGCAA
VRSKWGEVGRPYDVV
```

Figure 5.26: input file created to analyse the peptides selected with mAb JAR 36 by LocaPep; the homology model structure of fHbp variant 3 was used for the analysis.

In our case, the output file reports a total of seventeen residues as possible epitope of JAR 36. The interesting result is that eight of these residues (E192, L193, A194, V207, L209, R213, Y214 and G215) resided in the V_E segment and four of them (E192, L209,

R213 and G215) are conserved in V_E segments from lineage 2 and close to fHbp-fH bindig site (Fig. 5.27 and 5.28).

```
                195        205        215        225        235        245        255
E.2.6   TLEQNVELAA AELKADEKSH AVILGDTRYG SEEKGTYHLA LFGDRAQEIA GSATVKIGEK VHEIGIAGKQ
E.2.2   TPEQNVELAA AELKADEKSH AVILGDTRYG SEEKGTYHLA LFGDRAQEIA GSATVKIGEK VHEIGIAGKQ
E.2.1   TPEQNVELAS AELKADEKSH AVILGDTRYG GEEKGTYHLA LFGDRAQEIA GSATVKIREK VHEIGIAGKQ
E.2.4   TPEQNVELAS AELKADEKSH AVILGDTRYG SEEKGTYHLA LFGDRAQEIA GSATVKIGEK VHEIGIAGKQ
E.1.8   SPELNVDLAA ADIKPDGKRH AVISGSVLYN QAEKGSYSLG IFGGKAQEVA GSAEVKTVNG IRHIGLAAKQ
E.1.4   SPELNVDLAA ADIKPDEKHH AVISGSVLYN QAEKGSYSLG IFGGQAQEVA GSAEVETANG IRHIGLAAKQ
```

Figure 5.27: amino acid sequences of the six distinct variable E (V_E) segments. The eight residues predicted by LocaPep are highlighted in yellow.

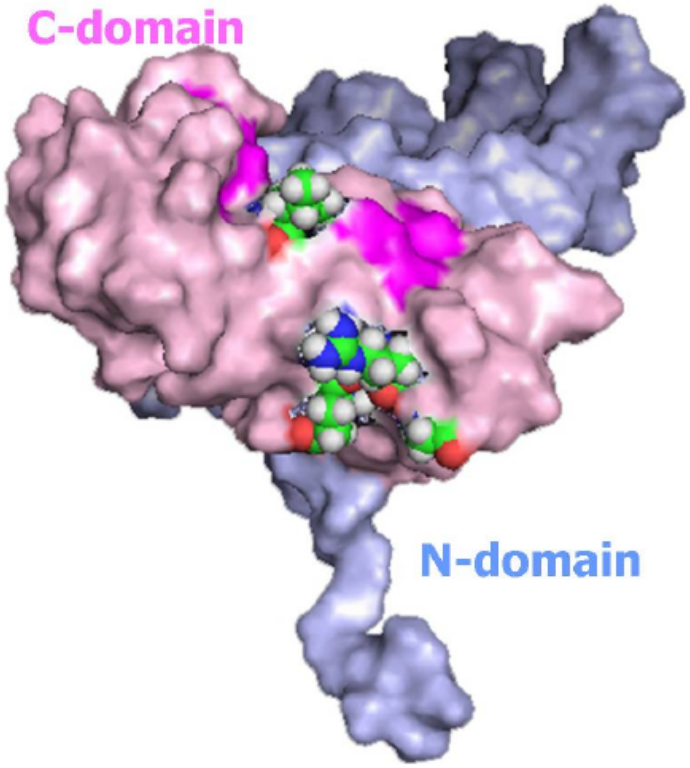

Figure 5.28: location on fHbp variant 3 of the four conserved residues predicted by LocaPep to affect binding of the JAR 36 mAb. The deep pink area indicates the fH-fHbp binding site in C-terminal domain.

Chapter 6

Discussion

Neisseria meningitidis causes severe, often fatal, septicemia and meningitis. Despite serogroup B of *N. meningitidis* is responsible of 50% of meningococcal-disease cases worldwide, it is the only serogroup whose infection is not yet vaccine-preventable. Instead, conjugate vaccines are available for preventing diseases caused by pathogenic serogroups A, C, Y, and W-135 in adolescents 11 years of age or older and adults 55 years of age or younger (Centers for Disease Control and Prevention, 2005).

The above conjugate approach cannot be easily applied to serogroup B because the capsular polysaccharide is a polymer of $\alpha(2\rightarrow8)$N-acetyl neuraminic acid or polysialic acid, a molecule which is partly identical to a widely distributed human carbohydrate. Thus being the serogroup B polysaccharide structure correspoding to that of a self-antigen, human hosts are in general immunologically tolerant to it and therefore fail to induce an effective immune response. On the other side, an immune response against it would risk to induce autoimmunity.

Recently, an effective protein-based vaccine, containing novel antigens discovered by *reverse vaccinology*, has been proposed and is currently under late-phase clinical investigation. One of these antigens is a membrane-anchored lipoprotein of 274 amino acids known as factor H binding protein (fHbp), also called GNA1870 or lipoprotein 2086. The gene encoding fHbp is present in all meningococcal strains, however fHbp exists in at least three variant groups or two sub-families based on amino acid sequence identity and antibody cross-reactivity.

This protein binds fH, an important negative regulatory molecule in the human complement cascade. The antigen elicits serum antibodies that both directly activate classical complement pathway bacteriolysis and also block the binding of fH. If fH is not bound on the bacterial surface, the organism becomes more susceptible to bacteriolysis

mediated by the alternative complement pathway.

Recently, the amino acid residues involved in the epitopes recognized by a panel of murine bactericidal monoclonal antibodies prepared against fHbp from each of three variant groups have been identified.

In the present study we have used phage displayed random peptide libraries to identify the epitope recognized by the mAb JAR 36. Indeed, in previous studies, it was not possible to identify the amino acid residues in fHbp that are responsible for the binding of the anti-fHbp mAb JAR 36 by using multiple sequence alignments, because this mAb reacts with all of the fHbp sequences tested from variant groups 2 and 3.

The phage display technology allows to select from a set of random peptide those which specifically bind to an Ab. The selected peptides are assumed to mimic the epitope in terms of spatial organization and physicochemical properties. In practice, the mimotopes and Ag are both recognized by the same Ab paratope, therefore mimotopes imitate the natural epitope. The power of phage display technology is that of allowing to screen, in a small volume, a number of peptide very large (10^8) moreover, the phage displayed ligands are physically associated with their genetic information which can be easily determined.

In this work we have used five different libraries, composed of random 9-mers, 12-mers and 15-mers fused to the N-terminal region of the major coat protein (pVIII) of filamentous phage. Fifteen peptides were isolated for their ability to bind the mAb JAR 36. Positive phage clones, carrying the specific peptides, were identified through several rounds of affinity selection, by using JAR 36 as target. The libraries were selected using two methods: dynabeads and biopanning. The phage pools selected through the two methods described, were tested in ELISA to verify their enrichment in phage particles reacting with the mAb JAR 36. The combined use of the dynabeads and biopanning was expected to help in minimizing the risk to select non-specific clones. However, the method with dynabeads alone has allowed us to select the phage particles with higher reactivity with JAR 36.

After three rounds of affinity selection, positive phage clones were identified through immunoscreening and positive phage recovery. Phage clones, tested in ELISA, show good reactivity with JAR 36, indicating their ability to mimic the original epitope of the mAb. The JAR 36 concentration to be used for detect its reactivity either with the phage pools and the single clones, was determined through a calibration curve. The libraries pVIII-9aa and pVIII-9aa.Cys allowed to select the larger number of clones, probably because the small size of peptides allows a more efficient expression on phage surface, consequently

these particles show stronger binding to the mAb. The peptides with the highest OD value in ELISA were selected from the constrained libraries. In these libraries, the presence of two cysteines in the peptide sequences represent a collection of disulphide constrained loops having different size. The peptides are presented in a cyclic and therefore more constrained conformation, which could strengthen binding with the mAb in comparison to a flexible linear peptide.

The amino acid sequence of the specific peptides was deduced by sequencing the DNA encoding for the insert of the positive clones. To avoid sequencing of phage particles carrying the same insert, for the pVIII-15aa library two additional primers were specifically sinthesized. The primer forward is complementary to the sequence that includes both the vector and the insert coding for the 15-mer peptide. Therefore, this primer can only amplify clones carrying this insert, while the samples not amplified by these two primers contain inserts with different sequences.

From the comparison of amino acid composition, obtained by the characterization of the nucleotide sequence of the positive clones inserts, it was not feasible to identify a clear consensus sequence common to the different peptides, therefore suggesting that the JAR 36 epitope is discontinuous and not linear.

With the aim of identifying the aminoacid residues critical for the interaction with the antibody, the observed frequency in the mimotopes was normalized by calculating, for every aminoacid, the ratio with the expected frequency in the libraries. The results show a higher abundance of Asp(D), Gly(G), Lys(K) and Trp(W) residues in the inserts, with a value $\geq$2, and Ala (A), Asn (N) and Glu (E) having a value between 1 and 1.5. The tryptophan residue is absent in all the fHbp sequences, whereas it has a very high frequency in the peptides. It very likely mimics a different amino acid present in the natural protein sequence, and/or helps folding of the peptide into the active conformation, suitable for antibody binding.

We have then analysed the presence of the above amino acid residues, found to be more abundant in the selected peptides, in the sequences of fH binding proteins belonging to different strains of *Neisseria meningitidis*. From the data of reactivity of JAR 36 with different variants of the protein, together with the comparison of homology in their amino acid composition, we hypothesized that the epitope recognized by JAR 36 mAb is residing in variable segment E (V_E) derived from lineage 2. Therefore our attention was focused on the regions that are conserved in the 2 and 3 variants (both recognized by JAR 36) of the variable E (V_E) segment, comprising the residues from 186 to 255.

Several interesting residues were identified and, considering that to be recognised

by the antibody the epitope must reside in an exposed region on the protein surface, we have verified that these residues were actually exposed to the solvent, and therefore available for interaction with the antibody JAR 36, this was obtained by examining their position in the three-dimensional structure of fHbp. To this aim an homology model for the tertiary structure of the fHbp variant 3 was made using the software MOE (Chemical Computing Group), based on a crystal structure of variant 1, the only one available in the database. The software MOE is written in a self-contained programming system, the Scientific Vector Language (SVL) and its CASP validated applications for protein structure prediction are powerful, intuitive and easy to use. In our case, the model building was made easier by the high ratio of homology shared between the different variants of the fHbp in terms of aminoacid composition. We used this information, along with reactivity with fHbp variants from different modular groups and protein structural informations, to predict residues potentially involved in the epitope recognized by JAR 36.

Using site-specific mutagenesis, it was prepared a panel of six recombinant fHbp mutants with alanine substitutions, which allowed us to identify the amino acid D201, which affects binding of JAR 36. This key residue D201 is present in the V_E segment of both JAR 36-reactive and non-reactive fHbp sequences. Therefore, it is very likely that neighboring residues affect the conformation of D201 in non-binding variants.

As previously reported, JAR 36 partially inhibits the binding of fH to fHbp. We have analyzed the crystal structure of fHbp in complex with the fH to better understand the interactions established by these two molecules. The fHbp-fH complex is held together by extensive interactions that involve both the N-terminal and C-terminal domains and that collectively form a very wide binding site. A total of nineteen residues of fHbp establish interactions with the fH. The residue D201 is included among these, but it does not establish strong interaction with fH. Therefore, its replacement with an alanine was expected to provide a fH binding not significantly different from the protein WT. In contrast and unexpectedly, binding of fH to the K199A mutant was much lower than that of the native protein. Its substitution probably influences the interaction of the neighboring residue D197 that, in contrast to D201, establishes a strong interaction with a tyrosine in position 344 in fH.

In previous studies, the properties of pairs of anti-fHbp mAbs relative to their synergistic functional activity were examined. It was reported that pairs of mAbs are bactericidal when at least one of them inhibits the binding of fH to fHbp and when the distance between the residues affecting the epitopes is between 16 and 20 Å. There is no

bactericidal activity when the distance is less than 16 Å or greater than 20 Å. Before the location of a residue contributing to the JAR 36 epitope was known, JAR 36 was shown to be bactericidal when assayed together with JAR 11 or JAR 13 against strain 8047, which expresses fHbp ID 77 in variant group 2. We have measured the distances of residues affecting the epitopes of these and other mAbs. The results show that bactericidal pairs of mAbs recognize epitopes that involve residues separated by 27 to 47 Å. Therefore, there is no obvious correlation of bactericidal versus non-bactericidal combinations with the distance of the epitopes recognized by these pairs of mAbs.

Since, as reported above, there was no obvious similarity between the affinity-selected peptides, among themselves or with the linear sequence of the antigen, we have used LocaPep, a recently introduced computer program, which uses an algorithm that focuses on the antigen surface features, by using peptides selected from phage display libraries to predict possible epitopes. A number of computational resources are available for mimotope-based epitope prediction that are based on different approaches. Findmap only works with sequence information from mimotopes and antigen. SiteLight, 3DEX, Mapitope and Pepsurf use both sequence informations and 3D structure of the antigen. The web servers MIMOX, MIMOP and Pepitope implement the two approaches described above. However, these tools often provide several alternatives that can correspond to different regions on the antigen surface, moreover some of them does not allow the analysis of peptides too long. LocaPep is written in Fortran90 and even if it runs in command line mode without a graphical user interface, it provides an easy and satisfactory tool to help in the epitope prediction. Its clusters algorithm is based on the idea that some exposed residues can act as "seeds" around which clusters of amino acids that are mimicked by the mimotopes are formed in the surface.

The results, contained in an output file, show that seventeen residues might play an important role in the binding of JAR 36 with fHbp. Eight of these residues reside in the V_E segment and four of them are common in variant groups 2 and 3.

Taking together all the results obtained in the present study, by using a phage display library screening approach, in combination with site-directed mutagenesis, we have identified the amino acid residue D201 of meningococcal factor H binding protein, affecting the epitope of mAb JAR 36. Moreover, a nearby substitution of a residue K199 with an alanine, decreases the binding of fH. We have also identified, by using a computational tool, the residues E192, L209, R213 and G215 as likely being important for binding to JAR 36. These latter results should be confirmed through site-specific mutagenesis experiments. However, either the residue D201 and the "in silico"-predicted

epitope are located in the proximity of the fH-binding site. This finding is according with experimental data, previously reported, of JAR 36 partially inhibiting binding of fH to fHbp.

A detailed knowledge of the epitopes recognized by protective antibodies is necessary for understanding the molecular mechanisms responsible for effective immune response. Particularly, the knowledge of epitope rcognized by JAR 36 is important for its ability to confer protection through dual mechanisms: by binding of the Abs to the surface of the pathogen and by blocking binding of the complement inhibitor fH. Moreover, the epitope mapping recognised by this mAb should allow us to better understand the basis of its cooperative bactericidal activity between different pairs of anti-fHbp mAbs, for the characterization of the molecular mechanism of immune protection against MenB, toward the development of safe and effective protein-based vaccines for the prevention of group B meningitis.

Bibliography

Arditi, M., Ables, L., Yogev, R. (1989). Cerebrospinal fluid endotoxin levels in children with H. influenzae meningitis before and after administration of intravenous ceftriaxone. *Journal of Infectious Disease*, **160**, 1005–1011.

Barbas III, C., Kang, A., Lerner, R., Benkovic, S. (1991). Assembly of combinatorial antibody libraries onnphage surfaces: the gene III site. *PNAS, U.S.A.*, **88**, 7978–7982.

Bass, S. H., Greene, R., Wells, J. A. (1990). Hormone phage: An enrichment method for variant proteins with altered binding properties. *Proteins*, **8**, 309–314.

Bauer, M. & Smith, G. P. (1988). Filamentous phage morphogenetic signal sequence and orientation of DNA in the virion and gene V protein comple. *Virology*, **167**, 166–175.

Beck, E. & Zink, B. (1981). Nucleotide sequence and genome organization of filamentous bacteriophages fl and fd. *Gene*, **16**, 35–58.

Beernink, P. & Granoff, D. (2009). The modular architecture of meningococcal factor H-binding protein. *Microbiology*, **155**, 2873–2883.

Beernink, P.T. & Granoff, D. (2008). Bactericidal Antibody Responses Induced by Meningococcal Recombinant Chimeric Factor H-Binding Protein Vaccines. *Infection and immunity*, **76**, 2568–2575.

Beernink, P., Welsch, J., Bar-Lev, M., Koeberling, O., Comanducci, M., Granoff, D. (2008). Fine antigenic specificity and cooperative bactericidal activity of monoclonal antibodies directed at the meningococcal vaccine candidate, factor H-binding protein. *Infection and Immunity*, **76**, 4232–4240.

Beernink, P., LoPasso, C., Angiolillo, A., Felici, F., Granoff, D. (2009). A region of the N-terminal domain of meningococcal factor H-binding protein that elicits bactericidal antibody across antigenic variant groups. *Molecular Immunology*, **46**, 1647–1653.

Beernink, P. T., Leipus, A., Granoff, D. M. (2006). Rapid genetic grouping of factor H-binding protein (genome-derived neisserial antigen 1870), a promising group B meningococcal vaccine candidate. *Clinical and Vaccine Immunology*, **13**, 758–763.

Bjune, G., Hoiby, E., Gronnesby, J., Arnesen, O., Fredriksen, J., Halstensen, A., Holten, E., Lindbak, A., Nokleby, H., Rosenqvist, E., et al. (1991). Effect of outer membrane vesicle vaccine against group B meningococcal disease in Norway. *Lancet*, **338**, 1093–1096.

Boeke, J.D. & Model, P. (1982). A prokaryotic membrane anchor sequence: carboxyl terminus of bacteriophage f1 gene III protein retains it in the membrane. *PNAS, U.S.A.*, **79**, 5200–5204.

Boslego, J., Garcia, J., Cruz, C., Zollinger, W., Brandt, B., Ruiz, S., Martinez, M., Arthur, J., Underwood, P., Silva, W., et al. (1995). Efficacy, safety, and immunogenicity of a meningococcal group B (15:P1.3) outer membrane protein vaccine in Iquique, Chile. *Vaccine*, **13**, 821–829.

Brandtzaeg, P. (2006). *Pathogenesis and pathophysiology of invasive meningococcal disease. Handbook of Meningococcal Disease: Infection Biology, Vaccination, Clinical Management.* Wiley-VCH, Weinheim.

Cantini, F., Savino, S., Scarselli, M., Masignani, V., Pizza, M., Romagnoli, G., Swennen, E., Veggi, D., Banci, L., Rappuoli, R. (2006). Solution structure of the immunodominant domain of protective antigen GNA1870 of Neisseria meningitidis. *Journal of Biological Chemistry*, **281**, 7220–7227.

Cantini, F., Veggi, D., Dragonetti, S., Scarselli, M., Romagnoli, G., Pizza, M., Banci, L., Rappuoli, R. (2009). Solution structure of the factor H-binding protein, a survival factor and protective antigen of Neisseria meningitidis. *Journal of Biologcal Chemistry*, **284**, 9022–9026.

Cartwright, K. (1995). Meningococcal Carriage and Disease. *John Wiley & Sons, Chichester.*

Caugant, D. (2008). Genetics and evolution of Neisseria meningitidis: importance for the epidemiology of meningococcal disease. *Infection, Genetics and Evolution*, **8**, 558–565.

Cendron, L., Veggi, D., Girardi, E., Zanotti, G. (2011). Structure of the uncomplexed Neisseria meningitidis factor H-binding protein fHbp (rLP2086). *Acta crystallographica. Structural Biology and Cristallization communications.*, **67**, 531–535.

Centers for Disease Control and Prevention (2005). Prevention and Control of meningococcal disease: reccomendations of the Advisory Committee on Immunization Practices (ACIP). *Morbidity and Mortality Weekly Report (MMWR)*, **54**, 1–21. http://www.cdc.gov/mmwr/preview/mmwrhtml/rr5407a1.htm.

Cesareni, G., Castagnoli, L., Dente, L., Iannolo, G., Vetriani, C., Felici, F., LuzzagoA., Monaci, P., Nicosia A., Cortese, R. (1995). Construction and utilization of peptide libraries displayed by filamentous bacteriophage. In: Immunological recognition of peptides in medicine and biology. *CRC Press*, pp. 43–59.

Cesareni, G. & Murray, J. (1987). Plasmid vectors carryng the replication origin of filamentous single stranded phage. *Genetic Engineering: principles and methods*, **8**, 135.

Chothia, C. & Lesk, A. (1986). The relation between the divergence of sequence and structure in proteins. *The EMBO Journal*, **5**, 823–826.

Claus, H., Vogel, U., Muhlenhoff, M., Gerardy-Schahn, R., Frosch, M. (1997). Molecular divergence of the sia locus in different serogroups of Neisseria meningitidis expressing polysialic acid capsules. *Molecular and General Genetics*, **257**, 28–34.

Connor, S., Morse, A., Thomson, M. (2003). Environmental risk and meningitis epidemics in Africa. *Emerging Infectious Diseases Journal*, **9**, 1287–1293.

Cwirla, S. E., Peters, E. A., Barrett, R. W., Dower, W. J. (1990). Peptides of phage: A vast library of peptides for identifying ligands. *PNAS, U.S.A.*, **87**, 6378–6382.

De la Cruz, V., Lal, A., McCutchan, T. (1988). Immunogenicity and epitope mapping of foreign sequences via genetically engineered filamentous phage. *Journal of Biological Chemistry*, **263**, 4318–4322.

DeLano, W. (2006). The PyMOL Molecular Graphics System. *DeLano Scientific, San Carlos, CA, USA*.

Dente, L., Cesareni, G., Cortese, R. (1983). pEMBL: a new family of single stranded plasmids. *Nucleic Acids Research*, **11**, 1645–1655.

Deroo, S. & Muller, C. (2001). Antigenic and immunogenic phage displayed mimotopes as substitute antigens: Applications and limitations. *Combinatorial Chemistry & high throughput creening*, **4**, 75–101.

Devlin, J. J., Panganiban, L. C., Devlin, P. E. (1990). Random peptide libraries: A source of specific protein binding molecules. *Science*, **249**, 404–406.

Endemann, H. & Model, P. (1995). Location of filamentous phage minor coat proteins in phage and in infected bacteria. *Journal of Molecular Biology*, **250**, 496–506.

Felici, F., Castagnoli, L., Musacchio, A., Jappelli, R., Cesareni, G. (1991). Selection of antibody ligands froma large library of oligopeptides expressed on amultivalent exposition vector. *Journal of Molecular Biology*, **222**, 301–310.

Felici, F., Luzzago, A., Folgori, A., Cortese, R. (1993). Mimicking of discontinuous epitopes by phage-displayed peptides, II. Selection of clones recognized by a protective monoclonal antibody against the Bordetella pertussis toxin from phage peptide libraries. *Gene*, **128**, 21–27.

Felici, F., Luzzago, A., Monaci, P., Nicosia, A., Sollazzo, M., Traboni, C. (1995). Peptide and protein display on the surface of filamentous bacteriophage. *Biotechnology Annual Review*, **1**, 149–183.

Finne, J., Leinonen, M., Makela, P. (1983). Antigenic similarities between brain components and bacteria causing meningitis. Implications for vaccine development and pathogenesis. *Lancet*, **2**, 355–357.

Finne, J., Bitter-Suermann, D., Goridis, C., Finne, U. (1987). An IgG monoclonal antibody to group B meningococci cross-reacts with developmentally regulated polysialic acid units of glycoproteins in neural and extraneural tissues. *Journal of Immunology*, **138**, 4402–4407.

Fletcher, L. D., Bernfield, L., Barniak, V., Farley, J. E., Howell, A., Knauf, M., Ooi, P., Smith, R. P., Weise, P., et al. (2004). Vaccine potential of the Neisseria meningitidis 2086 lipoprotein. *Infection and Immunity*, **72**, 2088–2100.

Frosch, M., Weisgerber, C., Meyer, T. F. (1989). Molecular characterization and expression in Escherichia coli of the gene complex encoding the polysaccharide capsule of Neisseria meningitidis group B. *PNAS, U.S.A.*, **86**, 1669–1673.

Fulford, W. & Model, P. (1984). Gene X of bacteriophage fl is required for phage DNA synthesis: Mutagenesis of in-frame overlapping gene. *Journal of molecula Biology*, **178**, 137–153.

Gagneux, S., Hodgson, A., Smith, T., Wirth, T., Ehrhard, I., Morelli, G. (2002). Prospective study of a serogroup X Neisseria meningitidis outbreak in northern Ghana. *Journal of Infectious Diseases*, **185**, 618–626.

Gao, C., Lin, C., Lo, C., Mao, S., Wirsching, P., Lerner, R., Janda, K. (1997). Making chemistry selectable by linking it to infectivity. *PNAS, U.S.A.*, **94**, 11777–11782.

Gao, C., Mao, S., Kaufmann, G., Wirsching, P., Lerner, R., Janda, K. (2002). A method for the generation of combinatorial antibody libraries using pIX phage display. *PNAS, U.S.A.*, **99**, 12612–12616.

Giuliani, M., Adu-Bobie, J., Comanducci, M., et al. (2006). A universal vaccine for serogroup B meningococcus. *PNAS, U.S.A*, **103**, 10834–10839.

Goldschneider, I., Gotschlich, E., Artenstein, M. (1969). Human immunity to the meningococcus. II. Development of natural immunity. *The Journal of Experimental Medicine*, **129**, 1327–1348.

Gotschlich, E., Liu, T., Artenstein, M. (1969). Human immunity to the meningococcus. Preparation and immunochemical properties of the group A, group B, and group C meningococcal polysaccharides. *The Journal of Experimental Medicine*, **129**, 1349–1365.

Granoff, D. (2010). Review of meningococcal group B vaccines. *Clinical Infectious Disease*, **50**, 54–65.

Granoff, D., Welsch, J., Ram, S. (2009). Binding of complement factor H (fH) to Neisseria meningitidis is specific for human fH and inhibits complement activation by rat and rabbit sera. *Infection and Immunity*, **77**, 764–769.

Gray, C. W. (1989). Three-dimensional structure of complexes of single-stranded DNA-binding proteins with DNA. IKe and fd gene 5 proteins from left-handed helices with single-stranded DNA. *Journal of Molecula Biology*, **208**, 57–64.

Greenwood, J., Willis, A., Perham, R. (1991). Multiple display of foreign peptides on a filamentous bacteriophage. Peptides from Plasmodium falciparum circumsporozoite protein as antigens. *Journal of Molecular Biology*, **220**, 821–827.

Griffiths, A., Malmqvist, M., Marks, J., Bye, J., Embleton, M., McCafferty, J., Baier, M., Holliger, K., Gorick, B., Hughes-Jones, N., et al. (1993). Human anti-self antibodies with high specificity from Ephage display libraries. *EMBO Journal*, **12**, 725–734.

Hill, D. F. & Petersen, G. (1982). Nucleotide sequence of bacteriophage fl DNA. *Journal of Virology*, **44**, 32–46.

Holliger, P., Riechmann, L., Williams, R. (1999). Crystal structure of the two N-terminal domains of g3p from filamentous phage fd at 1.9 A: evidence for conformational lability. *Journal of Molecular Biology*, **288**, 649–657.

Hufton, S., Moerkerk, P., Meulemans, E., de Bruïne, A., Arends, J., Hoogenboom, H. (1999). Phage display of cDNA repertoires: the pVI display system and its applications for the selection of immunogenic ligands. *Journal of Immunological methods*, **231**, 39–51.

Iannolo, G., Minenkova, O., Petruzzelli, R., Cesareni, G. (1995). Modifying filamentous phage capsid: limits in the size of the major capsid protein. *Journal of Molecular Biology*, **248**, 835–844.

Ilìchev, A., Minenkova, O., Tatìkov, S., et al. (1989). Production of a viable variant of the M13 phage with a foreign peptide inserted into the basic coat protein. *Dokl Akad Nauk SSSR*, **307**, 481.

Kaplan, S. (1999). Clinical manifestations, diagnosis, and prognostic factors of bacterial meningitis. *Infectious Disease Clinics of North America*, **13**, 579–590.

Krogh, A., Larsson, B., von Heijne, G., Sonnhammer, E. (2001). Predicting transmembrane protein topology with a hidden Markov model: application to complete genomes. *Journal of Molecular Biology*, **305**, 567–580.

Leib, S.L. & Tauber, M. (1999). Pathogenesis of bacterial meningitis. *Infectious Disease Clinics of North America*, **13**, 527–548.

Lepow, M., Beeler, J., Randolph, M., Samuelson, J., Hankins, W. (1986). Reactogenicity and immunogenicity of a quadrivalent combined meningococcal polysaccharide vaccine in children. *Journal of Infectious Diseases*, **154**, 1033–1036.

Løset, G., Roos, N., Bogen, B., Sandlie, I. (2011). Expanding the versatility of phage display II: improved affinity selection of folded domains on protein VII and IX of the filamentous phage. *PLoS One*, **6**, 17433.

Lubkowski, J., Hennecke, F., Pluckthun, A., Wlodawer, A. (1998). The structural basis of phage display elucidated by the crystal structure of the N-terminal domains of g3p. *Nature Structural Biology*, **5**, 140–147.

Luzzago, A., Felici F, Tramontano, A., Pess, i. A., Cortese, R. (1993). Mimicking of discontinuous epitopes by phage-displayed peptides, I. Epitope mapping of human H ferritin using a phage library of constrained peptides. *Gene*, **128**, 51–57.

Luzzago, A. & Felici, F. (1998). Construction of disulfide-constrained random peptide libraries displayed on phage coat protein VIII. *Methods in Molecular Biology*, **87**, 155–164.

Madico, G., Welsch, J., Lewis, L., McNaughton, A., Perlman, D., Costello, C., Ngampasutadol, J., Vogel, U., Granoff, D., Ram, S. (2006). The meningococcal vaccine candidate GNA1870 binds the complement regulatory protein factor H and enhances serum resistance. *Journal of Immunology*, **177**, 501–510.

Maiden, M., Bygraves, J., Feil, E., et al. (1998). Multilocus sequence typing: a portable approach to the identification of clones within populations of pathogenic microorganisms. *PNAS, U.S.A.*, **95**, 3140–3145.

Marvin, D., Welsh, L., Symmons, M., Scott, W., Straus, S. (2006). Molecular structure of fd (f1, M13) filamentous bacteriophage refined with respect to X-ray fibre diffraction and solid-state NMR data supports specific models of phage assembly at the bacterial membrane. *Journal of Molecula Biology*, **355**, 294–309.

Mascioni, A., Bentley, B., Camarda, R., Dilts, D., Fink, P., Gusarova, V., Hoiseth, S., Jacob, J., Lin, S., Malakian, K., McNeil, L., Mininni, T., Moy, F., Murphy, E., Novikova, E., Sigethy, S., Wen, Y., Zlotnick, G., Tsao, D. (2009). Structural Basis for the Immunogenic Properties of the Meningococcal Vaccine Candidate LP2086. *Journal of Biological Chemistry*, **284**, 8738–8746.

Masignani, V., Comanducci, M., Giuliani, M., Bambini, S., Adu-Bobie, J., Arico, B., et al. (2003). Vaccination against Neisseria meningitidis using three variants of the lipoprotein GNA1870. *The Journal of Experimental Medicine*, **197**, 789–799.

McDonnell, P. A., Shon, K., Kim, Y., Opella, S. J. (1983). fd coat protein structure in membrane environments. *Journal of Molecular Biology*, **233**, 447–463.

Mertsola, J., Ramilo, O., Mustafa, M., et al. (1989). Release of endotoxin after antibiotic treatment of gram negative bacterial meningitis. *Pediatric Infectious Disease Journal*, **8**, 904–906.

Model, P. & Russel, M. (1988). Filamentous bacteriophage. In "The Bacteriophages". *R. Calendar, ed.*, **2**, 375–456.

Oldenburg, K., Loganathan, D., Goldstein, I., Schultz, P., Gallop, M. (1992). Peptide ligands for a sugar-binding protein isolated from a random peptide library. *PNAS, U.S.A.*, **89**, 5393–5397.

Pace, D., Pollard, A., Messonier, N. (2009). Quadrivalent meningococcal conjugate vaccines. *Vaccine*, **27**, B30–B41.

Pacios, F. L., Tordesillas, L., Palacín, A., Sanchez-Monge, R., Salcedo, G., Díaz-Perales, A. (2011). LocaPep: Localization of Epitopes on Protein Surfaces Using Peptides from Phage Display Libraries. *Journal of Chemical Information and Modelling*, **51**, 1465–1473.

Parmley, S. E & Smith, G. E. (1988). Antibody-selectable filamentous fd phage vectors: Affinity purification of target genes. *Gene*, **73**, 305–318.

Pearson, W. (1996). Effective protein sequence comparison. *Methods in Enzimology*, **266**, 227–258.

Perrett, K., Snape, M., Ford, K., et al. (2009). Immunogenicity and immune memory of a nonadjuvanted quadrivalent meningococcal glycoconjugate vaccine in infants. *The Pediatric Infectious Disease Journal*, **28**, 186–193.

Pizza, M., Scarlato, V., Masignani, V., Giuliani, M., Aricò, B., Comanducci, M., Jennings, G., Baldi, L., Bartolini, E., Capecchi, B., e. a. (2000). Whole genome sequencing to identify vaccine candidates against serogroup B meningococcus. *Science*, **287**, 1816–1820.

Pizzi, E., Cortese, R., Tramontano, A. (1995). A mapping epitopes on protein surface. *Biopolymers*, **36**, 675–680.

Pollard, A., Probe, G., Trombley, C., et al. (2002). Evaluation of a diagnostic polymerase chain reaction assay for Neisseria meningitidis in North America and field experience during an outbreak. *Archives of Patology & Laboratory Medicine*, **126**, 1209–1215.

Portnoy, J.M. & Olsen, L. (1985). Normal cerebrospinal fluid values in children: another look. *Pediatrics*, **75**, 484–487.

Rakonjac, J., Feng, J., Model, P. (1999). Filamentous phage are released from the bacterial membrane by a two-step mechanism involving a short C-terminal fragment of pIII. *Journal of Molecular Biology*, **289**, 1253–1265.

Rakonjac, J. & Model, P. (1998). Roles of pIII in filamentous phage assembly. *Journal of Molecular Biology*, **282**, 25–41.

Ramsay, M., Andrews, N., Kaczmarski, E., Miller, E. (2001). Efficacy of meningococcal serogroup C conjugate vaccine in teenagers and toddlers in England. *Lancet*, **357**, 195–196.

Rapoza, M. P. & Webster, R. (1995). The products of gene I and the overlapping in-frame gene XI are required for filamentous phage assembly. *Journal of Molecula Biology*, **248**, 627–638.

Rodi, D.J. & Makowski, L. (1999). Phage-display technology-finding a needle in a vast molecular haystack. *Current opinion in Biotechnology*, **10**, 87–93.

Rosenstein, N., Bradley, B., Stephens, D., Popovic, T., Hughes, J. (2001). Meningococcal Disease. *The New England Journal of Medicine*, **344**, 1378–1388.

Russel, M. & Model, P. (1989). Genetic analysis of the filamentous bacteriophage packaging signal and of the proteins that interact with it. *Journal of Virology*, **63**, 3284–3295.

Sáez-Llorens, X., Ramilo, O., Mustafa, M., et al. (1990). Molecular pathophysiology of bacterial meningitis: current concepts and therapeutic implications. *Journal of Pediatrics*, **116**, 671–684.

Scarselli, M., Cantini, F., Santini, L., Veggi, D., Dragonetti, S., et al. (2009). Epitope mapping of a Bactericidal Monoclonal Antibody against the Factor H Binding Protein of Neisseria meningitidis. *Journal of Molecula Biology*, **386**, 97–108.

Schneider, M., Exley, R., Chan, H., et al. (2006). Functional significance of factor H binding to Neisseria meningitidis. *Journal of Immunology*, **176**, 7566–7575.

Schneider, M., Prosser, B., Caesar, J., et al. (2009). Neisseria meningitidis recruits factor H using protein mimicry of host carbohydrates. *Nature*, **458**, 890–893.

Scott, J. K. & Smith, G. P. (1990). Searching for peptide ligands with an epitope library. *Science*, **249**, 386–390.

Scott, J., Loganathan, D., Easley, R., Gong, X., Goldstein, I. (1992). A family of concanavalin A-binding peptides from a hexapeptide epitope library. *PNAS, U.S.A.*, **89**, 5398–5402.

Skinner, M. M., Zhang, H., Leschnitzer, D. H., Guan, Y., Bellamy, H., Sweet, R. M., Gray, C. W., Konings, R. N., Wang, A. H., Terwilliger, T. C. (1994). Structure of the gene V protein of bacteriophage fl determined by multiwavelength x-ray diffraction on the selenomethionyl protein. *PNAS U.S.A.*, **91**, 2071–2075.

Smith, G. P. (1985). Filamentous fusion phage: Novel expression vectors that display cloned antigens on the surface of the virion. *Science*, **228**, 1315–1317.

Stabler, R. A., Marsden, G. L., Witney, A. A., Li, Y., Bentley, S. D., Tang, C. M., Hinds, J. (2005). Identification of pathogen-specific genes through microarray analysis of pathogenic and commensal Neisseria species. *Microbioly*, **151**, 2907–2922.

Stephen, C. W. & Lane, D. P. (1992). Mutant conformation of p53: Precise epitope mapping using a filamentous phage epitope library. *Journal of Molecular Biology*, **225**, 577–583.

Stephens, D. S., Greenwood, B., Brandtzaeg, P. (2007). Epidemic meningitis, meningococcaemia, and Neisseria meningitidis. *Lancet*, **369**, 2196–2210.

Swartley, J. S., Marfin, A. A., Edupuganti, S., Liu, L. J., Cieslak, P., Perkins, B., Wenger, J. D., Stephens, D. S. (1997). Capsule switching of Neisseria meningitidis. *PNAS, U.S.A.*, **94**, 271–276.

Tettelin, H., Saunders, N., Heidelberg, J., Jeffries, A., Nelson, K., Eisen, J.A, ., Ketchum, K., Hood, D., Peden, J., Dodson, R., et al. (2000). Complete genome sequence of Neisseria meningitidis serogroup B strain MC58. *Science*, **287**, 1809–1815.

Theilen, U., Wilson, L., Wilson, G., Beattie, J., Qureshi, S., Simpson, D. (2008). Management of invasive meningococcal disease in children and young people: Summary of SIGN guidelines. *BMJ, Clinical research ed.*, **336**, 1367–1370.

Thomson, M., Molesworth, A., Djingarey, M., Yameogo, K., Belanger, F., Cuevas, L. (2006). Potential of environmental models to predict meningitis epidemics in Africa. *Tropical Medicine & International Health*, **11**, 781–788.

Van Wezenbeek, P., Hulsebos, T., Schoenmakers, J. (1980). Nucleotide sequence of the filamentous bacteriophage M13 DNA genome: Comparison with phage fd. *Gene*, **11**, 129–148.

Wang, J., Caugant, D., Li, X., et al. (1992). Clonal and antigenic analysis of serogroup A Neisseria meningitidis with particular reference to epidemiological features of epidemic meningitis in the People's Republic of China. *Infection and immunity*, **60**, 5267–5282.

Wang, J., Cieplak, P., Kollman, P. (2001). How Well Does a Restrained Electrostatic Potential (RESP) Model Perform in Calculating Conformational Energies of Organic and Biological Molecules. *Journal of Computational Chemistry*, **21**, 1049–1074.

Webster, R. E. & Lopez, J. (1985). *Structure and assembly of the class 1 filamentous bacteriophage. In "Virus Structure and Assembly"*, volume pp 235-268. Jones & Bartlett, Boston.

Welsch, J., Ram, S., Koeberling, O., Granoff, D. (2008). Complement-dependent synergistic bactericidal activity of antibodies against factor H-binding protein, a sparsely distributed meningococcal vaccine antigen. *Journal of Infectious Disease*, **197**, 1053–1061.

Welsch, J. A., Rossi, R., Comanducci, M., Granoff, D. M. (2004). Protective activity of monoclonal antibodies to genome-derived neisserial antigen 1870, a Neisseria meningitidis candidate vaccine. *Journal of Immunology*, **172**, 5606–5615.

Zwick, M., Shen, J., Scott, J. (1998). Phage-displayed peptide libraries. *Current opinion in Biotechnology*, **9**, 427–439.

Acknowledgement :

Let me begin by expressing my gratitude towards of Prof. Franco Felici, who patiently corrected this thesis and because he gave me the opportunity to be involved in this project.

My utmost gratitude goes to Antonella Angiolillo for her continous technical support and for the encouragement and advices. Thanks for making me feel immediately confortable in the early days at lab. I also want to thank Carla Lo Passo that taught me the phage display technology and for her hospitality during my stay at the University of Messina.

Special thanks to Denis Shields who welcomed me into his group of Clinical Bioinformatics at the University College of Dublin and giving me his knowledge and help in a research field little known for me. A big thanks to Antony Chubb who gave me invaluable suggestions and passed on his enthusiasm for his work as researcher.

I also want to thank all the colleagues and friends in Denis' lab (Alessandra, Federica, Bronagh, Naisha, Bob, Darren, Fergal, Kevin, Praveen, Nora, Niall, Eanna, Catherine, Therese, Ilias,) and Pollastri' group (Claudio, Alessandro A., Alessandro L., Viola and Luca) without whom the months in Dublin would have been very lonely. I will never forget the foosball matches and the cake and present for my birthday!

I want express the gratitude I feel towards the people met during these years of PhD programme and who have become great friends. Particularly Alessandra and Michele, Antonio and Emma with whom I have shared so many incredible moments that I will never forget.

I also want to thank Raimondo and Patrizia for their unforgettable hospitality.

Annex

Conferences :

- Computational Biology and Innovation, PhD Symposium, 6-7 December 2011, UCD Dublin, Ireland.
  Epitope mapping of meningococcal fHbp using experimental and bioinformatic tools
  Lorenza Zippilli, Antonella Angiolillo, Carla LoPasso, Anthony Chubb, Peter Beernink, Dan Granoff, Franco Felici.
  (Poster presentation)

- 36th FEBS Congress, 25-30 June 2011, Torino, Italy.
  Epitope mapping of Neisseria meningitidis factor H-binding protein (fHbp)
  Lo Passo C., Beernink P., Zippilli L., Angiolillo A., Costa I., Pernice I., Galbo R., Granoff D. and Felici F.
  (Poster presentation)

- XI FISV Congress, 23-25 September 2009, Riva del Garda (TN), Italy.
  A region of the N-terminal domain of meningococcal factor H-binding protein that elicits bactericidal antibody across antigenic variant groups
  A. Angiolillo, P.T. Beernink, C. Lo Passo, J.A. Welsch, L. Zippilli, D.M. Granoff, F. Felici
  (Poster presentation)

Epitope Mapping of Two Cross-reactive Monoclonal Antibodies to Meningococcal Factor H-binding Protein: Implications for Synergistic Bactericidal Activity

Lo Passo C.[1], Zippilli L.[2], Angiolillo A.[2], Costa, I.[1], Pernice I.[1], Galbo R.[1], Felici F.[2] and Beernink P.T.[3]

[1]Department of Life Science, University of Messina, Italy

[2]Department of S.T.A.T., University of Molise, Pesche, Italy

[3]Center for Immunobiology and Vaccine Development, Children's Hospital Oakland Research Institute, Oakland, CA, USA

Running title: Cross-reactive mAb to meningococcal fHbp

ABSTRACT

Background

Factor H-binding protein (fHbp) is a promising vaccine candidate for prevention of sepsis and meningitis caused by meningococci. This protein binds human factor H (fH) to the bacterial surface, which leads to evasion of host immunity. fHbp can be classified into three antigenic variant groups, with partial cross-protective antibody responses between variant groups 2 and 3. Antibodies against fHbp block binding of factor H and elicit complement-mediated killing.

Methodology/Principal Findings

We report epitope mapping studies of two murine IgG mAbs, designated JAR 31 and JAR 36, which were isolated from a mouse immunized with fHbp in variant group 3. These mAbs cross-react with fHbp in variant groups 2 and 3 (~30-40% of strains), bind to the bacterial surface and elicit complement-mediated bactericidal activity in combinations with other anti-fHbp mAbs. We screened bacteriophage-displayed peptide libraries to identify amino acid residues contributing to the JAR 36 epitope. Based on the frequent occurrences of aspartate and lysine residues in the bound peptides and the reactivities of JAR 31 and JAR 36 with natural chimeric fHbp variants, we selected six residues in the C-terminal region of fHbp for replacement with alanine. The D201A substitution eliminated binding of JAR 31 and JAR 36, and a nearby substitution, K199A, decreased binding of fH.

Conclusions

The epitopes recognized by anti-fHbp mAbs JAR 31 and JAR 36 are near the fH-binding site, which permits blocking of binding of fH to fHbp by the mAbs and increases their ability to confer protective activity.

INTRODUCTION

Meningococcal factor H-binding protein (fH) is a surface-exposed lipoprotein that binds human factor H (fH) to the bacterial surface [1]. Binding of fH, which is an important down-regulatory protein of the alternative complement pathway, leads to bacterial evasion of host-mediated immunity [1,2,3]. Recombinant fHbp is part of two vaccines in late-stage clinical development for prevention of meningococcal disease caused by capsular group B strains [4,5]. Currently there are no vaccines licensed in the U.S. or Europe for prevention of group B disease.

Antibodies to fHbp activate classical complement pathway bactericidal activity and also block binding of fH to the bacteria, which increases susceptibility of the organisms to complement-mediated bacteriolysis [6,7]. The development of a broadly protective fHbp-based meningococcal vaccine requires overcoming two limitations of the antigen. First, fHbp exists in different antigenic variant groups with minimal cross-reactivity among them [8,9]. Second, the protein is expressed at low levels by many strains, which limits susceptibility to anti-fHbp bacteriolysis [10,11].

In previous studies, we prepared a panel of 12 murine anti-fHbp mAbs against a representative fHbp sequence variant from each of the three major antigenic groups [12,13]. Against low fHbp-expressing strains, no individual mAb had complement-mediated bactericidal activity but binding of certain combinations of anti-fHbp mAbs yielded sufficient immune complex on the bacterial surface to activate complement-mediated bacteriolysis (i.e., synergistic or cooperative anti-fHbp mAb bactericidal activity [6,13,14]).

In previous studies, we used either multiple sequence alignments [13] or peptide

phage display [14], coupled with site-specific mutagenesis, to identify amino acid residues in fHbp that affected binding of 9 of the 12 anti-fHbp mAbs. Collectively, the data suggested that the distances between epitopes recognized by different combinations of mAbs were important for the ability of two IgG molecules to engage C1q, activate the classical complement pathway and elicit cooperative bactericidal activity.

Because of the central role of fHbp in meningococcal pathogenesis [1,2,6,15,16], and vaccine potential of this protein [8,9], it is important to increase our understanding of the mechanisms by which anti-fHbp antibodies elicit cooperative complement-mediated bactericidal activity. The purpose of the present study was to identify fHbp amino acid residues affecting binding by two anti-fHbp mAbs, designated JAR 31 and JAR 36, which are two of the three anti-fHbp mAbs in our panel whose epitopes remained undefined. The epitopes recognized by these mAbs were of interest because the two mAbs cross-reacted with all fHbp amino acid sequence variants tested from fHbp variant groups 2 and 3 [11], and JAR 36 elicited cooperative complement-mediated bacteriolysis when tested with other anti-fHbp mAbs [13].

RESULTS

Binding of JAR 31 and JAR 36 mAbs to natural fHbp sequence variants. JAR 31 and JAR 36 are IgG2b mAbs that were isolated from a mouse immunized with recombinant fHbp ID 28[1] from variant group 3. Both mAbs reacted with recombinant fHbp ID 28, which was the immunogen used to produce the mAb. Both JAR 31 and JAR 36 cross-reacted with fHbp ID 77 (in variant group 2) but not with fHbp ID 1 (in variant group 1) (**Figure 1, Panels A and B**). The JAR 31 and JAR 36 mAbs also cross-reacted with a natural chimeric fHbp, ID 207. As a control, mAb JAR 5, which is specific for fHbp sequence variants in variant group 1 [12], reacted with fHbp ID 1 (variant group 1) and with the chimeric fHbp ID 207, but not with fHbp ID 28 (variant group 3) or ID 77 (variant group 2) (**Panel C)**.

Amino acid residues 1 to 185 (variable segments V_A through V_D)[2] of the natural chimeric fHbp ID 207 have 96% identity with the corresponding segments of fHbp ID 1, while residues 186 to 255 of segment V_E of fHbp ID 207 have 96% identity with segment

---

[1] fHbp ID numbers are assigned in the fHbp database at http://pubmlst.org/neisseria/fHbp/

[2] fHbp can be classified into modular groups [11,17] based on different combinations of five variable segments, each encoded by genes from one of two lineages (shown in **Figure 2, Panel A** as white or gray symbols). The full-length protein can contain all five segments from the same lineage (i.e., modular groups I or II), or have individual segments derived from different lineages (i.e., natural chimeras, designated modular groups III to VII, **Figure 2, Panel A**).

V_E of fHbp ID 28.[3] JAR 31 and JAR 36 also reacted strongly with three additional recombinant fHbp variants, ID 22, ID 79 and ID 77, but not with ID 15 (data not shown). The fHbp variants that were bound by JAR 31 and JAR 36 are denoted with asterisks (**Figure 2, Panel A)**. Collectively, the data were consistent with the epitopes recognized by the two mAbs residing in variable segment E (V_E) derived from lineage 2 (white octagonal symbols).

Inhibition of JAR 31 binding by JAR 36. To test whether the JAR 31 and JAR 36 mAbs recognized overlapping epitopes, we used non-labeled mAbs to inhibit binding of alkaline phosphatase-labeled JAR 31 to fHbp ID 28 by ELISA. Both JAR 31 and JAR 36 yielded 95% inhibition at the highest concentration tested, 20 µg/ml (**Figure 3**). JAR 33 was used as a negative control and gave <25% inhibition at the highest concentration tested.

Epitope mapping of JAR 36 mAb by peptide phage display. Based on the hypothesis that the two mAbs recognized similar regions of fHbp, we sought to identify specific amino acid residues contributing to the epitope recognized by one of the mAbs, JAR 36. We screened five filamentous phage libraries displaying random peptides of different lengths fused to the N-terminus of the coat protein VIII. The screening was performed by immuno-affinity selection, using two different techniques to minimize the risk of selecting non-specific clones. For each library, either individually or in combination, three rounds of selection were performed using the JAR 36 mAb as bait. After each selection cycle, the reactivity of phage pools was tested by ELISA using the pC89 phage vector (not encoding a foreign peptide) as a negative control in order to

[3] amino acid numbering is based on the sequence of the mature fHbp ID 1, available at http://pubmlst.org/neisseria/fHbp/

detect enrichment of JAR 36-specific clones in the selected mixtures. Forty-five JAR 36-specific positive clones were identified by immuno-screening and the sequences of the respective PCR amplified DNA fragments were determined. Among these clones were 15 independent sequences, each of which showed an optical density ≥0.5 by ELISA (**Table 1**).

The phage display experiment did not identify a consensus sequence among the JAR 36-reactive peptides, which suggested that the JAR 36 epitope was either discontinuous or conformational. We hypothesized that the most abundant amino acids in the bound peptides (**Table 2**) might be important for the interaction between the immunogen and the mAb. The observed frequency of each amino acid in the mimotopes and the expected frequency of each amino acid in the collective libraries were used to calculate a ratio representing the relative frequency. The results indicated higher occurences of aspartate (D), glycine (G), lysine (K) and tryptophan (W), each with a normalized ratio >2.0 (**Table 2**). Tryptophan does not occur in any known fHbp sequence [11,17], and glycine has only a hydrogen atom as its side chain. Consequently, we predicted that the electrostatically-charged residues aspartate (D) or lysine (K) might contribute to the JAR 36 epitope.

Site-specific mutagenesis of D and K residues. Since JAR 31 and JAR 36 reacted with fHbp sequence variants containing variable E (V_E) segments from lineage 2 (**Figure 2, Panel A**), we focused our attention on the amino acid residues, D and K, which occurred frequently in the peptide sequences, and that were located between positions 186 and 255 of fHbp ID 28 (**Panel B**). This region of fHbp contained three aspartate (D) and five lysine (K) residues that were conserved in V_E segments from

lineage 2 (**Figure 2, Panel B**). To decrease further the number of possible residues to test experimentally, we examined the positions of the D and K residues in a homology model of the fHbp ID 28 protein (**Figure 4**). Six of these eight residues occurred in two clusters near the fH binding site of the protein; Cluster 1 included K199, D201 and K203 on one end of the C-terminal structural domain, and Cluster 2 included D211, K241 and K245 on the other end of the same domain.

We substituted the codons for residues K199, D201 and K203 in Cluster 1 with alanine (A) and expressed and purified the fHbp mutants. By ELISA, JAR 31 and JAR 36 reacted with the wild-type fHbp ID 28 and the K199A and K203A mutants but not with the D201A mutant (**Figure 5, Panels A and B**). As a positive control to demonstrate that D201 mutant was adsorbed to the wells of the microtiter plate, we tested binding of anti-fHbp mAb JAR 33, which reacted similarly with the native ID 28 and all three of the mutants (**Figure 5, Panel C**). Alanine substitutions of the three residues, in Cluster 2, had no effect on binding of JAR 31 by Western blotting or ELISA (data not shown).

Since JAR 36 previously was shown to inhibit binding of human fH [13], we also tested binding of fH to the fHbp mutants of Cluster 1. Binding of fH to the D201A and K203A mutants was not significantly different from that of the native ID 28 protein (**Figure 5, Panel D**). In contrast, binding of fH to the K199A mutant was lower than to the native protein. Thus, the amino acid residue D201, which affected binding of the JAR 31 and JAR 36 mAbs, while not decreasing fH binding, was in proximity to the fH-binding site.

Based on the location of residue D201, which affected the epitopes recognized

by JAR 31 and JAR 36, and those recognized by previously mapped anti-fHbp mAbs [13,14], we examined the distances between residues involved in the epitopes of bactericidal and non-bactericidal pairs of mAbs (**Table 3**). JAR 36 was bactericidal in combination with either mAb JAR 11 or JAR 13, but was not bactericidal with the mAbs JAR 10, JAR 4, JAR 32, JAR 33, or JAR 35. Bactericidal pairs of mAbs recognized epitopes that were 20 to 29 Å apart, and non-bactericidal pairs recognized epitopes that were 20 to 32 Å apart (**Table 3**).

DISCUSSION

In previous studies, we were not able to identify amino acid residues in fHbp that were responsible for binding the anti-fHbp mAbs JAR 31 or JAR 36 using multiple sequence alignments, because these mAbs reacted with all of the fHbp sequences tested from variant groups 2 and 3. Therefore, in the present study, we used peptide phage display, which had been successful in identifying residues involved in the epitope of another cross-reactive anti-fHbp mAb, JAR 4, which reacts with fHbp in variant groups 1 and 2 [14]. With JAR 4, we identified a tripeptide consensus sequence, DHK, that also was found in fHbp. In the present study we did not identify a consensus sequence but identified several amino acid residues that occurred more frequently than by chance in the bound phage peptide sequences. We used this information, along with reactivity with fHbp variants from different modular groups (**Figure 2**, **Panel A**) and protein structural information to predict residues potentially involved in the epitope recognized by JAR 36.

Using site-specific mutagenesis, we prepared six recombinant fHbp mutants with alanine substitutions and identified D201A, which affected binding of both JAR 31 and JAR 36. Residue D201 is present in the V_E segment of both JAR 36-reactive and non-reactive fHbp sequences (**Figure 2, Panel B**). Therefore, it is possible that a neighboring residue(s) affects the conformation of D201 in non-binding variants. As reported previously, JAR 36 partially inhibits binding of fH to fHbp [13]. Although the D201A substitution in fHbp eliminated binding of JAR 31 and JAR 36, it did not affect binding of human fH. Conversely, substitution of the nearby residue K199 in fHbp decreased the binding of fH to fHbp but not binding of JAR 31 or JAR 36. Since the

residues K199 and D201 are in proximity to each other, the binding sites for human fH and the two anti-fHbp mAbs likely overlap.

In two previous studies, we examined the properties of pairs of anti-fHbp mAbs relative to their synergistic functional activity. In the first study, pairs of mAbs were bactericidal when at least one mAb inhibited binding of fH to fHbp and when the distance between residues affecting the epitopes was between 16 and 20 Å [13]. There was no bactericidal activity when the distance was less than 16 Å or greater than 20 Å. In the second study, however, bactericidal pairs of mAbs recognized epitopes that involved residues separated by 27 to 47 Å [14]. In addition, there was one bactericidal pair, mAb502 and JAR 4, neither of which inhibited binding of fH to fHbp.

Before the location of a residue that contributed to the JAR 36 epitope was known, JAR 36 was shown to be bactericidal when assayed with JAR 11 or JAR 13 against strain 8047, which expresses fHbp ID 77 in variant group 2 [13]. JAR 36 also was bactericidal with JAR 13 against strain M1239, which expresses fHbp ID 28 in variant group 3. There was no obvious correlation of bactericidal versus non-bactericidal combinations with the distance between epitopes recognized by these pairs of mAbs. There also was no correlation with the respective IgG subclasses (for example, although JAR 36 (IgG2a) was bactericidal with JAR 11 or JAR 13 (both IgG2a), JAR 36 was not bactericidal with other IgG2a mAbs (JAR 4, JAR 32 or JAR 33). Although the spacing between epitopes recognized by the two mAbs appeared to be the most important determinant of cooperative bactericidal activity in our earlier study [13], there likely are other contributing factors such as the ability of a mAb to inhibit binding of fH to fHbp [7], and relative kinetics of association and dissociation of binding

between the mAb and fHbp [16].

One particularly interesting example was the combination of JAR 36 and JAR 11, which was bactericidal (BC_{50} = 1 µg/ml). This combination contrasted with that of JAR 36 and JAR 35, which was not bactericidal (BC_{50} >50 µg/ml). JAR 11 is an IgG2a mAb, whereas JAR 35 is an IgG2b. Alone, the IgG2b mAb might be expected to have higher bactericidal activity than the IgG2a, based on the differences in functional activity of four murine mAbs of different IgG subclasses bearing the same paratope, which recognized the meningococcal porin protein PorA [18]. Our previous studies [13,14] and the present study, which collectively have examined 32 different combinations of mAbs, did not indicate a correlation between synergistic bactericidal activity and IgG subclasses of anti-fHbp mAbs. Thus, the explanation for the observed differences in the functional activity of these two pairs of mAbs is not likely a result of their IgG subclasses.

Binding of JAR 11 and JAR 35 are both affected by amino acid substitutions at residue 174 in fHbp; JAR 11 binds when A174 is present and JAR 35 binds when K174 is present [13]. Although their epitopes appear to overlap, the large difference in their ability to elicit complement-mediated bactericidal activity in combination with JAR 36 suggests that the respective orientations of the bound JAR 11 and JAR 35 mAbs are considerably different from each other. The distance between the epitopes recognized by the two mAbs is not necessarily important for eliciting complement-mediated bactericidal activity; however, the distance between the Fc regions of the two mAbs needed to engage C1q is likely to be important for bactericidal activity. Developing a further understanding of the requirements for synergistic bactericidal activity of two mAbs that are directed at the same antigen will require structural studies or molecular

modeling of immune complexes containing mAbs bound to non-overlapping mAb epitopes of fHbp.

MATERIALS AND METHODS

Peptide phage display. Peptides that bound to the JAR 36 mAb were selected by panning five phage libraries constructed in the two-gene phagemid vector pC89 [19]. These libraries display random peptide sequences of different sizes, fused to the N-terminal region of the major coat protein (pVIII) of filamentous phage. The pVIII-9aa, pVIII-12aa and pVIII-15aa libraries are composed of random 9-mers, 12-mers and 15-mers, respectively. The pVIII-9aa.Cys library has random sequences of 9 residues flanked by two Cys residues, and the pVIII-Cys.Cys library has random sequences of 12 residues with two Cys residues present 2 to 10 residues apart, which creates a collection of disulfide constrained loops of different sizes [20].

Specific phage clones were isolated from the libraries using two different techniques. In the biopanning approach, 1 µg/ml of JAR 36 mAb was incubated overnight at 4 °C with 10^{10} transducing units of each library, in a total volume of 20 µl of PBS. The mixture was incubated with 0.8 µg of biotinylated goat anti-mouse IgG antibody (Fc specific, Sigma, St Louis, MO, USA), which had been pre-adsorbed overnight at 4 °C with $3x10^{10}$ UV-inactivated M13 KO7 phage particles to prevent non-specific binding. This mixture was added to a streptavidin-coated 6 cm Falcon plate and incubated for 10 min at room temperature. After 10 washes with 1 ml of washing solution, bound phages were eluted with 800 µl 0.1 N HCl, adjusted to pH 2.2 with glycine and 10mg/ml BSA. The solution was neutralized using 60 µl of 2 M Tris–HCl, pH 9.6 and the phage were amplified by infecting E.coli TG1 cells. The second and third rounds of selection were done in the same way, except 10 ng/ml and 1 ng/ml of the mAb were used, respectively.

The Dynabeads approach was described previously [12]. The JAR 36 mAb (1µg/ml) was incubated with magnetic beads conjugated with protein G (50 µg protein G-Dynabeads®, Dynal, Norway) for 1 h at room temperature under agitation. The beads were washed 3 times with washing solution (PBS, 0,5% Tween-20), and approximately 10^{10} ampicillin-transducing units of library preparation (~10^{11} phage particles) in a volume of 100 µl, were added to 900 µl of blocking solution (PBS, 5% non-fat dry milk, 0.05% Tween-20) and agitated for 3 to 4 h at room temperature. After 10 washes with 1ml of washing solution, bound phages were eluted with 500 µl 0.1 N HCl, adjusted to pH 2.2 with glycine and 10 mg/ml BSA. The solution was neutralized and the phages were amplified by infecting *E. coli* TG1 cells. The second and third rounds of panning were performed as described above, but using 10^{10} ampicillin-transducing units obtained from the first and the second round of amplified phage pools, respectively.

Identification of positive clones. Positive phage clones were identified through immunoscreening as described previously [21]. After three rounds of affinity selection, using the libraries either individually or in combination, phage particles were mixed with 2 ml of a culture of *E. coli* TG1 (OD_{600} ~0.4). Five hundred µl of this culture were infected with M13KO7 helper phage (~10^9 pfu) and incubated for 15 min at 37 °C and for an additional 30 min with shaking. Serial dilutions of infected bacteria were plated on Luria–Bertani (LB) agar plates containing ampicillin, kanamycin and IPTG, which were incubated overnight at 37°C. Nitrocellulose filters (Protran BA85, 0.45 µm, Schleicher & Schuell, Keene, NH) were layered on the plates containing 50–200 colonies, and left at room temperature for 1 h. Filters were blocked for 1 h with blocking

295solution, and incubated with mAb JAR 36 (1 µg/ml in blocking solution) for 2 h at room
296temperature with gentle shaking. After 3 washes, an alkaline phosphatase-conjugated
297anti-mouse IgG Ab (Sigma, St. Louis, MO, 1:5,000) was added for 1 h at room
298temperature. Filters were washed and developed with nitro blue tetrazolium and 5-
299bromo-4-chloro-3-indolyl-phosphate (Sigma). Positive colonies were suspended in 50
300µl of 1x PBS and heated at 70°C for 15 min to kill the bacterial cells. After centrifugation
301for 5 min at 16,000 x *g*, the supernatant containing the positive phage particles was
302collected. Five µl of recovered supernatant was amplified by infecting *E. coli* TG1.

303 *Direct binding ELISA.* Binding of JAR 36 mAb to peptides displayed by the
304phage library selected clones was confirmed by phage ELISA. Ninety-six well plates
305were coated with mAb JAR 36 (100 µl per well, 0.2 µg/ml in 50 mM $NaHCO_3$, 0.02%
306(w/v) NaN_3, pH 9.6) and incubated overnight at 4°C. The plates were washed 8 times
307with TBST (50 mM Tris –HCl,150 mM NaCl, pH 7.5, 0.05% (v/v) Tween- 20). One
308hundred µl per well of phage supernatant were added and the plates were incubated for
3092 h at 37 °C. After washing, 100 µl of an horseradish peroxidase conjugated anti-M13
310mAb (Amersham Biosciences, Buckinghamshire, UK, 1:5,000) were added and
311incubated for 1 h at 37°C. Antibody binding was detected by adding 3,3',5,5'-
312tetramethylbenzidine (TMB) (Sigma) and reading the OD at 450 nm after 45 min.

313 *Construction of site-specific mutants.* Site-specific mutants were chosen by
314targeting charged residues (Lys or Asp) that were present in the last 70 residues of the
315fHbp ID 28 sequence and that were predicted to be surface-exposed based on the
316crystal structure of fHbp ID 1 in a complex with a fragment of human fH [22]. The
317sequences of the mutagenic oligonucleotides were: K199A_fwd,

GCAGCAGATGAAAAATCACACG; K199A_rev, GAGTTCGGCGGCGGCA; D201A_fwd, GCTGAAAAATCACACGCCG; D201A_rev, TGCTTTGAGTTCGGCGG; K203A_fwd, GCATCACACGCCGTCAT; K203A_rev, TTCATCTGCTTTGAGTTCGGC; D211A_fwd, GCCACGCGCTACGGCAGC; D211A_rev, GCCCAAAATGACGGCGT; K241A_fwd; GCGATAGGGGAAAAGGTTCACGAAATC; K241A_rev: CACGGTTGCCGAGCCG; K245A_fwd, CAGTTCACGAAATCGGCATC; and K245A_rev,_CTTCCCCTATCTTCACGGTTGC; mutated nucleotides in the forward oligonucleotide sequences are underlined. The oligonucleotides were phosphorylated with T4 polynucleotide kinase (New England Biolabs, Ipswich, MA) prior to PCR amplification. Mutants were constructed using the Phusion Site-Directed Mutagenesis Kit (Thermo Scientific, Waltham, MA) using the manufacturer's protocols. The mutagenesis reactions were transformed in to chemically competent *E. coli* DH5α (Invitrogen, Carlsbad, CA) and independent mutant clones were verified by DNA sequencing (Davis Sequencing, Davis, CA).

Purification of recombinant fHbp. The wild-type fHbp ID 28 and site-specific mutant proteins were expressed from the T7 promotor using the *E. coli* plasmid pET21b (Novagen, Madison, WI) as described previously [8,23]. The recombinant proteins were purified by immobilized metal ion chromatography using Ni-NTA agarose (Qiagen, Valencia, CA) as described previously. Purified fHbps were dialyzed against PBS, sterilized by filtration (Millex 0.22 µm; Millipore, Billerica, MA), and stored at 4 °C prior to use. The protein concentrations were determined by UV absorbance (Nanodrop 1000, Wilmington, DE) based on the extinction coefficient calculated from the amino acid sequence [24].

Binding of mAbs and fH to fHbp. Binding of anti-fHbp mAbs to purified recombinant fHbp was measured by ELISA. Purified fHbp (2 µg/ml) was adsorbed to the wells of a microtiter plate overnight, which subsequently were blocked with PBS containing 0.1% (v/v) Tween-20 (Sigma-Aldrich, St. Louis, MO) and 1% (w/v) BSA. Anti-fHbp mAbs were added at concentrations ranging from 0.008 to 25 µg/ml and incubated for 1 h at 37 °C. Bound antibody was detected (1 h at room temperature) with goat anti-mouse IgG conjugated with alkaline phosphatase (Invitrogen, Carlsbad, CA). After 30 min of incubation with p-nitrophenyl phosphate (1 mg/ml; Sigma) at room temperature, the optical density at 405 nm was measured.

For measuring inhibition of binding of anti-fHbp mAbs to fHbp, JAR 31 harvested from hybridoma culture supernatant was purified by chromatography using a protein G column (HiTrap Protein G HP 1 ml, GE Life Sciences) and conjugated to alkaline phosphatase (EasyLink Alkaline Phosphatase Conjugation Kit, AbCam) according to the manufacturer's protocol. Equal volumes of AP-conjugated JAR 31 (2µg/ml) and anti-fHbp mAb inhibitors (starting concentration of 40 µg/ml) were premixed and 100 µl were added to the wells of a microtiter plate that had been sensitized and blocked as described above. After addition of the antibody mixtures, the reactions were incubated for 2 hours at room temperature. The alkaline phosphatase was detected as described above.

For measuring binding of human fH to fHbp, the wells of a microtiter plate were sensitized with fHbp and blocked as described above for mAb binding. Purified human fH (Complement Technologies, Tyler, TX) was added at concentrations ranging from 0.008 to 25 µg/ml and the plate was incubated for 2 h at room temperature. The

primary antibody was sheep anti-human fH (1:5,000; Abcam, Cambridge, MA) and the secondary antibody was donkey anti-sheep IgG conjugated with alkaline phosphatase (1:5,000; Sigma). The incubation conditions for the primary and secondary antibodies and the development steps were the same as described above for mAb binding to fHbp.

ACKNOWLEDGEMENTS

We thank Emily Braga and Jennifer Thweatt (Children's Hospital Oakland Research Institute) for expert technical assistance, Rolando Pajon for construction of the fHbp ID 28 homology model and Dan Granoff for helpful discussions and comments on the manuscript.

REFERENCES

1. Madico G, Welsch JA, Lewis LA, McNaughton A, Perlman DH, et al. (2006) The meningococcal vaccine candidate GNA1870 binds the complement regulatory protein factor H and enhances serum resistance. J Immunol 177: 501-510.

2. Schneider MC, Exley RM, Chan H, Feavers I, Kang YH, et al. (2006) Functional significance of factor H binding to Neisseria meningitidis. J Immunol 176: 7566-7575.

3. Lewis LA, Ngampasutadol J, Wallace R, Reid JE, Vogel U, et al. (2010) The meningococcal vaccine candidate neisserial surface protein A (NspA) binds to factor H and enhances meningococcal resistance to complement. PLoS Pathog 6: e1001027.

4. Giuliani MM, Biolchi A, Serruto D, Ferlicca F, Vienken K, et al. (2010) Measuring antigen-specific bactericidal responses to a multicomponent vaccine against serogroup B meningococcus. Vaccine 28: 5023-5030.

5. Jiang HQ, Hoiseth SK, Harris SL, McNeil LK, Zhu D, et al. (2010) Broad vaccine coverage predicted for a bivalent recombinant factor H binding protein based vaccine to prevent serogroup B meningococcal disease. Vaccine 28: 6086-6093.

6. Welsch JA, Ram S, Koeberling O, Granoff DM (2008) Complement-dependent synergistic bactericidal activity of antibodies against factor H-binding protein, a sparsely distributed meningococcal vaccine antigen. J Infect Dis 197: 1053-1061.

7. Giuntini S, Reason DC, Granoff DM (2011) Complement-mediated Bactericidal Activity of Anti-fHbp Monoclonal Antibodies Against the Meningococcus Relies Upon Blocking Factor H Binding. Infect Immun.

8. Masignani V, Comanducci M, Giuliani MM, Bambini S, Adu-Bobie J, et al. (2003) Vaccination against Neisseria meningitidis using three variants of the lipoprotein GNA1870. J Exp Med 197: 789-799.

9. Fletcher LD, Bernfield L, Barniak V, Farley JE, Howell A, et al. (2004) Vaccine potential of the Neisseria meningitidis 2086 lipoprotein. Infect Immun 72: 2088-2100.

10. McNeil LK, Murphy E, Zhao XJ, Guttmann S, Harris SL, et al. (2009) Detection of LP2086 on the cell surface of Neisseria meningitidis and its accessibility in the presence of serogroup B capsular polysaccharide. Vaccine 27: 3417-3421.

11. Pajon R, Beernink PT, Harrison LH, Granoff DM (2010) Frequency of factor H-binding protein modular groups and susceptibility to cross-reactive bactericidal activity in invasive meningococcal isolates. Vaccine 28: 2122-2129.

12. Welsch JA, Rossi R, Comanducci M, Granoff DM (2004) Protective activity of monoclonal antibodies to genome-derived neisserial antigen 1870, a Neisseria meningitidis candidate vaccine. J Immunol 172: 5606-5615.

13. Beernink PT, Welsch JA, Bar-Lev M, Koeberling O, Comanducci M, et al. (2008) Fine antigenic specificity and cooperative bactericidal activity of monoclonal antibodies directed at the meningococcal vaccine candidate factor h-binding protein. Infect Immun 76: 4232-4240.

14. Beernink PT, LoPasso C, Angiolillo A, Felici F, Granoff D (2009) A region of the N-terminal domain of meningococcal factor H-binding protein that elicits bactericidal antibody across antigenic variant groups. Mol Immunol 46: 1647-1653.

15. Seib KL, Brunelli B, Brogioni B, Palumbo E, Bambini S, et al. (2011) Characterization of diverse subvariants of the meningococcal factor H (fH) binding protein for their ability to bind fH, to mediate serum resistance, and to induce bactericidal antibodies. Infect Immun 79: 970-981.

16. Dunphy KY, Beernink PT, Brogioni B, Granoff DM (2011) Effect of factor H-binding protein sequence variation on factor H binding and survival of Neisseria meningitidis in human blood. Infect Immun 79: 353-359.

17. Murphy E, Andrew L, Lee KL, Dilts DA, Nunez L, et al. (2009) Sequence diversity of the factor H binding protein vaccine candidate in epidemiologically relevant strains of serogroup B Neisseria meningitidis. J Infect Dis 200: 379-389.

18. Michaelsen TE, Kolberg J, Aase A, Herstad TK, Hoiby EA (2004) The four mouse IgG isotypes differ extensively in bactericidal and opsonophagocytic activity when reacting with the P1.16 epitope on the outer membrane PorA protein of *Neisseria meningitidis*. Scand J Immunol 59: 34-39.

19. Felici F, Castagnoli L, Musacchio A, Jappelli R, Cesareni G (1991) Selection of antibody ligands from a large library of oligopeptides expressed on a multivalent exposition vector. J Mol Biol 222: 301-310.

20. Luzzago A, Felici F (1998) Construction of disulfide-constrained random peptide libraries displayed on phage coat protein VIII. Methods Mol Biol 87: 155-164.

21. Luzzago A, Felici F, Tramontano A, Pessi A, Cortese R (1993) Mimicking of discontinuous epitopes by phage-displayed peptides, I. Epitope mapping of human H ferritin using a phage library of constrained peptides. Gene 128: 51-57.

22. Schneider MC, Prosser BE, Caesar JJ, Kugelberg E, Li S, et al. (2009) Neisseria meningitidis recruits factor H using protein mimicry of host carbohydrates. Nature 458: 890-893.

23. Beernink PT, Granoff DM (2008) Bactericidal antibody responses induced by meningococcal recombinant chimeric factor H-binding protein vaccines. Infect Immun 76: 2568-2575.

24. Gasteiger E, Hoogland C, Gattiker A, Duvaud S, Wilkins MR, et al. (2005) Protein identification and analysis tools on the ExPASy server. In: Walker JM, editor: Humana Press. pp. 571-607.

25. Beernink PT, Granoff DM (2009) The modular architecture of meningococcal factor H-binding protein. Microbiology 155: 2873-2883.

26. Schwede T, Kopp J, Guex N, Peitsch MC (2003) SWISS-MODEL: An automated protein homology-modeling server. Nucleic Acids Res 31: 3381-3385.

27. Cendron L, Veggi D, Girardi E, Zanotti G (2011) Structure of the uncomplexed Neisseria meningitidis factor H-binding protein fHbp (rLP2086). Acta Crystallogr Sect F Struct Biol Cryst Commun 67: 531-535.

Table 1. Amino acid sequences of the phage-displayed peptides mimicking the JAR 36 epitope[a]

Sequence[b]	No. of Clones	ELISA OD[c]	SD[d]
AKWCAQFCQGYL	2	3.10	0.42
AKWCNLWCTWVG	3	2.25	0.35
GKQCAAWCEWFA	1	1.10	0.14
GKGCTRRGCDVD	2	1.00	0.39
WSDKDRNLWGLWYRE	4	0.78	0.05
QARCIVEECKWA	3	0.68	0.16
LGWCGDGLCKGV	2	0.65	0.14
NKFVSLGLA	5	0.65	0.09
QKWFALGAPWYD	3	0.60	0.10
WNINWGKPTRDE	1	0.57	0.04
GKWCLLVDCNRD	1	0.57	0.04
RPGPGDIDI	13	0.57	0.16
KVCQLWGNNCGE	2	0.55	0.07
GCGKWELDGCAA	2	0.55	0.07
VRSKWGEVGRPYDVV	1	0.45	0.08

[a] positive phage clones ranked by their reactivity with JAR 36

[b] deduced amino acid sequences of the peptide inserts displayed through pVIII fusion on the phage library clones positive for JAR 36

[c] reactivity of phage clone with mAb JAR 36, determined by ELISA

[d] SD value is the standard deviation of the mean (n = 2)

Table 2. Amino acid frequencies in the distinctive phage clones bound by JAR 36

Amino acid[a]	Observed[b]	Expected[c]	Obs./Exp. (95% CI)[d]
Alanine (A)	0.072	0.063	1.16 (0.62, 1.94)
Arginine (R)	0.061	0.088	0.69 (0.35, 1.22)
Asparagine (N)	0.050	0.038	1.33 (0.61, 2.48)
Aspartate (D)	0.078	0.038	2.07 (1.15, 3.39)
Glutamine (Q)	0.039	0.038	1.04 (0.43, 2.11)
Glutamate (E)	0.050	0.038	1.33 (0.61, 2.48)
Glycine (G)	0.139	0.063	2.22 (1.47, 3.17)
Histidine (H)	0.006	0.038	0.15 (0.00, 0.83)
Isoleucine (I)	0.028	0.045	0.61 (0.20, 1.41)
Leucine (L)	0.078	0.088	0.89 (0.49, 1.45)
Lysine (K)	0.083	0.038	2.22 (1.25, 3.57)
Methionine (M)	0.006	0.030	0.19 (0.00, 1.04)
Phenylalanine (F)	0.028	0.038	0.74 (0.24, 1.71)
Proline (P)	0.033	0.063	0.53 (0.19, 1.15)
Serine (S)	0.017	0.088	0.19 (0.05, 0.55)
Threonine (T)	0.022	0.063	0.36 (0.10, 0.90)
Tryptophan (W)	0.111	0.030	3.74 (2.32, 5.61)
Tyrosine (Y)	0.028	0.038	0.74 (0.24, 1.71)
Valine (V)	0.067	0.063	1.07 (0.56, 1.82)

[a] Cys (C) residues were eliminated from the analysis because they were fixed in a subset of the phage libraries

[b] Observed frequency of each amino acid in unique peptides bound by JAR 36

[c] Expected frequency of each amino acid in the five phage libraries used. For the construction of pVIII-9aa and pVIII-9aa.Cys libraries, all 64 codons were used; for the pVII-Cys.Cys and pVIII-15aa libraries, 32 codons were used; and for the pVIII-12aa 20 codons were used, one for each amino acid.

[d] Ratio between observed frequency and expected frequency and 95% confidence interval (CI) calculated from the Gaussian distribution.

Table 3. Anti-fHbp mAbs JAR 31 and JAR 36 (IgG2b) elicit cooperative bactericidal activity in pair-wise combinations with other anti-fHbp mAbs[a]

mAb (IgG Subclass)	Reactive Residue(s)[a]	Approximate Distance (Å)[b]	Test Strain (fHbp ID[c])	Combination BC_{50}, µg/ml[c]	
				JAR 31	JAR 36
JAR 4 (2a)	D25, H26, K27	30-32	8047 (77)	TBD	>50
JAR 10 (1)	K180, E192	24	8047 (77)	TBD	>50
JAR 11 (2a)	A174	20	8047 (77)	TBD	1
JAR 13 (2a)	S216	29	8047 (77)	TBD	1
JAR 13 (2a)	S216	29	M1239 (28)	ND	1
JAR 32 (2a)	K174	20	M1239 (28)	ND	>50
JAR 33 (2a)	R180, E192	24	M1239 (28)	ND	>50
JAR 35 (2b)	K174	20	M1239 (28)	ND	>50

[a] Reactive residue(s), amino acid residue affecting epitope expression [13] [14].

[b] Distance between respective alpha carbons of D201 and reactive residue(s) of second mAb, measured with PyMol (http://www.pymol.org) using the model described in the legend to Figure 3.

[c] fHbp ID numbers are from the database at http://pubmlst.org/neisseria/fHbp/ and the corresponding variant groups and modular groups are shown in **Figure 2, Panel A**.

[d] None of the mAbs individually was bactericidal (BC_{50}>50 µg/ml). JAR 4, JAR 10, JAR 32, JAR 33 and JAR 35 elicited cooperative bactericidal activity (BC_{50}<50 µg/ml) with other anti-fHbp mAbs not shown [13].

FIGURE LEGENDS

Figure 1. Binding of anti-fHbp mAbs to purified recombinant fHbp variants by ELISA. **A,** Binding of mAb JAR 31 to fHbp ID 1 (filled circles), ID 28 (open triangles), ID 77 (open squares) and ID 207 (asterisks). **B,** Binding of mAb JAR 36 to fHbp ID 1. **C,** Binding of a control mAb, JAR 5, showed that fHbp ID 1, which was negative for JAR 31 and JAR 36 binding, was present on the plate in a similar quantity as the other fHbp variants. The symbols used in Panels B and C are the same as those in Panel A.

Figure 2. Schematic of the modular architecture of fHbp. **A,** Seven different fHbp sequence variants, designated by ID numbers, are shown along with their classifications into modular groups and variant groups. fHbp is composed of five variable segments, each from one of two genetic lineages [11,25]. fHbp ID 1 and ID 28 are designated as comprising variable segments from lineage 1 (shaded) and 2 (white), respectively. In this panel, each distinctive V_E segment is designated by two numbers, separated by a decimal point with the first number, 1 or 2, referring to the genetic lineage, and the second number referring to the ID number of the segment as annotated on the website http://pubmlst.org/neisseria/fHbp/. The variants that bind the JAR 31 and JAR 36 mAbs are designated with an asterisk. **B,** Amino acid sequences of the six distinct variable E (V_E) segments shown in panel A. The residues D and K, which were over-represented in the phage sequences, are shown in bold in the sequence of E.2.6, which is present in fHbp ID 28.

Figure 3. Inhibition of binding of mAb JAR 31 to fHbp ID 28 by mAb inhibitors. JAR 31 conjugated to alkaline phosphatase was held at a fixed concentration and the concentrations of the mAb inhibitors (JAR 31, circular symbols; JAR 36, asterisks; JAR 33, squares) were varied. Percent inhibition was calculated relative to the optical density of wells containing no mAb inhibitor.

Figure 4. Location of residues predicted to affect binding of the JAR 31 and JAR 36 mAbs. A homology model of fHbp ID 28 was constructed using SwissModel [26] based on the atomic coordinates of the crystal structure of fHbp ID 1 (PDB accession number 3KVD) [27]. The figure was generated using PyMol (http://www.pymol.org). **A,** The protein is oriented with the C-terminal (beta-barrel) domain on the left and the fH-binding surface at the top. The two clusters of D and K residues near the fH-binding surface (top) are shown in green and blue, respectively. Two D or K residues that did not cluster with other residues are shown in yellow. **B,** Same as panel A, with view rotated 90° around the X-axis.

Figure 5. Binding of JAR 36 or human fH to site-specific mutants of fHbp ID 28 by ELISA. **A,** Binding of mAb JAR 31 to fHbp ID 28 wild-type (WT, open circles) K199A (open triangles), D201A (open squares) and K203A (asterisks) mutants. **B,** Binding of mAb JAR 36 to fHbp ID 28 wild-type and mutants. **C,** Binding of control mAb JAR 33. **D,** Binding of human fH. The symbols are the same as in Panel A. For each data point, the mean and range of two independent measurements is shown.

536**Figure 1.**

537

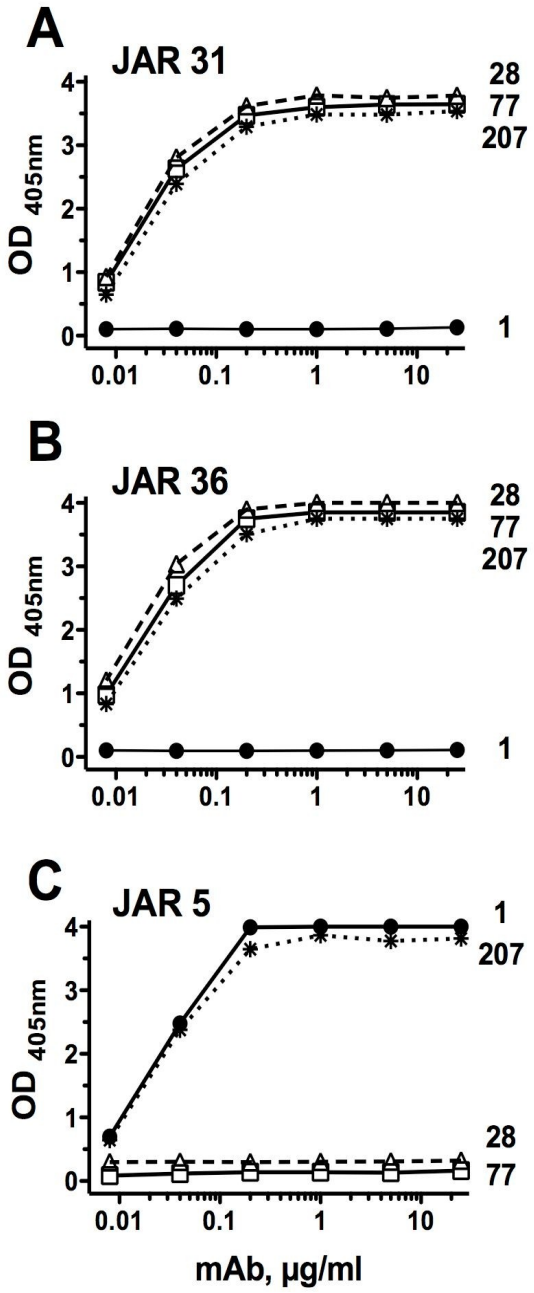

Figure 2

A

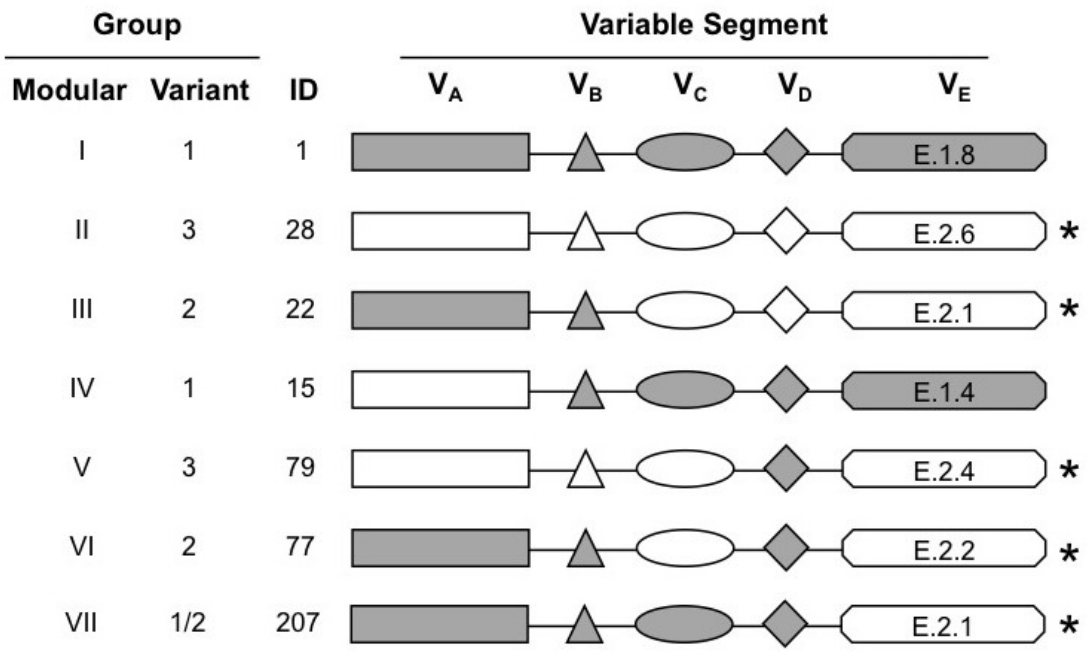

B

```
Seg ID        195        205        215        225        235        245        255
E.2.6  TLEQNVELAA AELKADEKSH AVILGDTRYG SEEKGTYHLA LFGDRAQEIA GSATVKIGEK VHEIGIAGKQ
E.2.2  TPEQNVELAA AELKADEKSH AVILGDTRYG SEEKGTYHLA LFGDRAQEIA GSATVKIGEK VHEIGIAGKQ
E.2.1  TPEQNVELAS AELKADEKSH AVILGDTRYG GEEKGTYHLA LFGDRAQEIA GSATVKIREK VHEIGIAGKQ
E.2.4  TPEQNVELAS AELKADEKSH AVILGDTRYG SEEKGTYHLA LFGDRAQEIA GSATVKIGEK VHEIGIAGKQ

E.1.8  SPELNVDLAA ADIKPDGKRH AVISGSVLYN QAEKGSYSLG IFGGKAQEVA GSAEVKTVNG IRHIGLAAKQ
E.1.4  SPELNVDLAA ADIKPDEKHH AVISGSVLYN QAEKGSYSLG IFGGQAQEVA GSAEVETANG IRHIGLAAKQ
```

Figure 3.

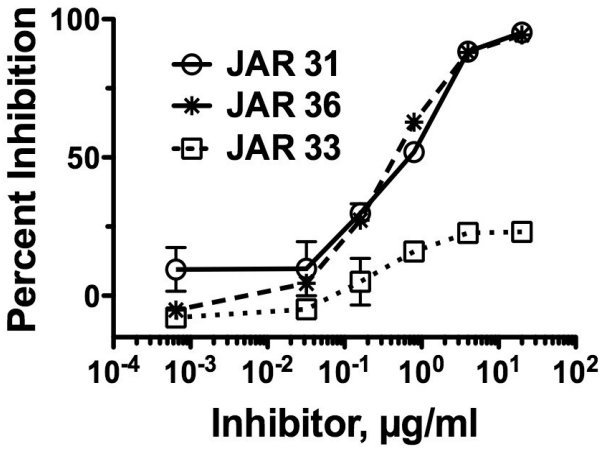
Percent Inhibition
100
50
0
JAR 31
JAR 36
JAR 33
10-4 10-3 10-2 10-1 100 101 102
Inhibitor, µg/ml

552**Figure 4.**
553

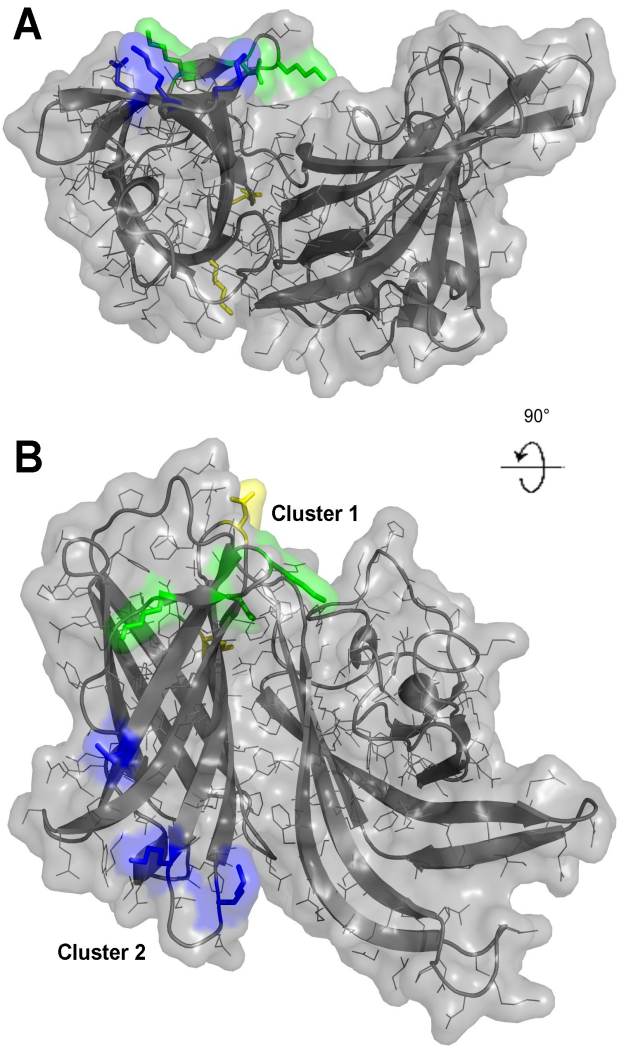

554**Figure 5.**

555

556